SUPPORTING INFORMATION

Discovery of (*S*)-3'-hydroxyblebbistatin and (*S*)-3'-aminoblebbistatin: polar myosin II inhibitors with superior research tool properties

Sigrid Verhasselt,[a] Bart I. Roman,[a]* Olivier De Wever,[b] Kristof Van Hecke,[c] Rik Van Deun,[c] Marc E. Bracke,[b] and Christian V. Stevens[a]*

[a] SynBioC Research Group, Department of Sustainable Organic Chemistry and Technology, Ghent University, Coupure Links 653, 9000 Ghent (Belgium)

*E-mail: bart1.roman@ugent.be, chris.stevens@ugent.be

[b] Laboratory of Experimental Cancer Research, Department of Radiation Oncology and Experimental Cancer Research, Ghent University, De Pintelaan 185, 9000 Ghent (Belgium)

[c] Department of Inorganic and Physical Chemistry, Ghent University, Krijgslaan 281 S3, 9000 Ghent (Belgium)

Table of contents

7. References

1. Synthetic protocols and compound characterization

1.1. Reagents and materials

Dichloromethane was dried by heating under reflux over CaH_2 and distilled under an atmosphere of nitrogen. Tetrahydrofuran was dried by heating under reflux with sodium/benzophenone under a nitrogen atmosphere and collected by distillation. Dry 1,4-dioxane and dry methanol were purchased from Sigma-Aldrich and Acros Organics, respectively. Reagents were purchased at the highest commercial quality and were used as received without further purification.

Yields refer to chromatographically and spectroscopically (^{1}H NMR) homogeneous material, unless otherwise stated.

Reactions were monitored on an Agilent 1200 series HPLC system fitted with an Ascentis® Express C18-column (2.7 µm particle size, 4.6 mm internal diameter), using acetonitrile/water (5 mM NH_4OAc) as eluent. Low-resolution mass spectra were recorded on an Agilent 1100 series VL mass spectrometer (ESI, 70 eV). High-resolution mass spectra (HRMS) were recorded using an Agilent Technologies 6210 series time-of-flight (TOF) mass spectrometer equipped with an ESI/APCI-multimode source. Thin layer chromatography (TLC) was carried out on 0.25 mm Merck silica plates (60 F_{254}) and spots were visualized by UV light (254 nm). Flash column chromatography was performed on an automated Reveleris® X2 flash chromatography system, using Reveleris® C18 or Reveleris® silica cartridges. Melting points were determined using a Wagner & Munz WME Heizbank Kofler bench.

NMR spectra were recorded on a Bruker Avance III instrument. ^{1}H NMR (400 MHz) chemical shifts are recorded in $CDCl_3$ or DMSO-d_6, reported in ppm and measured relative to tetramethylsilane or the residual undeuterated solvent as the internal reference, respectively. ^{13}C NMR (100.6 MHz) chemical shifts are reported in ppm and were measured relative to the residual undeuterated solvent as the internal reference. The following abbreviations were used to explain NMR peak multiplicities: s = singlet, d = doublet, t = triplet, q = quartet, p = pentet, m = multiplet, br = broad.

The enantiomeric excess (ee) of chiral compounds was determined *via* chiral HPLC analysis using a Daicel Chiralpak IA column (5 µm particle size, 150 mm length, 2.1 mm internal diameter). Detection wavelengths were set at 268, 234 and 296 nm. Analyses under reversed phase and normal phase conditions were performed at 25 °C and 35 °C, respectively. Optical rotations were obtained on a Jasco P-2000 polarimeter and are reported in deg mL g^{-1} dm^{-1}; concentrations are reported in grams per 100 mL.

1.2. Synthesis of aryl iodide 4b

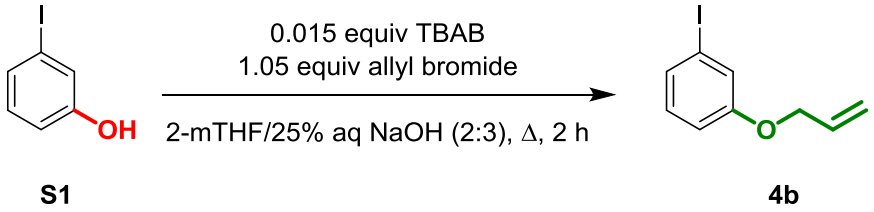

S1 **4b**

Allylation of 3-iodophenol (**S1**) to afford aryl iodide **4b** was based on a publication of Brown Ripin and Vetelino.[1]

In a bulb of 500 mL containing 225 mL of 2-methyltetrahydrofuran, 39.0 g of 3-iodophenol (**S1**) (177 mmol, 1 equiv), 340 mL of 25% aqueous NaOH, 0.857 g of tetra-*n*-butylammonium bromide (2.66 mmol, 0.015 equiv) and 16.2 mL of allyl bromide (186 mmol, 1.05 equiv) were brought together. The resulting mixture was stirred under reflux for 2 hours, cooled down to room temperature and diluted with 350 mL of diethyl ether and 175 mL of water. The two layers were separated and the aqueous layer was extracted with 350 mL of diethyl ether. The combined organic layers were concentrated under reduced pressure to a volume of 350 mL, washed with 175 mL of brine and dried over magnesium sulfate. Evaporation *in vacuo* afforded aryl iodide **4b** (46.1 g, quant.) as a yellow-orange oil.

1-(Allyloxy)-3-iodobenzene (4b)[2,3]

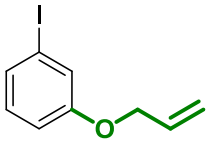

Yield = quant. Yellow-orange oil. **^{1}H NMR** (400 MHz, $CDCl_3$): δ = 4.50 (dt, J = 5.2, 1.4 Hz, 2H), 5.29 (dq, J = 10.5, 1.4 Hz, 1H), 5.40 (dq, J = 17.3, 1.4 Hz, 1H), 6.02 (ddt, J = 17.3, 10.5 Hz, 1H), 6.85–6.90 (m, 1H), 6.99 (t, J = 8.0 Hz, 1H), 7.26–7.28 (m, 1H), 7.26–7.30 (m, 1H). **MW** = 260.07. ^{1}H NMR spectrum is provided in Figure S5.

1.3. Synthesis of aryl iodide 4c

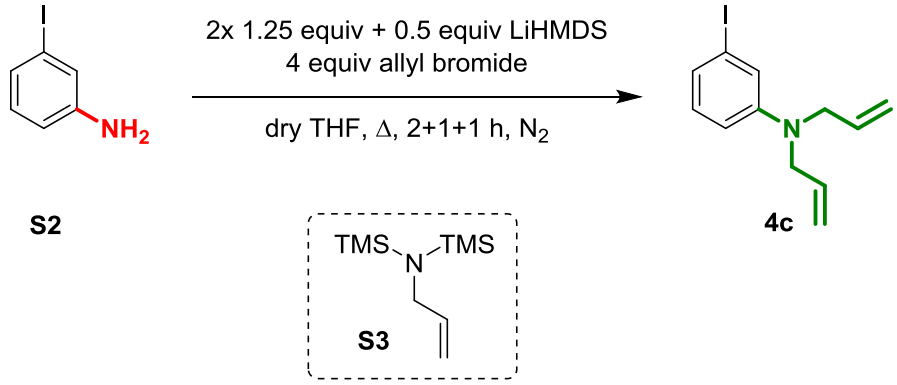

The allylation of 3-iodoaniline (**S2**) to produce aryl iodide **4c** was based on a publication of Vandekerckhove et al.[4]

A bulb of 500 mL, equipped with an oven-dried reflux condenser and kept under a nitrogen atmosphere, was loaded with 100 mL of dry tetrahydrofuran and 11.5 mL of 3-iodoaniline (**S2**) (95.6 mmol, 1 equiv). Then, the solution was cooled to 0 °C and 120 mL of lithiumbis(trimethylsilyl)amide (1 M solution in tetrahydrofuran, 120 mmol, 1.25 equiv) and 33.1 mL of allyl bromide (382 mmol, 4 equiv) were added. The reaction was stirred for 2 hours at reflux temperature. Next, the solution was cooled to 0 °C, a second portion of lithiumbis(trimethylsilyl)amide (1 M solution in tetrahydrofuran, 120 mL, 120 mmol, 1.25 equiv) was added and the reaction mixture was refluxed for 1 hour. The solution was again cooled to 0 °C, a third portion of lithiumbis(trimethylsilyl)amide (1 M solution in tetrahydrofuran, 47.8 mL, 47.8 mmol, 0.5 equiv) was added and the solution was stirred for another hour at reflux temperature. Subsequently, the mixture was cooled down to room temperature, quenched with 800 mL of saturated aqueous NH_4Cl and evaporated under reduced pressure. The residual aqueous layer was extracted with an equal volume of ethyl acetate (3×). The combined organic layers were concentrated *in vacuo* to a volume of 600 mL, washed with an equal volume of saturated aqueous $NaHCO_3$ and brine. Drying with magnesium sulfate and evaporation *in vacuo* resulted in a red oil. The side product *N*,*N*-bis(trimethylsilyl)allylamine (**S3**) was distilled off (20 mbar, 56–63 °C). The residue (28.8 g) was dissolved in 17 mL of hexane and half of the total volume was manually injected on a Reveleris® 120 g silica cartridge (12% sample loading) for purification *via* automated flash chromatography (flow rate: 80 mL min^{-1}; eluent: 7 CV of 100% hexane, followed by 4 CV of 100% ethyl acetate; detection wavelength: 254 nm). The same conditions were applied to purify the other half of the crude mixture. Evaporation of the combined fractions resulted in aryl iodide **4c** (21.4 g, 75%) as a yellow oil.

***N*,*N*-diallyl-3-iodoaniline (4c)**

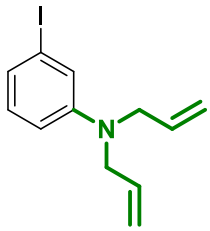

Yield = 75%. Yellow oil. R_f = 0.24 (hexane). **^{1}H NMR** (400 MHz, $CDCl_3$): δ = 3.88 (dt, J = 4.7, 1.7 Hz, 4H), 5.16 (dq, J = 17.5, 1.7 Hz, 2H), 5.17 (dq, J = 10.0, 1.7 Hz, 2H), 5.82 (ddt, J = 17.5, 10.0, 4.7 Hz, 2H), 6.63 (ddd, J = 8.2, 2.5, 0.8 Hz, 1H), 6.88 (t, J = 8.2 Hz, 1H), 6.97–7.01 (m, 1H), 6.99–7.01 (m, 1H). **^{13}C NMR** (100.6 MHz, $CDCl_3$): δ = 52.6, 95.4, 111.5, 116.3, 120.9, 125.1, 130.4, 133.2, 149.8. **MS** (ESI): *m/z* (%) = 299.6 ($[M+H]^+$, 100). **HRMS** (ESI): calculated for $C_{12}H_{15}IN$ ($[M+H]^+$) 300.0244; found 300.0254. **MW** = 299.16. ^{1}H NMR spectrum and ^{13}C NMR spectrum are provided in Figures S6–S7.

1.4. Synthesis of tris(3,5-dimethyl-1*H*-pyrazolyl-1-yl)methane (S5)

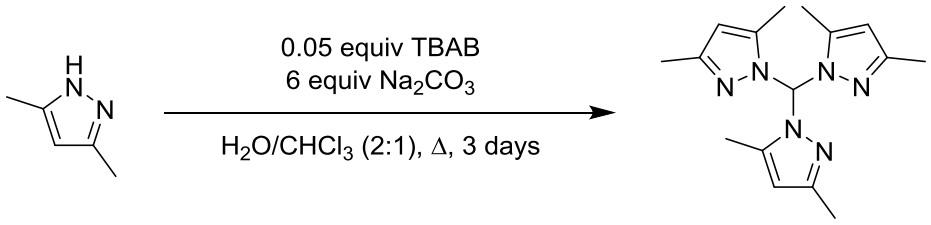

S4 **S5**

Tris(3,5-dimethyl-1*H*-pyrazol-1-yl)methane (**S5**) was synthesized *via* a procedure reported by Reger et al.[5]

In a bulb of 1 L containing 500 mL of demineralized water, 48.1 g of 3,5-dimethylpyrazole (**S4**) (500 mmol, 1 equiv) and 8.06 g of tetra-*n*-butylammonium bromide (25.0 mmol, 0.05 equiv) were brought together. With vigorous mechanical stirring, 318 g of sodium carbonate (3.00 mol, 6 equiv) was added gradually to the reaction mixture. After cooling to room temperature, 250 mL of chloroform was added and the mixture was refluxed for 3 days during which an orange-red emulsion had formed. Next, the solids were filtered off on a sintered glass Büchner funnel and the filter cake was rinsed with chloroform until the filtrate turned colorless. The organic and aqueous layers in the filtrate were separated. The organic layer was washed with an equal volume of brine and dried over magnesium sulfate. Evaporation *in vacuo* afforded a dark brown solid (60.6 g) which was recrystallized from absolute ethanol to give tris(3,5-dimethyl-1*H*-pyrazol-1-yl)methane (**S5**) (19.2 g, 39%) as an off-white powder.

Tris(3,5-dimethyl-1*H*-pyrazol-1-yl)methane (S5)[6,7]

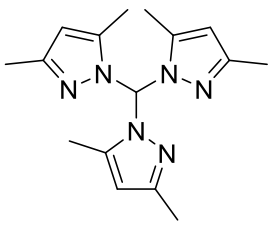

Yield = 39%. Off-white powder (from absolute ethanol). **^{1}H NMR** (400 MHz, $CDCl_3$): δ = 2.01 (br. s, 9H), 2.18 (s, 9H), 5.88 (s, 3H), 8.07 (s, 1H). **MW** = 298.39. ^{1}H NMR spectrum is provided in Figure S8.

1.5. General procedure for the *N*-arylation of 2-pyrrolidinone with aryl iodides

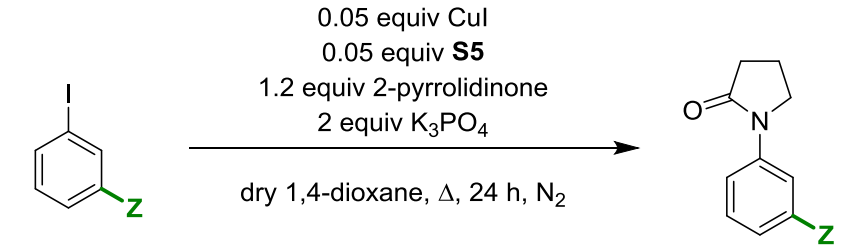

4a (Z = H)
4b (Z = OAllyl)
4d (Z = CN)

6a (Z = H)
6b (Z = OAllyl)
6d (Z = CN)

The preparation of pyrrolidinones **6a**,**b**,**d** was adopted from Haldón et al.[8]

In a flame-dried bulb of 250 mL containing 100 mL of dry 1,4-dioxane, 0.952 g of CuI (5.00 mmol, 0.05 equiv) and 1.49 g of tris(3,5-dimethyl-1*H*-pyrazol-1-yl)methane (**S5**) (5.00 mmol, 0.05 equiv) were brought together under a nitrogen atmosphere. Then, aryl iodide (100 mmol, 1 equiv), 9.12 mL of 2-pyrrolidinone (120 mmol, 1.2 equiv) and 42.4 g of K_3PO_4 (200 mmol, 2 equiv) were added and the reaction mixture was stirred at reflux temperature for 24 hours. A beige suspension was formed during this step. Next, the suspension was cooled down to room temperature and the solids were filtered off on a sintered glass Büchner funnel. The filter cake was rinsed with ethyl acetate until the filtrate turned colorless. The filtrate was washed with an equal volume of 3 M aqueous HCl (3×) and brine, after which the organic layer was dried over magnesium sulfate and evaporated *in vacuo*.

1.5.1. Synthesis of pyrrolidinone 6a

Pyrrolidinone **6a** was synthesized from aryl iodide **4a** (11.2 mL, 100 mmol, 1 equiv) and 2-pyrrolidinone (9.12 mL, 120 mmol, 1.2 equiv). Evaporation *in vacuo* afforded pyrrolidinone **6a** (14.3 g, 89%) as beige fibers. An analytical sample was prepared by recrystallization from absolute ethanol.

1-Phenylpyrrolidin-2-one (6a)[9,10]

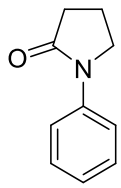

Yield = 89%. Beige fibers. **^{1}H NMR** (400 MHz, $CDCl_3$): δ = 2.16 (p, J = 7.6 Hz, 2H), 2.61 (t, J = 7.6 Hz, 2H), 3.87 (t, J = 7.6 Hz, 2H), 7.11–7.17 (m, 1H), 7.33–7.40 (m, 2H), 7.58–7.64 (m, 2H). **MW** = 161.20. ^{1}H NMR spectrum is provided in Figure S9.

1.5.2. Synthesis of pyrrolidinone 6b

Pyrrolidinone **6b** was synthesized from aryl iodide **4b** (45.0 g, 173 mmol, 1 equiv) and 2-pyrrolidinone (15.8 mL, 208 mmol, 1.2 equiv). Evaporation *in vacuo* afforded a red oil (38.9 g) which was further purified *via* automated flash chromatography with hexane/ethyl acetate as eluent. Half of the crude mixture was manually injected on a

Reveleris® 120 g silica cartridge (16% sample loading) and the injection valve was subsequently rinsed twice with 5 mL of the initial mobile phase (flow rate: 80 mL min^{-1}; eluent: 2 column volumes (CV) of 12% ethyl acetate, followed by a gradient from 12% to 100% ethyl acetate over 10 CV and finally 2 CV of 100% ethyl acetate; detection wavelengths: 254 nm and 268 nm). Next, the same conditions were applied to purify the other half of the crude mixture and evaporation of the combined fractions yielded pyrrolidinone **6b** (28.2 g, 75%) as a yellow-orange oil.

1-(3-(Allyloxy)phenyl)pyrrolidin-2-one (6b)

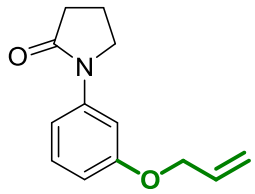

Yield = 75%. Yellow-orange oil. R_f = 0.51 (ethyl acetate). **^{1}H NMR** (400 MHz, $CDCl_3$): δ = 2.15 (p, J = 7.6 Hz, 2H), 2.61 (t, J = 7.6 Hz, 2H), 3.84 (t, J = 7.6 Hz, 2H), 4.55 (dt, J = 5.3, 1.4 Hz, 2H), 5.29 (dq, J = 10.6, 1.4 Hz, 1H), 5.42 (dq, J = 17.3, 1.4 Hz, 1H), 6.06 (ddt, J = 17.3, 10.6, 5.3 Hz, 1H), 6.71 (ddd, J = 8.2, 2.2, 0.7 Hz, 1H), 7.13 (ddd, J = 8.2, 2.2, 0.7 Hz, 1H), 7.25 (t, J = 8.2 Hz, 1H), 7.37 (t, J = 2.2 Hz, 1H). **^{13}C NMR** (100.6 MHz, $CDCl_3$): δ = 18.0, 32.9, 48.9, 68.9, 106.8, 110.8, 112.1, 117.8, 129.5, 133.2, 140.6, 158.9, 174.3. **MS** (ESI): *m/z* (%) = 218.1 ($[M+H]^+$, 100). **HRMS** (ESI): calculated for $C_{13}H_{16}NO_2$ ($[M+H]^+$) 218.1176; found 218.1178. **MW** = 217.26. ^{1}H NMR spectrum and ^{13}C NMR spectrum are provided in Figures S10–S11.

1.5.3. Synthesis of pyrrolidinone 6d

Pyrrolidinone **6d** was synthesized from aryl iodide **4d** (28.5 g, 124 mmol, 1 equiv) and 2-pyrrolidinone (11.3 mL, 149 mmol, 1.2 equiv). Evaporation *in vacuo* afforded pyrrolidinone **6d** (20.4 g, 88%) as beige crystals. An analytical sample was prepared by recrystallization from absolute ethanol.

3-(2-Oxopyrrolidin-1-yl)benzonitrile (6d)[11]

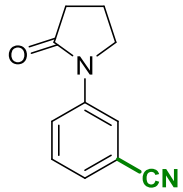

Yield = 88%. Beige crystals (mp 83 °C). **^{1}H NMR** (400 MHz, $CDCl_3$): δ = 2.21 (p, J = 7.6 Hz, 2H), 2.64 (t, J = 7.6 Hz, 2H), 3.87 (t, J = 7.6 Hz, 2H), 7.40 (dt, J = 8.0, 1.3 Hz, 1H), 7.46 (t, J = 8.0 Hz, 1H), 7.91 (ddd, J = 8.0, 2.3, 1.3 Hz, 1H), 7.96–7.99 (m, 1H). **^{13}C NMR** (100.6 MHz, $CDCl_3$): δ = 17.8, 32.6, 48.3, 112.9, 118.6, 122.5, 123.5, 127.6, 129.7, 140.2, 175.6. **MS** (ESI): *m/z* (%) = 186.9 ($[M+H]^+$, 100). **HRMS** (ESI): calculated for $C_{11}H_{11}N_2O$ ($[M+H]^+$) 187.0866; found 187.0860. **MW** = 186.21. ^{1}H NMR spectrum and ^{13}C NMR spectrum are provided in Figures S12–S13.

1.6. Synthesis of pyrrolidinone 6c

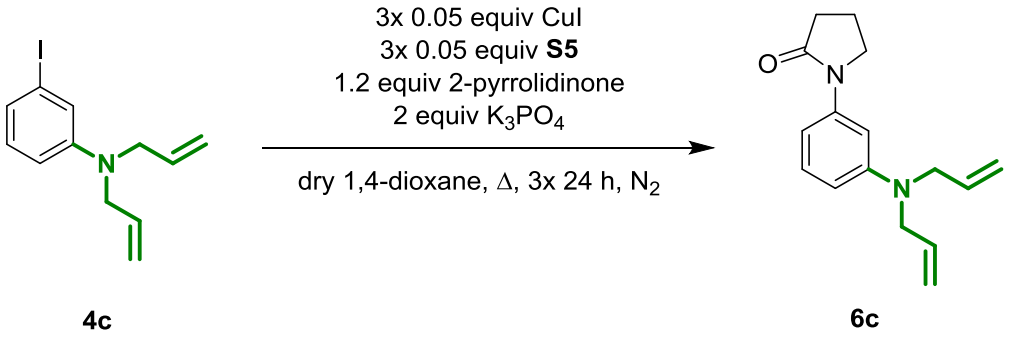

4c **6c**

For the synthesis of pyrrolidinone **6c**, the general procedure for the *N*-arylation of 2-pyrrolidinone with aryl iodides was slightly modified.

In a flame-dried bulb of 250 mL containing 96 mL of dry 1,4-dioxane, 0.909 g of CuI (4.76 mmol, 0.05 equiv) and 1.42 g of tris(3,5-dimethyl-1*H*-pyrazol-1-yl)methane (**S5**) (4.76 mmol, 0.05 equiv) were brought together under a nitrogen atmosphere. Then, 28.5 g of aryl iodide **4c** (95.3 mmol, 1 equiv), 8.68 mL of 2-pyrrolidinone (114 mmol, 1.2 equiv) and 40.5 g of K_3PO_4 (191 mmol, 2 equiv) were added under a nitrogen atmosphere and the reaction mixture was stirred under reflux for 24 hours. Next, a second portion of CuI (0.909 g, 4.76 mmol, 0.05 equiv) and of tris(3,5-dimethyl-1*H*-pyrazol-1-yl)methane (**S6**) (1.42 g, 4.76 mmol, 0.05 equiv) were added and the reaction mixture was refluxed for 24 hours. Afterwards, a third portion of CuI (0.909 g, 4.76 mmol, 0.05 equiv) and of tris(3,5-dimethyl-1*H*-pyrazol-1-yl)methane (**S6**) (1.42 g, 4.76 mmol, 0.05 equiv) were added and the mixture was stirred for another 24 hours at reflux temperature. A beige suspension was formed during this reaction. After cooling to room temperature, the solids were filtered off on a sintered glass Büchner funnel and the filter cake was rinsed with ethyl acetate until the filtrate turned colorless. The filtrate was washed with an equal volume of saturated aqueous NH_4Cl (3×) and brine, after which the organic layer was isolated and dried with magnesium sulfate. Evaporation *in vacuo* afforded an orange-red oil (32.5 g) of which 5.41 g was dissolved in acetonitrile and coated under reduced pressure onto 10.8 g of Davisil® C18 silica. Subsequently, purification was performed *via* automated flash chromatography with water/acetonitrile as eluent on a Reveleris® 120 g C18 cartridge (5% sample loading; flow rate: 80 mL min^{-1}; eluent: 2 CV of 20% acetonitrile, followed by a gradient from 20% to 40% acetonitrile over 30 CV and finally a gradient from 40% to 100% acetonitrile over 20 CV; detection wavelengths: 222 nm and 262 nm). Next, the same conditions were repeated another 5 times to purify the remaining parts of the crude mixture. Coevaporation of the combined fractions with chloroform, to remove traces of water, resulted in pyrrolidinone **6c** (19.3 g, 79%) as a yellow-orange oil.

1-(3-(Diallylamino)phenyl)pyrrolidin-2-one (6c)

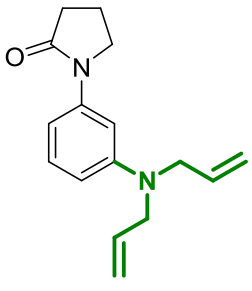

Yield = 79%. Yellow oil. R_f = 0.27 (hexane/ethyl acetate, 3:2). **^{1}H NMR** (400 MHz, $CDCl_3$): δ = 2.12 (p, J = 7.6 Hz, 2H), 2.58 (t, J = 7.6 Hz, 2H), 3.83 (t, J = 7.6 Hz, 2H),

3.93 (dt, J = 4.9, 1.7 Hz, 4H), 5.16 (dq, J = 9.3, 1.7 Hz, 2H), 5.19 (dq, J = 16.3, 1.7 Hz, 2H), 5.85 (ddt, J = 16.3, 9.3, 4.9 Hz, 2H), 6.47–6.52 (m, 1H), 6.75 (ddd, J = 8.1, 2.1, 0.6 Hz, 1H), 7.16 (t, J = 8.1 Hz, 1H), 7.16 (t, J = 2.1 Hz, 1H). **^{13}C NMR** (100.6 MHz, $CDCl_3$): δ = 18.1, 32.9, 49.1, 52.9, 104.7, 108.0, 108.9, 116.1, 129.2, 133.9, 140.3, 149.2, 174.1. **MS** (ESI): *m/z* (%) = 256.8 ($[M+H]^+$, 100). **HRMS** (ESI): calculated for $C_{16}H_{21}N_2O$ ($[M+H]^+$) 257.1648; found 257.1647. **MW** = 256.35. ^{1}H NMR spectrum and ^{13}C NMR spectrum are provided in Figures S14–S15.

1.7. Synthesis of pyrrolidinethione 10

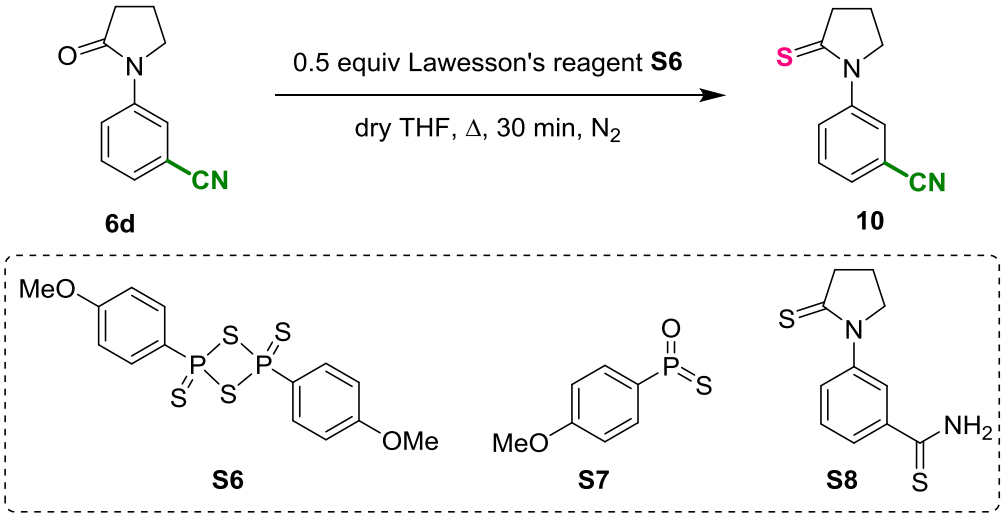

In a flame-dried bulb of 100 mL containing 50 mL of dry tetrahydrofuran, 1.86 g of pyrrolidinone **6d** (1.00 mmol, 1 equiv) and 2.00 g of Lawesson's reagent **S6** (0.500 mmol, 0.5 equiv) were brought together under a nitrogen atmosphere and stirred for 30 minutes at reflux temperature. Then, the reaction mixture was cooled to 0 °C, diluted with 50 mL of diethyl ether and the resulting slurry was filtered off over celite. Evaporation of the filtrate *in vacuo* afforded a yellow solid (3.70 g) which was dissolved in toluene and coated under reduced pressure onto 14.8 g of silica. Subsequently, purification was performed *via* automated flash chromatography with hexane/ethyl acetate as eluent on a Reveleris® 80 g silica cartridge (5% sample loading; flow rate: 60 mL min^{-1}; eluent: 2 CV of 0% ethyl acetate, followed by a gradient from 0% to 30% ethyl acetate over 60 CV and finally 5 CV of 100% ethyl acetate; detection wavelength: 272 nm). This afforded pyrrolidinethione **10** (1.60 g, 79%) as off-white fibers.

When excess Lawesson's reagent **S6** (more than 0.5 equivalents) and/or prolonged reaction times (more than 30 minutes) were used at elevated temperatures (70 °C), thionation of the nitrile functionality in pyrrolidinethione **10** also occurred, resulting in side product **S8**. Moreover, it should be noted it is crucial to use toluene to dissolve the crude product prior to flash chromatography: in order to obtain a high yield and good separation between desired product **10**, Lawesson's reagent byproduct **S7** and thiobenzamide **S8** during chromatography, it is important to obtain a free-flowing, well-coated mixture. From an extensive series of solvents (toluene, ethyl acetate, acetone, tetrahydrofuran, dichloromethane, chloroform, methanol and acetonitrile), toluene was the only solvent able to do so.

3-(2-Thioxopyrrolidin-1-yl)benzonitrile (10)

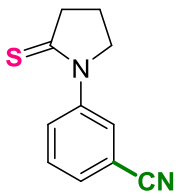

Yield = 79%. Off-white fibers (mp 132 °C). **^{1}H NMR** (400 MHz, $CDCl_3$): δ = 2.27 (p, J = 7.5 Hz, 2H), 3.24 (t, J = 7.5 Hz, 2H), 4.15 (t, J = 7.5 Hz, 2H), 7.53–7.63 (m, 2H), 7.87–7.92 (m, 2H). **^{13}C NMR** (100.6 MHz, $CDCl_3$): δ = 20.7, 46.4, 58.1, 113.2, 117.9, 128.3, 129.4, 130.0,

130.9, 141.2, 204.0. **MS** (ESI): *m/z* (%) = 203.2 ($[M+H]^+$, 100). **MW** = 202.28. ^{1}H NMR spectrum and ^{13}C NMR spectrum are provided in Figures S16–S17.

1.8. Synthesis of methyl 2-amino-5-methylbenzoate (7)

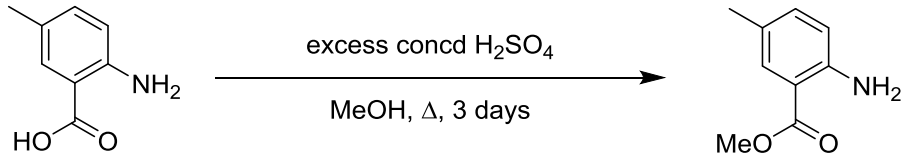

S9 **7**

The preparation of methyl 2-amino-5-methylbenzoate (**7**) was adopted from Lawson et al.[12]

To a solution of 30.5 g of 2-amino-5-methylbenzoic acid (**S9**) (184 mmol, 1 equiv) in 500 mL of methanol, 30 mL of concentrated H_2SO_4 was added and the resulting mixture was stirred at reflux temperature for 3 days. After cooling to room temperature, the solvent was removed *in vacuo*. The yellow residue was taken up in 250 mL of ethyl acetate and washed subsequently with an equal volume of 1 M aqueous NaOH. The organic layer was dried over magnesium sulfate and evaporated *in vacuo* to afford methyl 2-amino-5-methylbenzoate (**7**) (31.0 g, quant.) as a beige-orange powder.

Methyl 2-amino-5-methylbenzoate (7)[13,14]

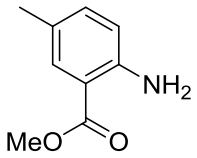

Yield = quant. Beige-orange powder. **^{1}H NMR** (400 MHz, $CDCl_3$): δ = 2.22 (s, 3H), 3.85 (s, 3H), 5.53 (br. s, 2H), 6.59 (d, J = 8.3 Hz, 1H), 7.09 (dd, J = 8.3, 2.2 Hz, 1H), 7.66 (d, J = 2.2 Hz, 1H). **MW** = 165.19. ^{1}H NMR spectrum is provided in Figure S18.

1.9. General procedure for the synthesis of amidines from pyrrolidinones

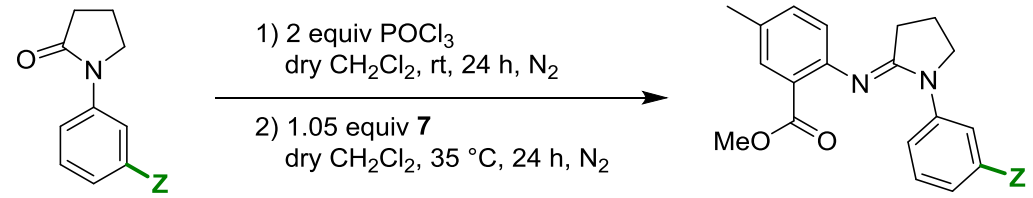

6a (Z = H)
6b (Z = OAllyl)
6d (Z = CN)

8a (Z = H)
8b (Z = OAllyl)
8d (Z = CN)

The synthesis of amidines **8a**,**b**,**d** from pyrrolidinones **6a**,**b**,**d** was performed *via* a modified procedure of Lucas-Lopez et al.[15]

A flame-dried bulb of 100 mL, kept under a nitrogen atmosphere, was loaded with 40 mL of dry dichloromethane and pyrrolidinone (15.0 mmol, 1 equiv). Next, 2.80 mL of $POCl_3$ (30.0 mmol, 2 equiv) was added and the resulting mixture was stirred at room temperature for 24 hours. Afterwards, a solution of methyl 2-amino-5-methylbenzoate (**7**) (2.60 g, 15.8 mmol, 1.05 equiv) in dry dichloromethane (15 mL) was added *via* syringe and the reaction mixture was heated to 35 °C for 24 hours. Then, the reaction mixture was cooled to 0 °C, basified with 3 M aqueous NaOH until the pH equaled 10, and subsequently extracted with an equal volume of ethyl acetate (3×). The combined organic layers were washed with an equal volume of brine, dried over magnesium sulfate and evaporated *in vacuo*.

1.9.1. Synthesis of amidine 8a

Amidine **8a** was synthesized from pyrrolidinone **6a** (2.42 g, 15.0 mmol, 1 equiv) and methyl 2-amino-5-methylbenzoate (**7**) (2.60 g, 15.8 mmol, 1.05 equiv). Evaporation *in vacuo* afforded an orange-brown oil (5.71 g) which was dissolved in acetonitrile/dichloromethane (1:1) and coated under reduced pressure onto 11.4 g of Davisil® C18 silica. Subsequently, purification was performed *via* automated flash chromatography with water/acetonitrile as eluent on a Reveleris® 120 g C18 cartridge (5% sample loading; flow rate: 80 mL min^{-1}; eluent: 2 CV of 30% acetonitrile, followed by a gradient from 30% to 100% acetonitrile over 20 CV and finally 2 CV of 100% acetonitrile; detection wavelengths: 218 nm and 246 nm). Coevaporation with chloroform, to remove traces of water, afforded amidine **8a** (3.90 g, 78%) as an off-white powder. An analytical sample was prepared by recrystallization from absolute ethanol.

Methyl 5-methyl-2-((1-phenylpyrrolidin-2-ylidene)amino)benzoate (8a)[15]

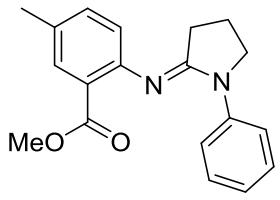

Yield = 78%. Off-white powder. **^{1}H NMR** (400 MHz, $CDCl_3$): δ = 2.03 (p, J = 7.3 Hz, 2H), 2.31 (s, 3H), 2.46 (t, J = 7.3 Hz, 2H), 3.81 (s, 3H), 3.87 (t, J = 7.3 Hz, 2H), 6.71 (d, J = 8.1 Hz, 1H), 7.02–7.08 (m, 1H), 7.18 (dd, J = 8.1, 1.7 Hz, 1H), 7.31–7.38 (m, 2H),

7.65 (d, J = 1.7 Hz, 1H), 7.79–7.84 (m, 2H). **MW** = 308.37. ^{1}H NMR spectrum is provided in Figure S19.

1.9.2. Synthesis of amidine 8b

Amidine **8b** was synthesized from pyrrolidinone **6b** (26.5 g, 122 mmol, 1 equiv) and methyl 2-amino-5-methylbenzoate (**7**) (21.1 g, 128 mmol, 1.05 equiv). Evaporation *in vacuo* afforded an orange-brown oil (42.9 g) of which 14.3 g was dissolved in dichloromethane and coated under reduced pressure onto 28.6 g of silica. Subsequently, purification was performed *via* automated flash chromatography with hexane/ethyl acetate/triethylamine as eluent on a Reveleris® 120 g silica cartridge (12% sample loading; flow rate: 80 mL min^{-1}; eluent: 2 CV of a 7% ethyl acetate/triethylamine mixture (ethyl acetate + 16% triethylamine), followed by a gradient from 7% to 60% ethyl acetate/triethylamine mixture over 10 CV and finally 3 CV of a 60% ethyl acetate/triethylamine mixture; detection wavelengths: 246 nm and 298 nm). Next, the same conditions were repeated twice to purify the remaining parts of the crude mixture. Evaporation of the combined fractions afforded amidine **8b** (22.2 g, 50%) as a light yellow powder.

Methyl 2-((1-(3-(allyloxy)phenyl)pyrrolidin-2-ylidene)amino)-5-methyl-benzoate (8b)

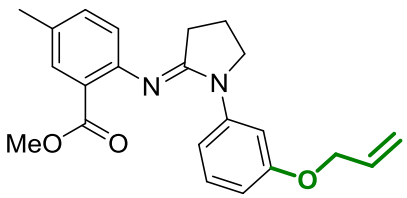

Yield = 50%. Light yellow powder (mp 66 °C). R_f = 0.42 (hexane/ethyl acetate/triethylamine, 7:3:0.5). **^{1}H NMR** (400 MHz, $CDCl_3$): δ = 2.03 (p, J = 7.3 Hz, 2H), 2.32 (s, 3H), 2.46 (t, J = 7.3 Hz, 2H), 3.83 (s, 3H), 3.85 (t, J = 7.3 Hz, 2H), 4.53 (dt, J = 5.4, 1.4 Hz, 2H), 5.25 (dq, J = 10.6, 1.4 Hz, 1H), 5.39 (dq, J = 17.2, 1.4 Hz, 1H), 6.05 (ddt, J = 17.2, 10.6, 5.4 Hz, 1H), 6.62 (ddd, J = 8.1, 2.2, 0.8 Hz, 1H), 6.70 (d, J = 8.1 Hz, 1H), 7.18 (dd, J = 8.1, 1.8 Hz, 1H), 7.22 (t, J = 8.1 Hz, 1H), 7.30 (ddd, J = 8.1, 2.2, 0.8 Hz, 1H), 7.65 (d, J = 1.8 Hz, 1H), 7.67 (t, J = 2.2 Hz, 1H). **^{13}C NMR** (100.6 MHz, $CDCl_3$): δ = 19.7, 20.6, 29.2, 50.7, 51.7, 68.8, 107.3, 109.4, 112.6, 117.7, 121.9, 122.9, 129.2, 131.0, 133.5, 133.5, 142.7, 150.6, 158.8, 159.7, 167.8. **MS** (ESI): *m/z* (%) = 364.6 ([M+H]$^+$, 100). **HRMS** (ESI): calculated for $C_{22}H_{25}N_2O_3$ ([M+H]$^+$) 365.1860; found 365.1848. **MW** = 364.44. ^{1}H NMR spectrum and ^{13}C NMR spectrum are provided in Figures S20–S21.

1.9.3. Synthesis of amidine 8d

Amidine **8d** was synthesized from pyrrolidinone **6d** (20.8 g, 112 mmol, 1 equiv) and methyl 2-amino-5-methylbenzoate (**7**) (19.4 g, 117 mmol, 1.05 equiv). Evaporation *in vacuo* afforded a red-brown oil (38.8 g) of which 6.47 g was dissolved in acetonitrile/dichloromethane (1:1) and coated under reduced pressure onto 12.9 g of Davisil® C18 silica. Subsequently, purification was performed *via* automated flash chromatography with water/acetonitrile as eluent on a Reveleris® 120 g C18 cartridge (5% sample loading; flow rate: 80 mL min^{-1}; eluent: 2 CV of 30% acetonitrile, followed by a gradient from 30% to 100% acetonitrile over 20 CV and finally 2 CV of 100% acetonitrile; detection wavelengths: 216 nm and 274 nm). Next, the same conditions were repeated

another 5 times to purify the remaining parts of the crude mixture. Coevaporation of the combined fractions with chloroform, to remove traces of water, yielded amidine **8d** (11.2 g, 30%) as an off-white powder.

Methyl 2-((1-(3-cyanophenyl)pyrrolidin-2-ylidene)amino)-5-methylbenzoate (8d)

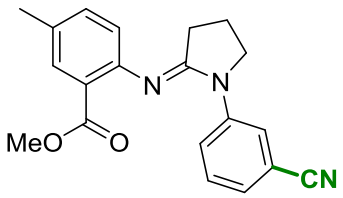

Yield = 30%. Off-white powder (mp 116 °C). R_f = 0.32 (hexane/ethyl acetate/triethylamine, 7:3:0.5). **^{1}H NMR** (400 MHz, $CDCl_3$): δ = 2.08 (p, J = 7.4 Hz, 2H), 2.33 (s, 3H), 2.49 (t, J = 7.4 Hz, 2H), 3.82 (s, 3H), 3.86 (t, J = 7.4 Hz, 2H), 6.69 (d, J = 8.1 Hz, 1H), 7.21 (dd, J = 8.1, 1.6 Hz, 1H), 7.31 (dt, J = 7.8, 1.3 Hz, 1H), 7.42 (t, J = 7.8 Hz, 1H), 7.69 (d, J = 1.6 Hz, 1H), 8.08–8.17 (m, 1H), 8.21 (t, J = 1.3 Hz, 1H). **^{13}C NMR** (100.6 MHz, $CDCl_3$): δ = 19.6, 20.6, 29.0, 50.2, 51.8, 112.4, 119.2, 121.2, 122.5, 123.0, 124.0, 125.9, 129.4, 131.2, 131.6, 133.7, 142.2, 149.8, 159.8, 167.4. **MS** (ESI): *m/z* (%) = 333.6 ($[M+H]^+$, 100). **HRMS** (ESI): calculcated for $C_{20}H_{20}N_3O_2$ ($[M+H]^+$) 334.1550; found 334.1543. **MW** = 333.38. ^{1}H NMR spectrum and ^{13}C NMR spectrum are provided in Figures S22–S23.

1.10. General procedure for the synthesis of quinolones from amidines

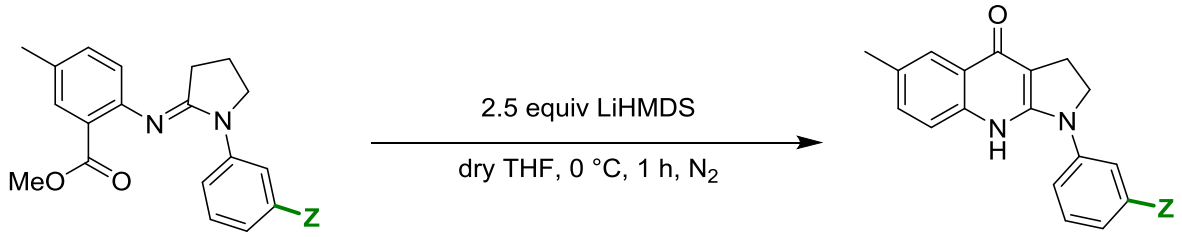

8a (Z = H)
8b (Z = OAllyl)
8d (Z = CN)

9a (Z = H)
9b (Z = OAllyl)
9d (Z = CN)

The synthesis of quinolones **9a**,**b**,**d** from amidines **8a**,**b**,**d** was performed *via* a modified procedure of Lawson et al.[12]

A flame-dried bulb of 100 mL, kept under a nitrogen atmosphere, was loaded with 15 mL of dry tetrahydrofuran and amidine (14.7 mmol, 1 equiv). Then, the solution was cooled to −78 °C and 36.8 mL of lithiumbis(trimethylsilyl)amide (1 M solution in tetrahydrofuran, 36.8 mmol, 2.5 equiv) was added. Subsequently, the mixture was stirred at 0 °C for 1 hour before being quenched by the addition of 60 mL of saturated aqueous NH_4Cl. The layers were separated and the organic layer was washed with an equal volume of saturated aqueous NH_4Cl (2×) and concentrated *in vacuo* to approximately 10 mL. Next, the residue was diluted with 75 mL of ethyl acetate, dried over magnesium sulfate and evaporated *in vacuo*.

1.10.1. Synthesis of quinolone 9a

Quinolone **9a** was synthesized from amidine **8a** (4.54 g, 14.7 mmol, 1 equiv). Evaporation *in vacuo* gave a yellow-orange powder which was washed on a sintered glass Büchner funnel with ice cold ethyl acetate until the filtrate turned colorless. This afforded quinolone **9a** (3.98 g, 98%) as a beige powder.

6-Methyl-1-phenyl-1,2,3,9-tetrahydro-4*H*-pyrrolo[2,3-*b*]quinolin-4-one (9a)[15]

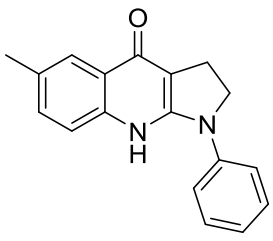

Yield = 98%. Beige powder. **^{1}H NMR** (400 MHz, DMSO-d^6): δ = 2.41 (s, 3H), 3.17 (t, J = 7.9 Hz, 2H), 4.07 (t, J = 7.9 Hz, 2H), 7.01 (t, J = 7.2 Hz, 1H), 7.32 (dd, J = 8.4, 1.8 Hz, 1H), 7.39 (t, J = 7.2 Hz, 2H), 7.51 (d, J = 8.4 Hz, 1H), 7.77 (br. s, 1H), 8.05 (br. s, 2H), 10.46 (br. s, 1H). **MW** = 276.33. ^{1}H NMR spectrum is provided in Figure S24.

1.10.2. Synthesis of quinolone 9b

Quinolone **9b** was prepared from amidine **8b** (19.9 g, 54.6 mmol, 1 equiv). Evaporation *in vacuo* resulted in an orange powder (18.7 g) which was washed on a sintered glass Büchner funnel with ice cold ethyl acetate until the filtrate turned colorless. This afforded quinolone **8b** (15.0 g, 82%) as an off-white powder.

1-(3-(Allyloxy)phenyl)-6-methyl-1,2,3,9-tetrahydro-4*H*-pyrrolo[2,3-*b*]quinolin-4-one (9b)

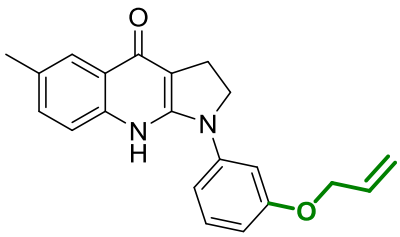

Yield = 82%. Off-white powder (mp 203 °C). R_f = 0.13 (ethyl acetate). **^{1}H NMR** (400 MHz, DMSO-d^6): δ = 2.42 (s, 3H), 3.17 (t, J = 7.9 Hz, 2H), 4.06 (t, J = 7.9 Hz, 2H), 4.63 (dt, J = 5.2, 1.5 Hz, 2H), 5.29 (dq, J = 10.6, 1.5 Hz, 1H), 5.46 (dq, J = 17.2, 1.5 Hz, 1H), 6.11 (ddt, J = 17.2, 10.6, 5.2 Hz, 1H), 6.60 (d, J = 7.7 Hz, 1H), 7.26 (t, J = 7.7 Hz, 1H), 7.32 (dd, J = 8.4, 1.5 Hz, 1H), 7.45 (d, J = 7.7 Hz, 1H), 7.52 (d, J = 8.4 Hz, 1H), 7.77 (br. s, 1H), 8.04 (br. s, 1H), 10.46 (br. s, 1H). **^{13}C NMR** (100.6 MHz, DMSO-d^6): δ = 21.5, 22.3, 48.6, 68.6, 104.5, 106.9, 107.5, 110.0, 117.9, 119.1, 121.0, 126.7, 129.6, 130.8, 131.2, 134.4, 143.8, 146.8, 154.2, 158.9, 159.8. **MS** (ESI): *m/z* (%) = 332.7 ([M+H]$^+$, 100). **HRMS** (ESI): calculated for $C_{21}H_{21}N_2O_2$ ([M+H]$^+$) 333.1598; found 333.1604. **MW** = 332.40. ^{1}H NMR spectrum and ^{13}C NMR spectrum are provided in Figures S25–S26.

1.10.3. Synthesis of quinolone 9d

Quinolone **9d** was obtained from amidine **8d** (10.8 g, 30.9 mmol, 1 equiv). Evaporation *in vacuo* resulted in an ochreous powder (12.3 g) which was washed on a sintered glass Büchner funnel with ice cold ethyl acetate until the filtrate turned colorless. This afforded quinolone **9d** (8.01 g, 86%) as a beige powder.

3-(6-Methyl-4-oxo-2,3,4,9-tetrahydro-1*H*-pyrrolo[2,3-*b*]quinolin-1-yl)benzonitrile (9d)

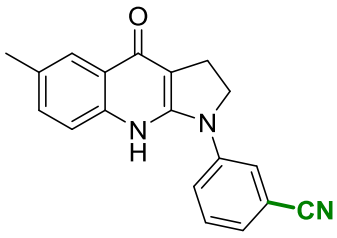

Yield = 86%. Beige powder (mp 252 °C). **^{1}H NMR** (400 MHz, DMSO-d^6): δ = 2.43 (s, 3H), 3.20 (t, J = 7.6 Hz, 2H), 4.10 (t, J = 7.6 Hz, 2H), 7.36 (d, J = 8.2 Hz, 1H), 7.41 (d, J = 7.9 Hz, 1H), 7.57 (d, J = 8.2 Hz, 1H), 7.58 (t, J = 7.9 Hz, 1H), 7.80 (br. s, 1H), 8.39 (d, J = 7.9 Hz, 1H), 8.62 (br. s, 1H), 10.63 (br. s, 1H). **^{13}C NMR** (100.6 MHz, DMSO-d^6): δ = 21.5, 22.3, 48.4, 106.8, 111.8, 119.2, 119.8, 120.1, 121.0, 121.8, 124.1, 126.8, 130.3, 131.1, 131.8, 143.2, 146.5, 154.7, 159.4. **MS** (ESI): *m/z* (%) = 301.7 ([M+H]$^+$, 100). **HRMS** (ESI): calculated for $C_{19}H_{16}N_3O$ ([M+H]$^+$) 302.1288; found 302.1296. **MW** = 301.34. ^{1}H NMR spectrum and ^{13}C NMR spectrum are provided in Figures S27–S28.

1.11. Synthesis of (*S*)-3'-diallylaminoblebbistatin ((*S*)-12) and (*S*)-3'-diallylaminoblebbistatin ((*S*)-12)

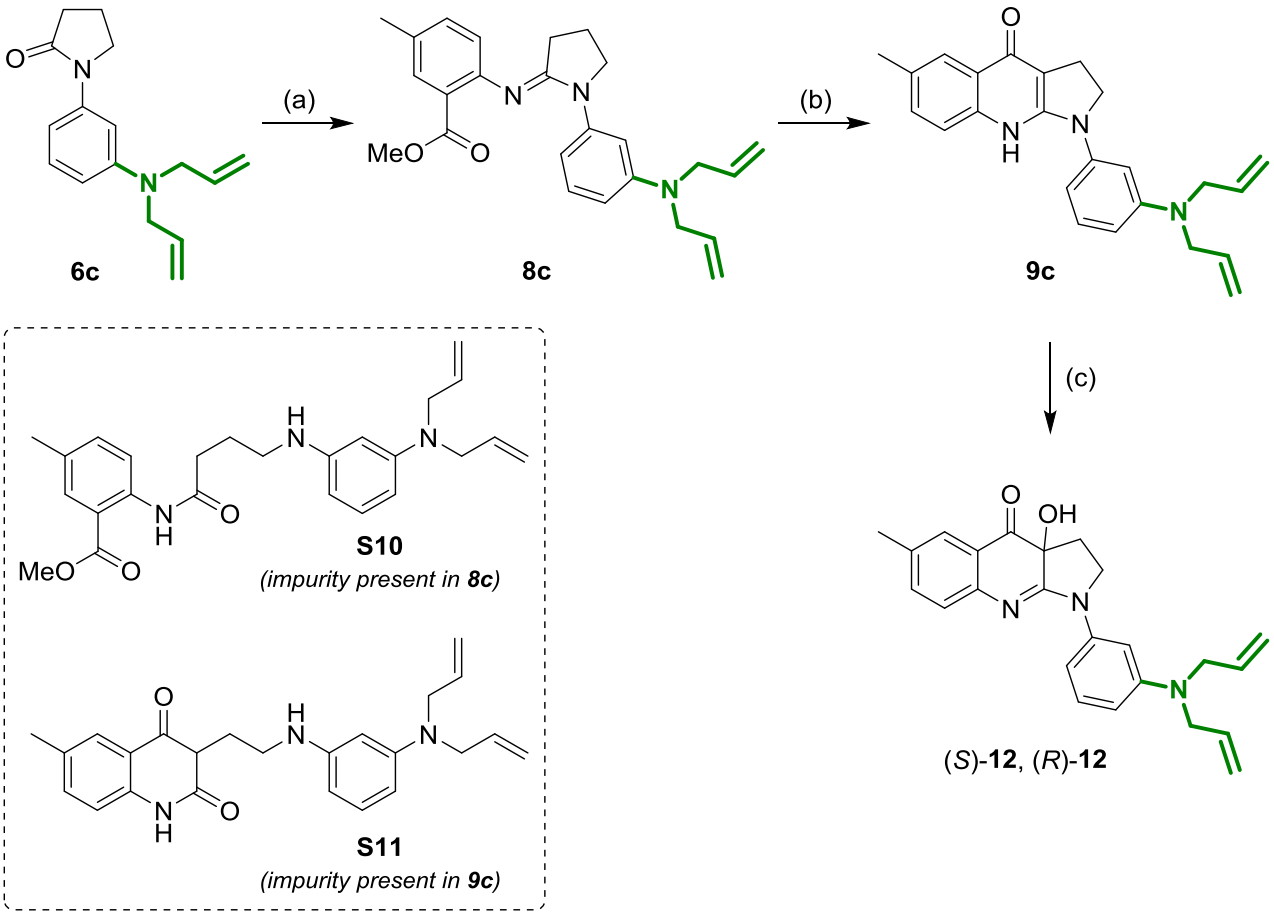

(a) i) 2 equiv $POCl_3$, dry CH_2Cl_2, rt, 24 h, N_2; ii) 1.05 equiv **7**, dry CH_2Cl_2, 35 °C, 24 h, N_2
(b) 2.5 equiv LiHMDS, dry THF, 0 °C, 1 h, N_2
(c) i) 1.2 equiv LiHMDS, dry THF, -78 °C, 30 min, Ar;
ii) 2.4 equiv **14** (for (*S*)-**12**) or **15** (for (*R*)-**12**), dry THF, -15 °C, 16 h, Ar

Amidine **8c** was obtained from pyrrolidinone **6c** (24.6 g, 96.0 mmol, 1 equiv) and methyl 2-amino-5-methylbenzoate (**7**) (16.7 g, 101 mmol, 1.05 equiv) *via* the general procedure for the synthesis of amidines from pyrrolidinones. During aqueous work-up, part of the amidine **8c** was converted into side product **S10** due to hydrolysis of the amidine functionality. Evaporation *in vacuo* afforded a red-brown oil (39.0 g) of which 6.50 g was dissolved in acetonitrile/dichloromethane (1:1) and coated under reduced pressure onto 13.0 g of Davisil® C18 silica. Subsequently, purification was performed *via* automated flash chromatography with water/acetonitrile as eluent on a Reveleris® 120 g C18 cartridge (5% sample loading; flow rate: 80 mL min^{-1}; eluent: 2 CV of 40% acetonitrile, a gradient from 40% to 80% acetonitrile over 20 CV, 4 CV of 80% acetonitrile and finally 3 CV of 100% acetonitrile; detection wavelengths: 256 nm and 330 nm). Next, the same conditions were repeated another 5 times to purify the remaining parts of the crude mixture. Coevaporation of the combined fractions with chloroform, to remove traces of water, resulted in crude amidine **8c** as a red-brown oil (11.9 g) that still contained side product **S10** as impurity.

Quinolone **9c** was synthesized from the crude amidine **8c** (8.69 g, 21.5 mmol, 1 equiv) *via* the general procedure for the synthesis of quinolones from amidines. Evaporation *in vacuo* resulted in a red oil (8.83 g) which was dissolved in tetrahydrofuran and coated under reduced pressure onto 26.5 g of silica. Subsequently, purification was performed *via* automated flash chromatography with hexane/ethyl acetate/methanol as eluent on a Reveleris® 80 g silica cartridge (11% sample loading; flow rate: 60 mL min^{-1}; eluent: 2 CV of 50% ethyl acetate, a gradient from 50% to 100% ethyl acetate over 10 CV, 5 CV of 100% ethyl acetate and finally 25 CV of a 10% methanol/90% ethyl acetate; detection wavelengths: 256 nm and 334 nm). Evaporation resulted in crude quinolone **9c** as an orange oil (4.97 g) that still contained side product **S11** (formed out of side product **S10** during reaction) as impurity.

Synthesis of (S)-3'-diallylaminoblebbistatin (S)-12

(*S*)-3'-diallylaminoblebbistatin (*S*)-**12** was synthesized from the crude quinolone **9c** (3.96 g, 10.7 mmol, 1 equiv) *via* the general procedure for the asymmetric *α*-hydroxylation of quinolones and using Davis' oxaziridine **14** (7.64 g, 25.6 mmol, 2.4 equiv). Evaporation *in vacuo* resulted in (*S*)-**12** (3.02 g, 73%) as an orange powder. The enantiomeric excess was 76% as determined by chiral HPLC analysis (Daicel Chiralpak IA column, acetonitrile/water (45:55), 1.0 mL min^{-1}, 25 °C). The powder was redissolved in 60 mL of boiling absolute ethanol and left untouched for 1 hour at room temperature. After 40 minutes fibers had formed, which were filtered off after an additional 20 minutes. This resulted in (*S*)-3'-diallylaminoblebbistatin (*S*)-**12** (1.03 g, 25%) as bright orange cotton-like fibers with an enantiomeric excess of >99%.

(*S*)-1-(3-(diallylamino)phenyl)-3a-hydroxy-6-methyl-1,2,3,3a-tetrahydro-4*H*-pyrrolo[2,3-*b*]quinolin-4-one ((*S*)-12)

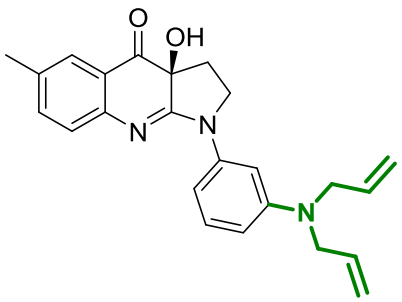

Yield = 25%. Bright orange, cotton-like fibers (from absolute ethanol, mp 167 °C). **ee** >99%, chiral HPLC: t_R ((*S*)-**11**) = 27.1 min, t_R ((*R*)-**11**) = 31.1 min (Daicel Chiralpak IA column, acetonitrile/water (45:55), 1.0 mL min^{-1}, 25 °C). $[\alpha]^{25}_D$ = −248 ± 2 (*c* = 0.11 in tetrahydrofuran). **^{1}H NMR** (400 MHz, DMSO-d_6): δ = 2.19–2.27 (m, 2H), 2.30 (s, 3H), 3.87–3.95 (m, 1H), 3.94–4.07 (m, 5H), 3.12–5.24 (m, 4H), 5.92 (ddt, *J* = 17.1, 10.2, 5.1 Hz, 2H), 6.47 (dd, *J* = 8.1, 2.0 Hz, 1H), 6.79 (s, 1H), 6.98 (dd, *J* = 8.1, 2.0 Hz, 1H), 7.07 (d, *J* = 8.1 Hz, 1H), 7.15 (t, *J* = 8.1 Hz, 1H), 7.38 (dd, *J* = 8.1, 1.8 Hz, 1H), 7.52 (d, *J* = 1.8 Hz, 1H), 7.94 (t, *J* = 2.0 Hz, 1H). **^{13}C NMR** (100.6 MHz, DMSO-d_6): δ = 20.7, 28.8, 47.9, 53.0, 73.5, 104.8, 107.4, 108.3, 116.4, 121.4, 126.2, 126.8, 129.4, 132.5, 134.8, 137.0, 141.9, 148.9, 149.8, 165.7, 195.1. **MS** (ESI): *m/z* (%) = 387.5 ($[M+H]^+$, 100). **HRMS** (ESI): calculated for $C_{24}H_{26}N_3O_2$ ($[M+H]^+$) 388.2020; found 388.2035. **MW** = 387.47. ^{1}H NMR spectrum, ^{13}C NMR spectrum and chiral HPLC chromatograms are provided in Figures S35–S36 and Figures S57–S58.

Synthesis of (R)-3'-diallylaminoblebbistatin (R)-12

(*R*)-3'-diallylaminoblebbistatin (*R*)-**12** was synthesized from the crude quinolone **9c** (0.967 g, 2.60 mmol, 1 equiv) *via* the general procedure for the asymmetric *α*-hydroxylation of quinolones and using Davis' oxaziridine **15** (1.86 g, 6.24 mmol, 2.4 equiv). Evaporation *in vacuo* resulted in (*R*)-3'-diallylaminoblebbistatin (*R*)-**12** (0.686 g, 68%) as an orange powder. The enantiomeric excess was 74% as determined by chiral HPLC analysis (Daicel Chiralpak IA column, acetonitrile/water (45:55), 1.0 mL min^{-1}, 25 °C). The powder was redissolved in 15 mL of boiling absolute ethanol and left untouched for 50 minutes at room temperature. After 30 minutes fibers had formed, which were filtered off after an additional 20 minutes. This resulted in (*R*)-3'-diallylaminoblebbistatin (*R*)-**12** (0.160 g, 16%) as bright orange cotton-like fibers with an enantiomeric excess of 98%.

(*R*)-1-(3-(diallyl-amino)phenyl)-3a-hydroxy-6-methyl-1,2,3,3a-tetrahydro-4*H*-pyrrolo[2,3-*b*]quinolin-4 one ((*R*)-12)

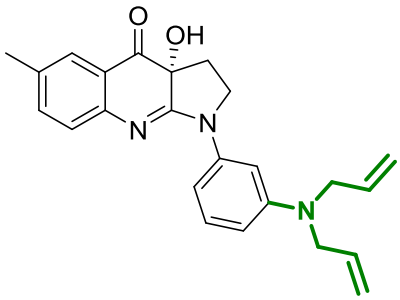

Yield = 16%. Bright orange cotton-like fibers (from absolute ethanol, mp 167 °C). **ee** 98%, chiral HPLC: t_R ((*R*)-**11**) = 31.1 min, t_R ((*S*)-**11**) = 27.7 min (Daicel Chiralpak IA column, acetonitrile/water (45:55), 1.0 mL min^{-1}, 25 °C). $[\alpha]^{25}_D$ = +327 ± 3 (*c* = 0.18 in tetrahydrofuran). **^{1}H NMR** (400 MHz, DMSO-d_6): δ = 2.19–2.27 (m, 2H), 2.30 (s, 3H), 3.87–3.95 (m, 1H), 3.94–4.07 (m, 5H), 3.12–5.24 (m, 4H), 5.92 (ddt, *J* = 17.1, 10.2, 5.1 Hz, 2H), 6.47 (dd, *J* = 8.1, 2.0 Hz, 1H), 6.79 (s, 1H), 6.98 (dd, *J* = 8.1, 2.0 Hz, 1H), 7.07 (d, *J* = 8.1 Hz, 1H), 7.15 (t, *J* = 8.1 Hz, 1H), 7.38 (dd, *J* = 8.1, 1.8 Hz, 1H), 7.52 (d, *J* = 1.8 Hz, 1H), 7.94 (t, *J* = 2.0 Hz, 1H). **^{13}C NMR** (100.6 MHz, DMSO-d_6): δ = 20.7, 28.8, 47.9, 53.0, 73.5, 104.8, 107.4, 108.3, 116.4, 121.4, 126.2, 126.8, 129.4, 132.5, 134.8, 137.0, 141.9, 148.9, 149.8, 165.7, 195.1. **MS** (ESI): *m/z* (%) = 387.5 ($[M+H]^+$, 100). **HRMS** (ESI): calculated for $C_{24}H_{26}N_3O_2$ ($[M+H]^+$) 388.2020; found 388.2023. **MW** = 387.47. Chiral HPLC chromatogram is provided in Figure S59.

1.12. Synthesis of diazomethane (CH_2N_2)

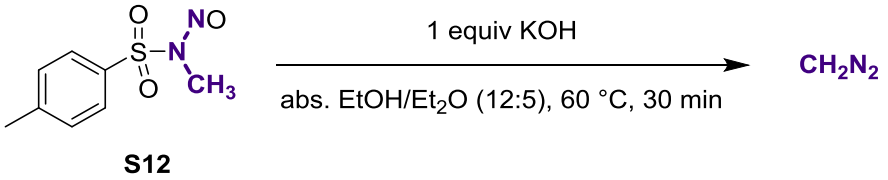

S12

CAUTION! Diazomethane is a toxic and explosive compound! When dealing with diazomethane, the experimenter should first thoroughly study the literature on the properties and safe generation and handling of this hazardous reagent![16,17] **The synthesis must be carried out in a properly working hood using dedicated and thoroughly inspected equipment! Do not use sharp-edged glassware or ground joints!**

A 250 mL distilling flask was fitted with a condenser set for distillation and with a dropping funnel by means of special cork stoppers. The condenser was connected to an L-shaped glass tube which in his turn was connected to an ice-cooled 250 mL Büchner flask by means of special cork stoppers. Pressure build-up has to be avoided by means of an opening to the environment.

A solution of 2.14 g of *N*-methyl-*N*-nitroso-*para*-toluenesulfonamide (**S12**) (10.0 mmol, 1 equiv) in 25 mL of diethyl ether was added to the distilling flask which was cooled to 0 °C. A solution of 0.561 g of KOH (10.0 mmol, 1 equiv) in 60 mL of absolute ethanol was added dropwise by means of an addition funnel (without mechanical stirring!). After complete addition, a solution of diazomethane in diethyl ether was distilled off by heating the reaction mixture to 60 °C for about 30 minutes, using a warm **(but CERTAINLY BELOW 70 °C)** water bath. **CAUTION! At no time the water should boil! Never use other means of heating! Diazomethane may explode at 100 °C!** During distillation, diethyl ether was added *via* the dropping funnel until the distillate turned colorless. The yellow distillate, a dilute solution of diazomethane in diethyl ether, was collected in a Büchner flask cooled to 0 °C. **CAUTION! Explosion hazard! The solution should be dilute!**

2. X-ray christallographic data

For the reported structures, X-ray intensity data were collected, at 100 K, on an Agilent Supernova Dual Source (Cu at zero) diffractometer equipped with an Atlas CCD detector using ω scans and CuKα (λ = 1.54184 Å) radiation. The images were interpreted and integrated with the program CrysAlisPro (Rigaku Oxford Diffraction).[18] Using Olex2,[19] the structures were solved by direct methods using the ShelXS structure solution program and refined by full-matrix least-squares on F^2 using the ShelXL program package.[20] Non-hydrogen atoms were anisotropically refined and the hydrogen atoms in the riding mode and isotropic temperature factors fixed at 1.2 times U(eq) of the parent atoms (1.5 times U(eq) for methyl and hydroxyl groups).

CCDC 1485738 and 1485739 contain the supplementary crystallographic data for this paper and can be obtained free of charge *via* www.ccdc.cam.ac.uk/conts/retrieving.html (or from the Cambridge Crystallographic Data Centre, 12, Union Road, Cambridge CB2 1EZ, UK; fax: +44-1223-336033; or deposit@ccdc.cam.ac.uk).

2.1. X-ray christallographic data of (*S*)-2

*Crystal data for compound (S)-**2***. $C_{18}H_{16}N_2O_3$, M = 308.33, orthorhombic, space group $P2_12_12_1$ (No. 19), a = 4.87924(5) Å, b = 14.43858(15) Å, c = 20.3657(2) Å, V = 1434.75(3) $Å^3$, Z = 4, T = 100 K, ρ_{calc} = 1.427 g cm^{-3}, μ(Cu-Kα) = 0.805 mm^{-1}, F(000) = 648, 63297 reflections measured, 2948 unique (R_{int} = 0.1028) which were used in all calculations. The final $R1$ was 0.0477 ($I > 2\sigma(I)$) and $wR2$ was 0.1282 (all data).

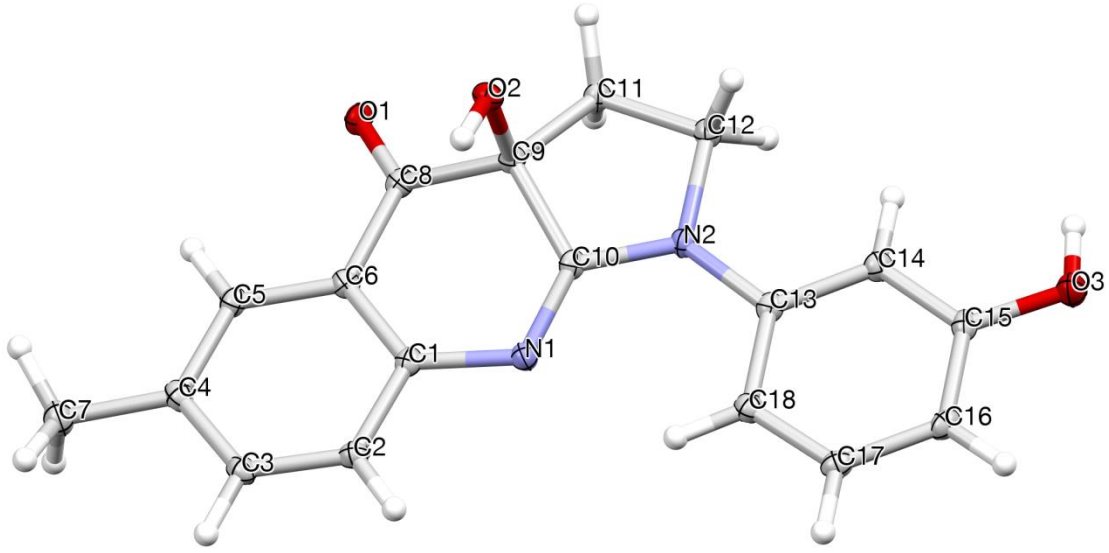

Figure S1. Molecular structure of compound (*S*)-**2**, showing thermal displacement ellipsoids at the 50% probability level and atom labeling scheme of the non-hydrogen atoms.

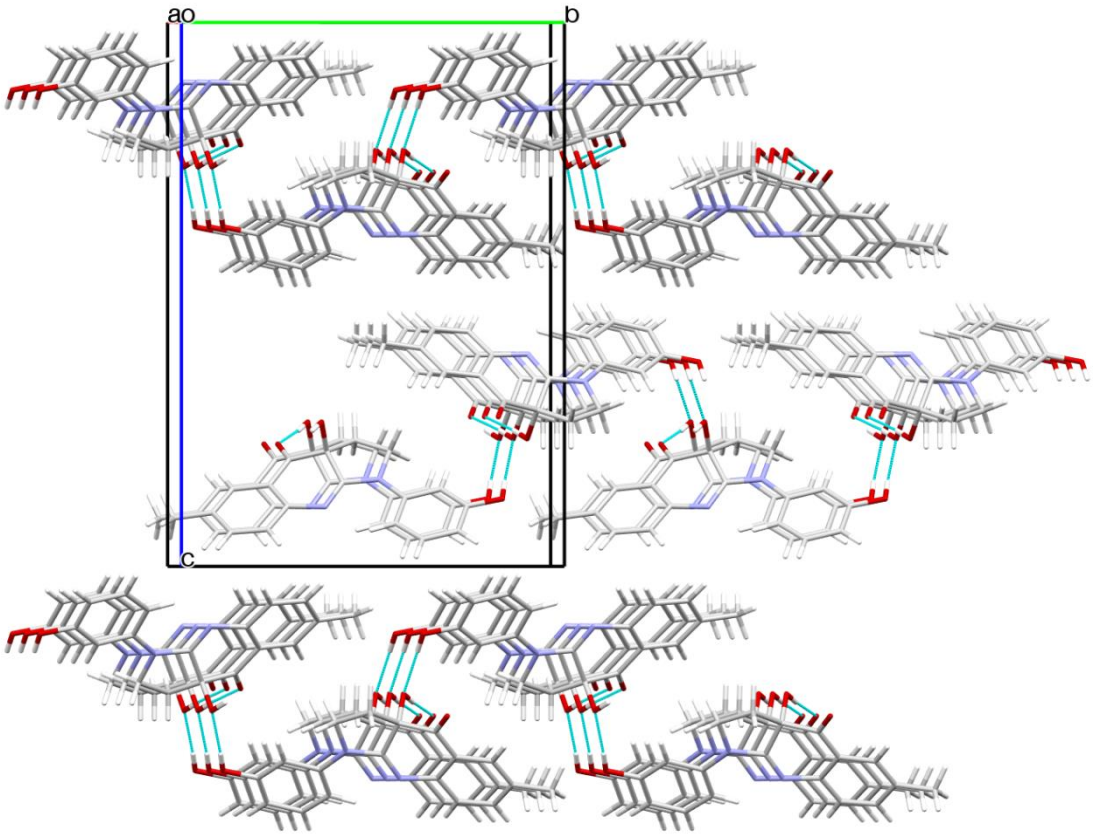

Figure S2. Packing in the crystal structure of compound (*S*)-**2**, along the a-axis. Hydrogen bonds, formed between the hydroxyl groups, are indicated.

2.2. X-ray christallographic data of (*R*)-2

*Crystal data for compound (R)-**2***. $C_{18}H_{16}N_2O_3$, M = 308.33, orthorhombic, space group $P2_12_12_1$ (No. 19), a = 4.88084(6) Å, b = 14.45507(15) Å, c = 20.3743(2) Å, V = 1437.47(3) Å^3, Z = 4, T = 100 K, ρ_{calc} = 1.425 g cm^{-3}, μ(Cu-Kα) = 0.803 mm^{-1}, F(000) = 648, 31031 reflections measured, 49208 unique (R_{int} = 0.1088) which were used in all calculations. The final R1 was 0.0498 ($I > 2\sigma(I)$) and wR2 was 0.0498 (all data).

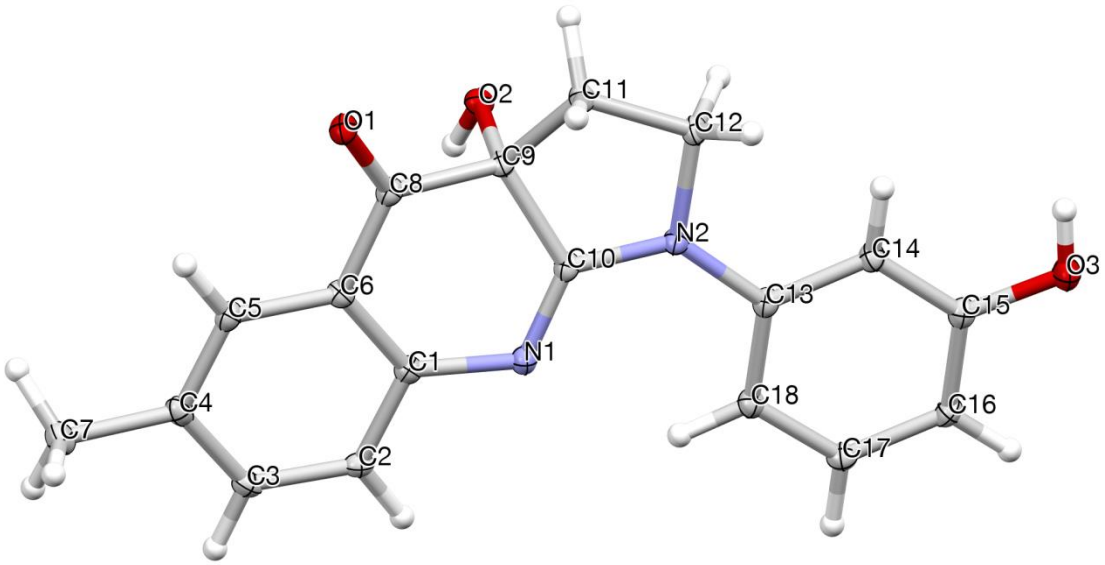

Figure S3. Molecular structure of compound (*R*)-**2**, showing thermal displacement ellipsoids at the 50% probability level and atom labeling scheme of the non-hydrogen atoms.

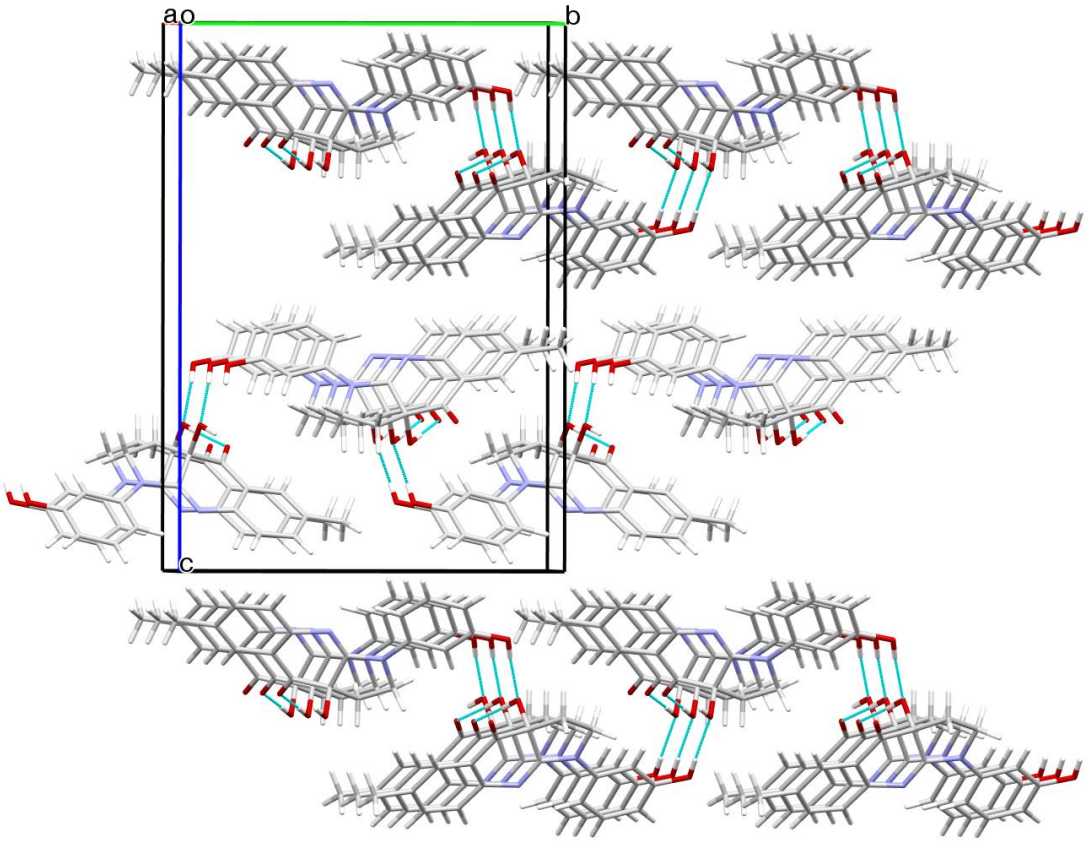

Figure S4. Packing in the crystal structure of compound (*R*)-**2**, along the a-axis. Hydrogen bonds, formed between the hydroxyl groups, are indicated.

3. ^{1}H NMR spectra, ^{13}C NMR spectra and LC-MS chromatograms

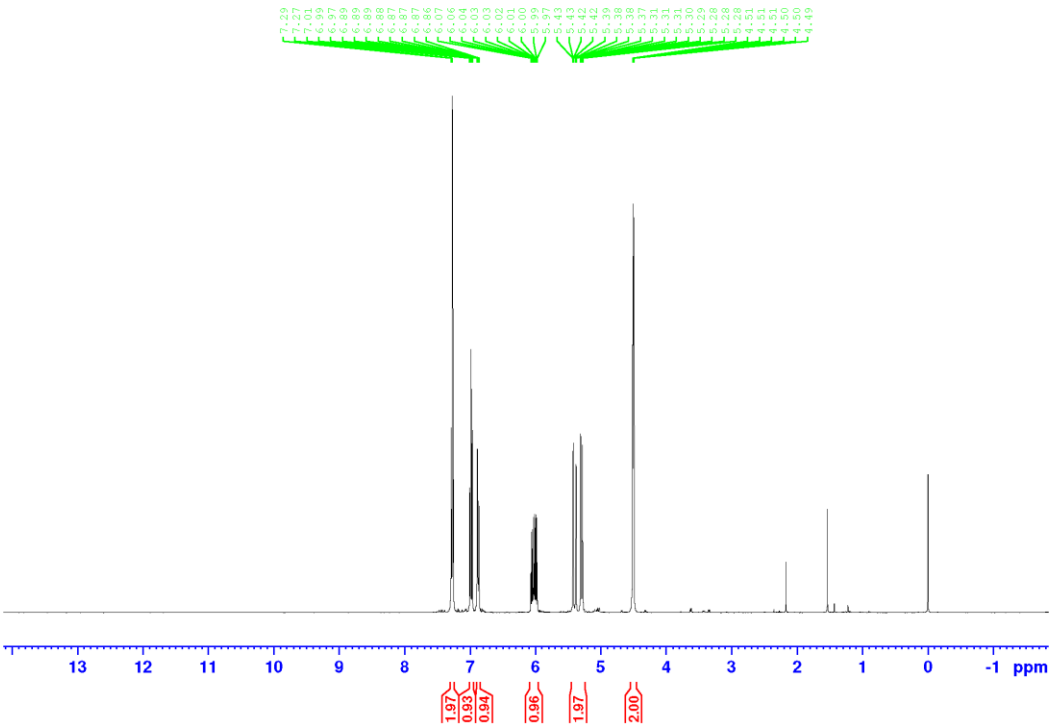

Figure S5. ^{1}H NMR spectrum of **4b**.

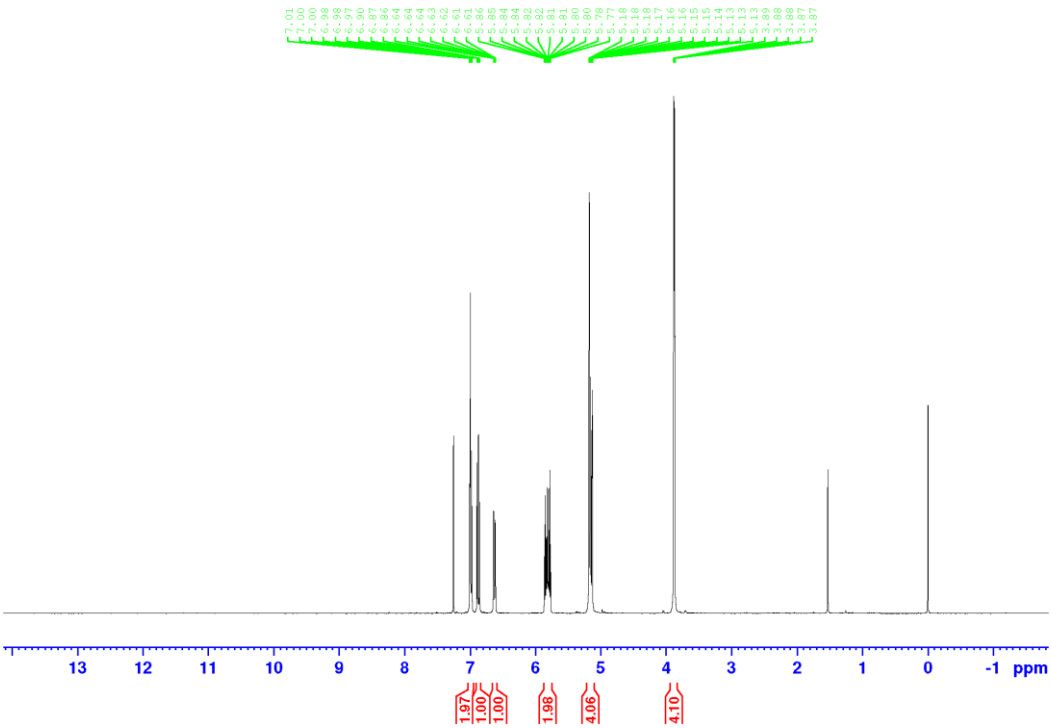

Figure S6. ^{1}H NMR spectrum of **4c**.

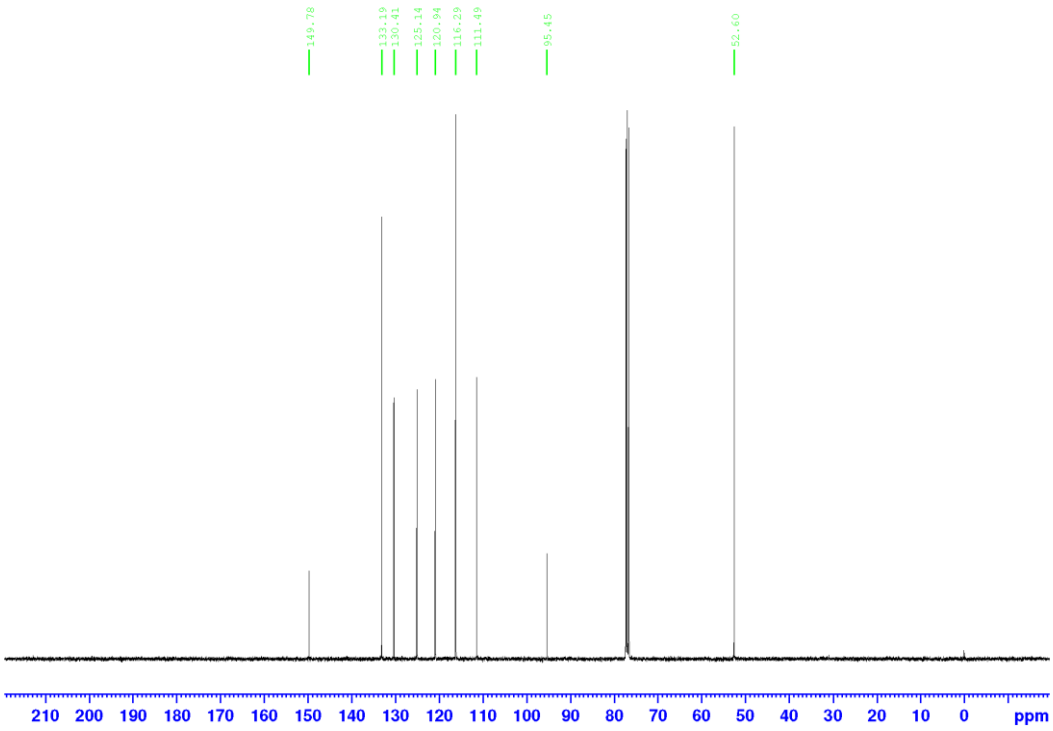

Figure S7. ^{13}C NMR spectrum of **4c**.

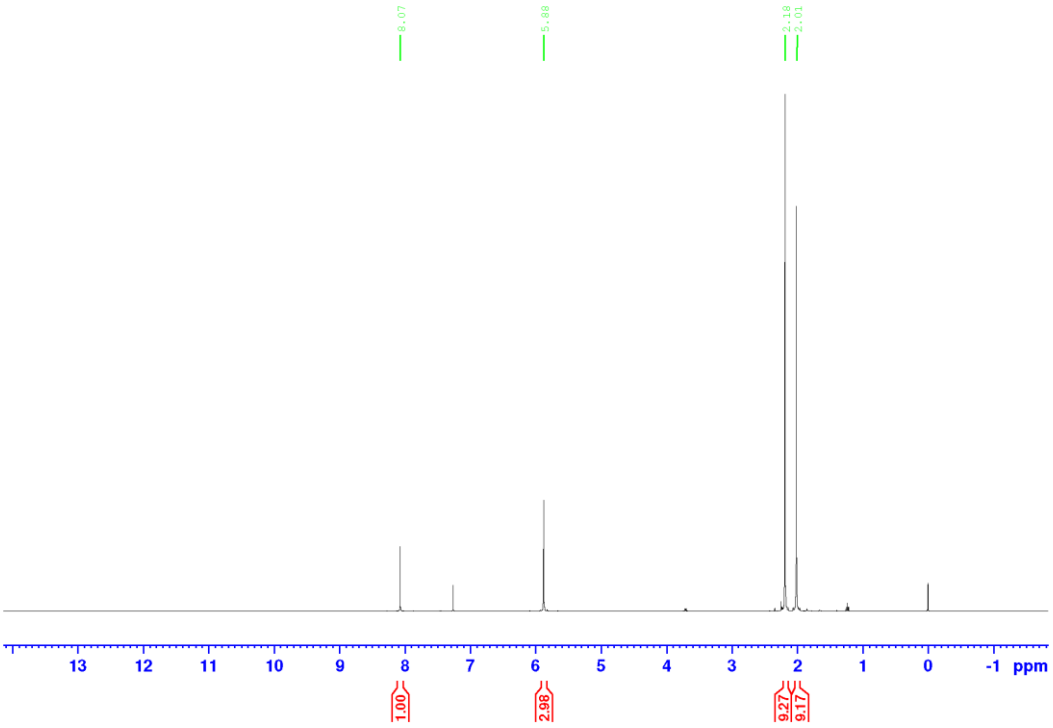

Figure S8. ^{1}H NMR spectrum of **S6**.

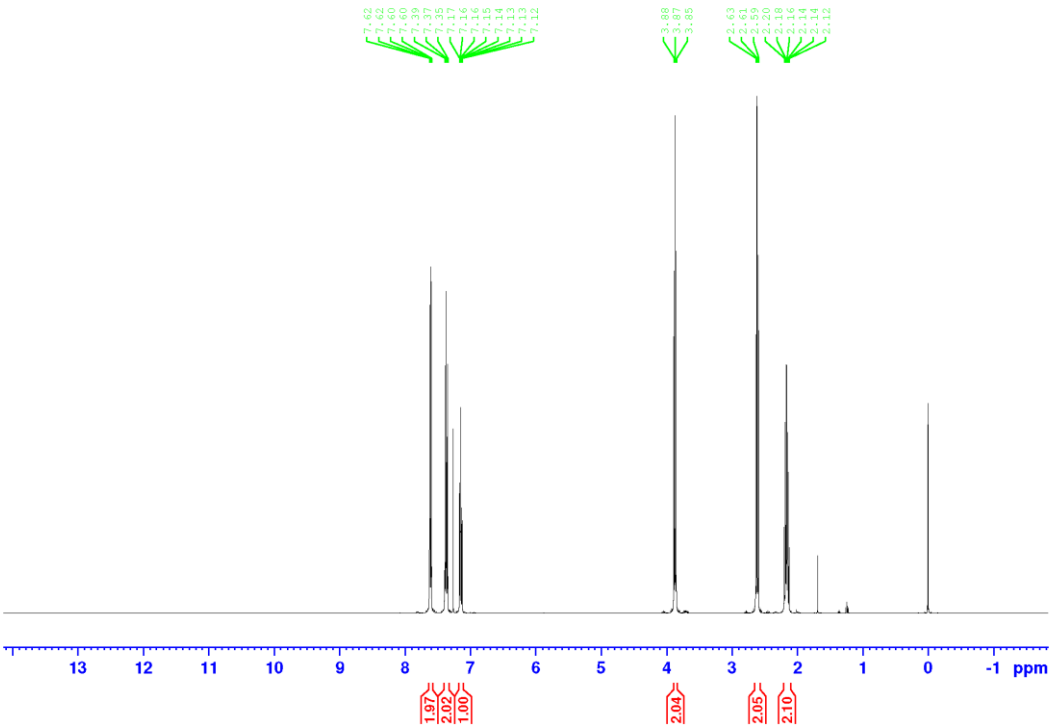

Figure S9. ^{1}H NMR spectrum of **6a**.

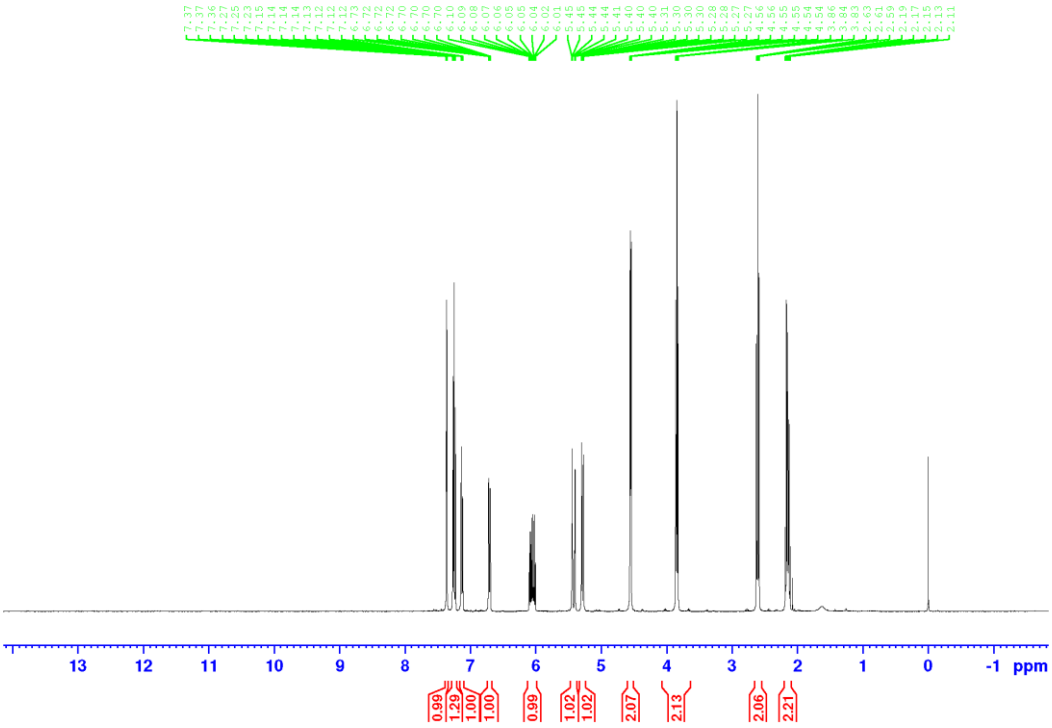

Figure S10. ^{1}H NMR spectrum of **6b**.

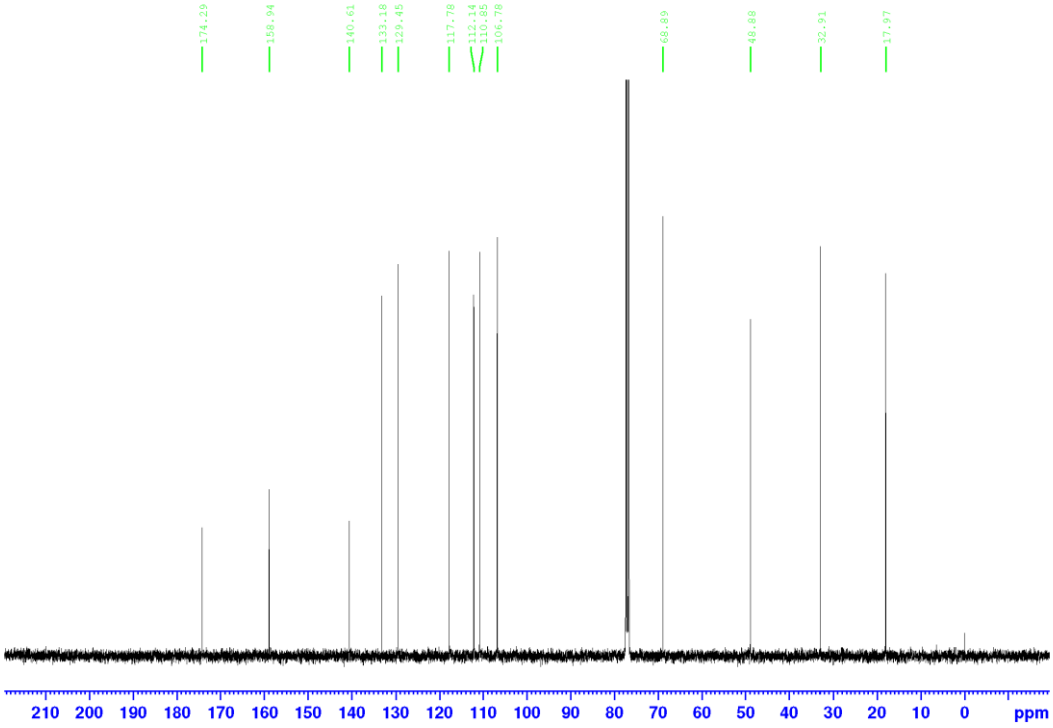

Figure S11. ^{13}C NMR spectrum of **6b**.

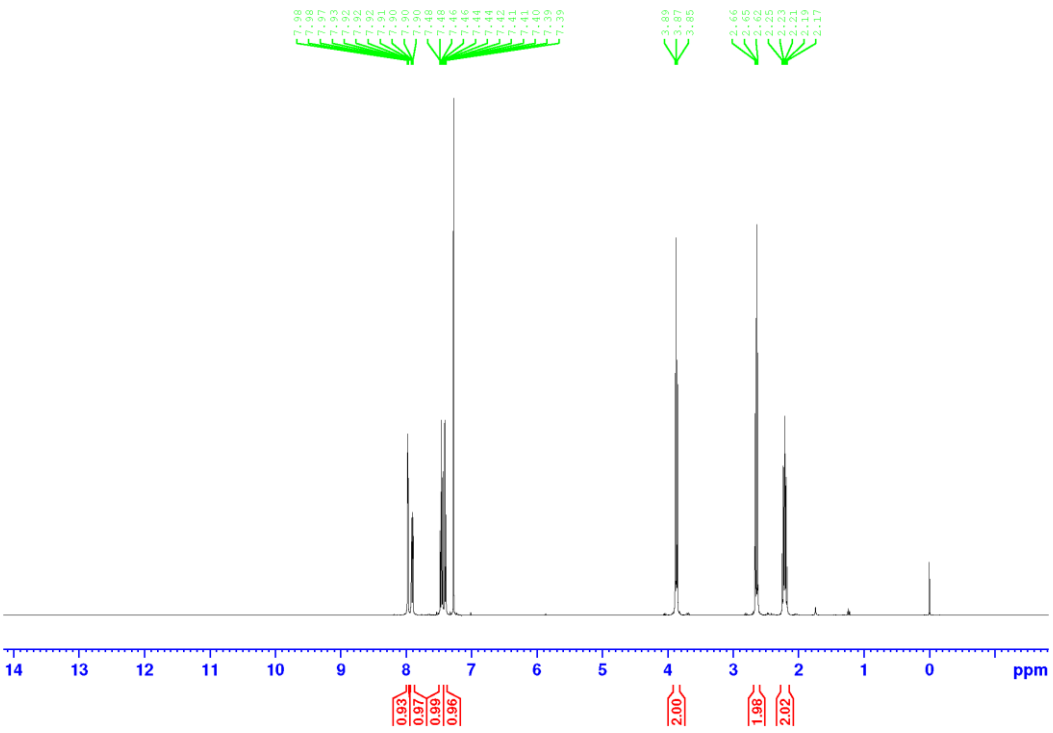

Figure S12. ^{1}H NMR spectrum of **6d**.

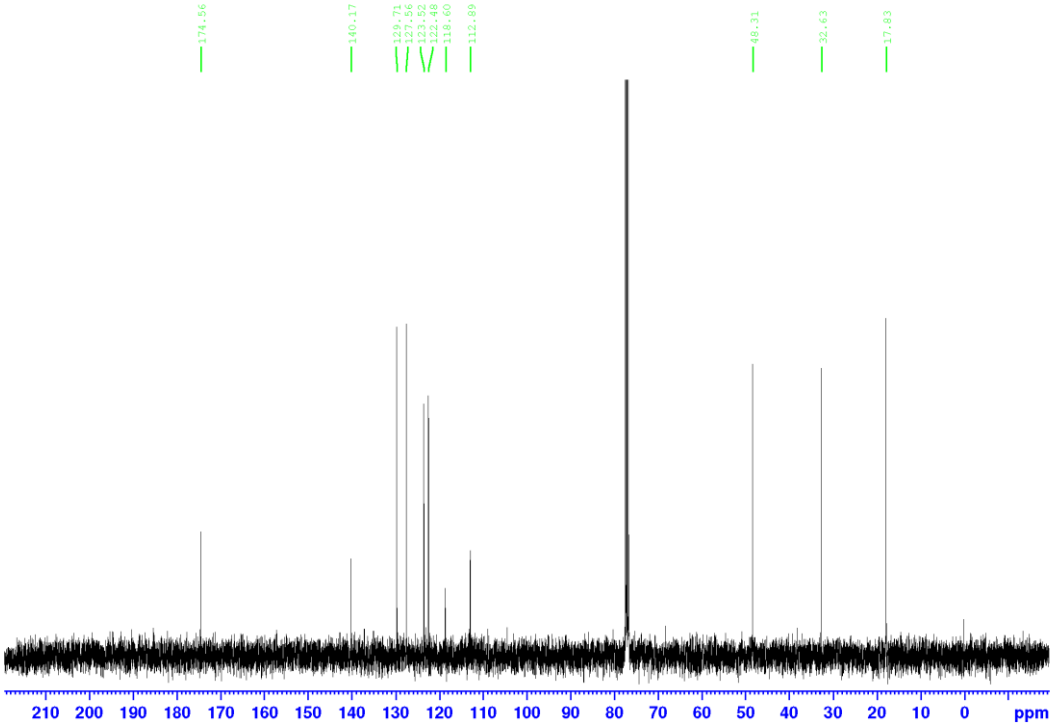

Figure S13. ^{13}C NMR spectrum of **6d**.

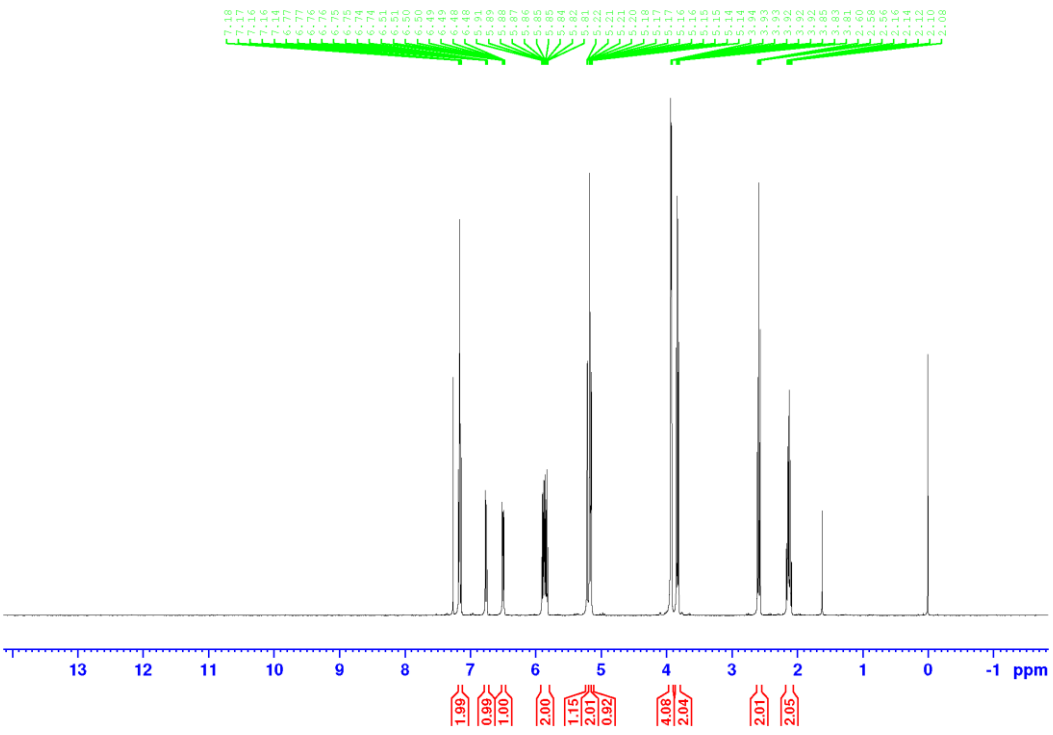

Figure S14. ^{1}H NMR spectrum of **6c**.

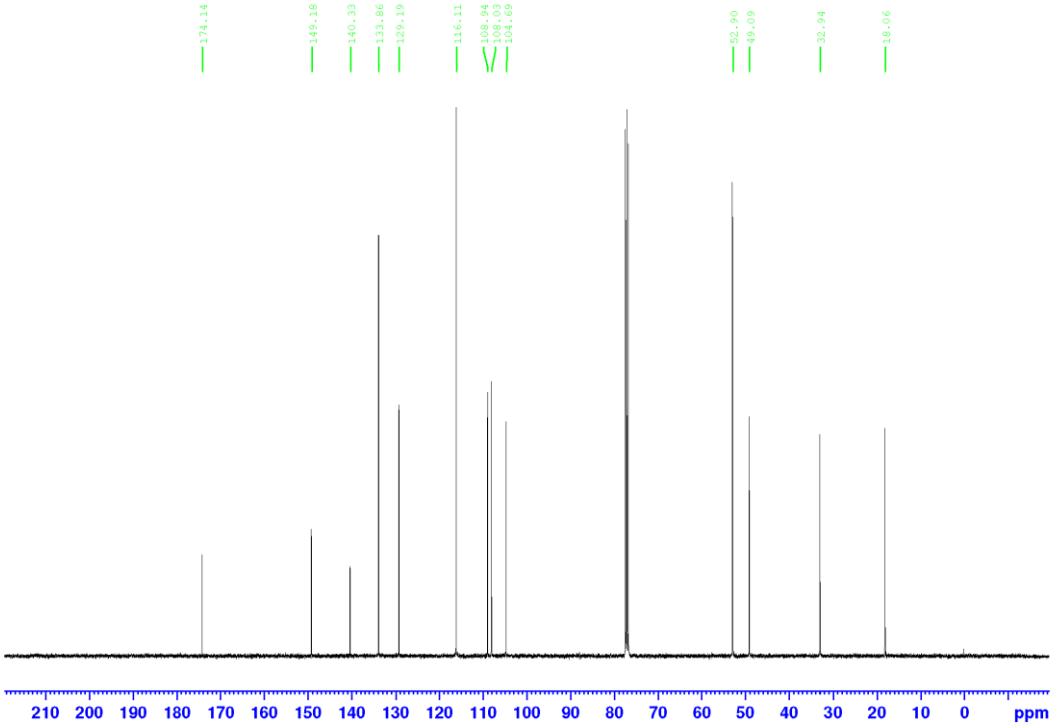

Figure S15. ^{13}C NMR spectrum of **6c**.

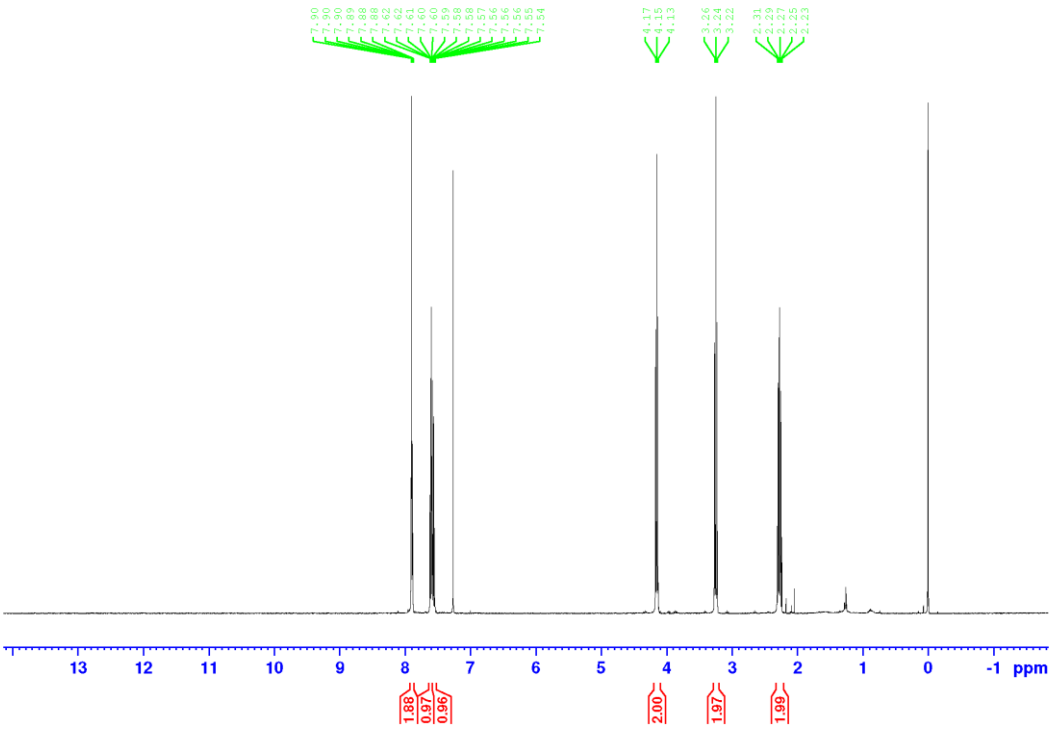

Figure S16. ^{1}H NMR spectrum of **10**.

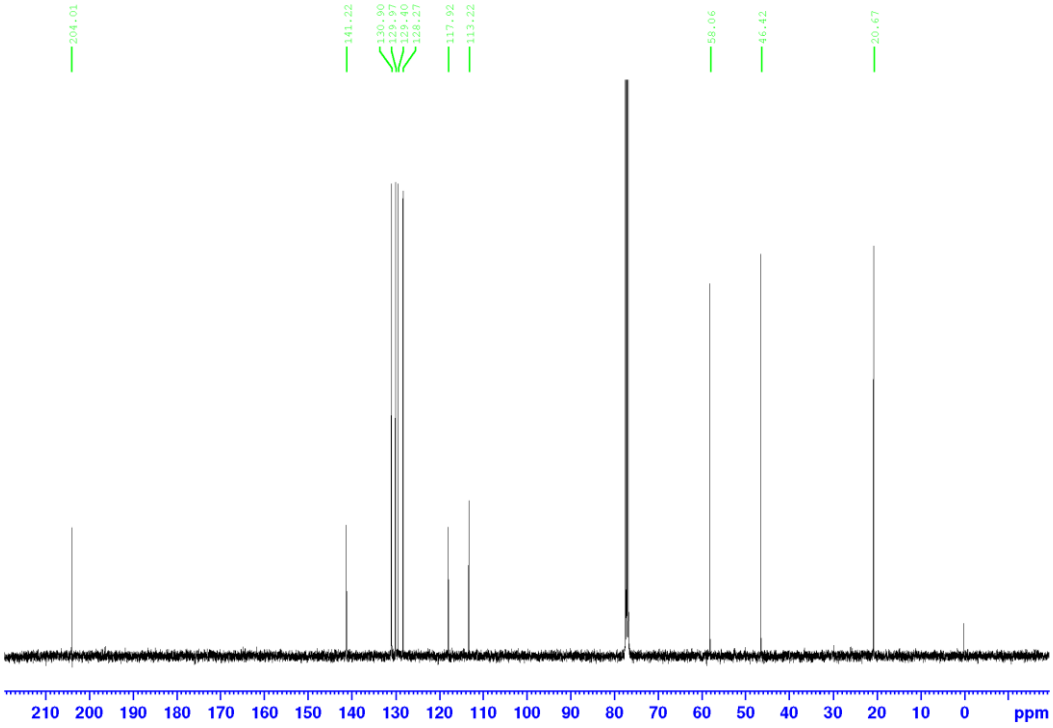

Figure S17. ^{13}C NMR spectrum of **10**.

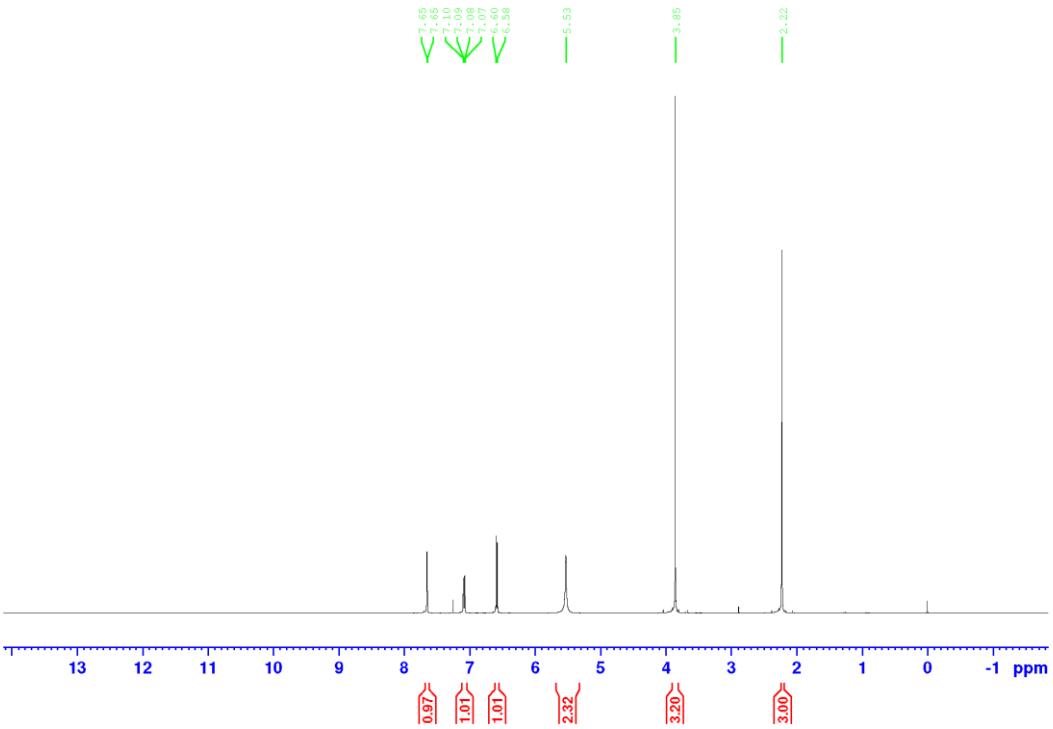

Figure S18. ^{1}H NMR spectrum of **7**.

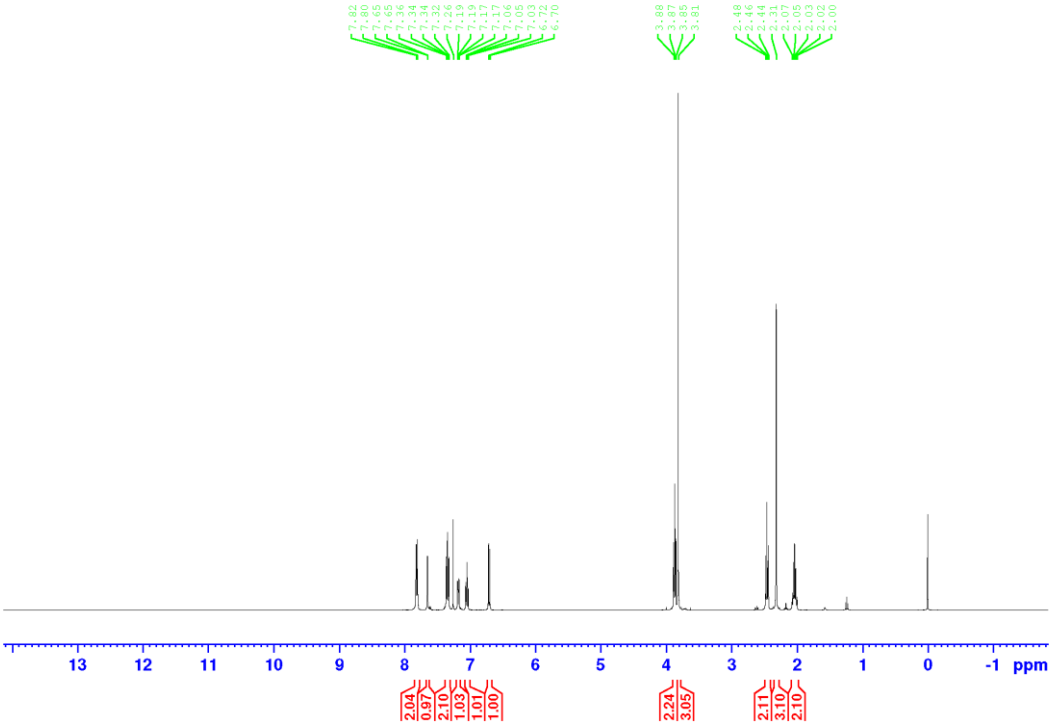

Figure S19. [1]H NMR spectrum of **8a**.

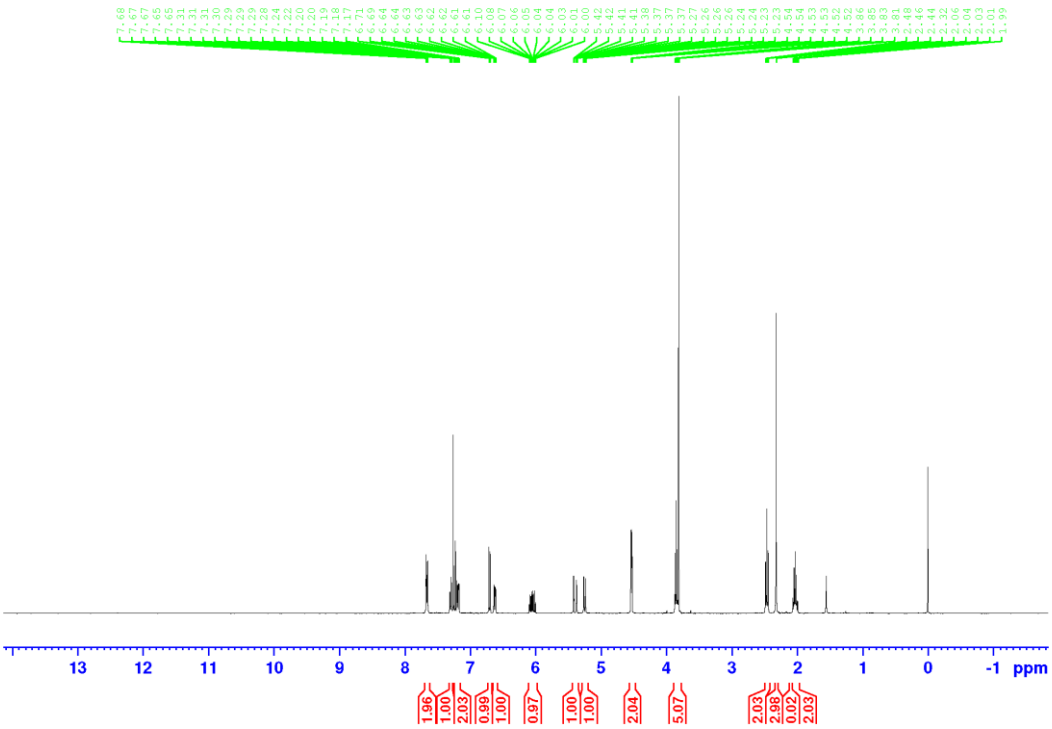

Figure S20. [1]H NMR spectrum of **8b**.

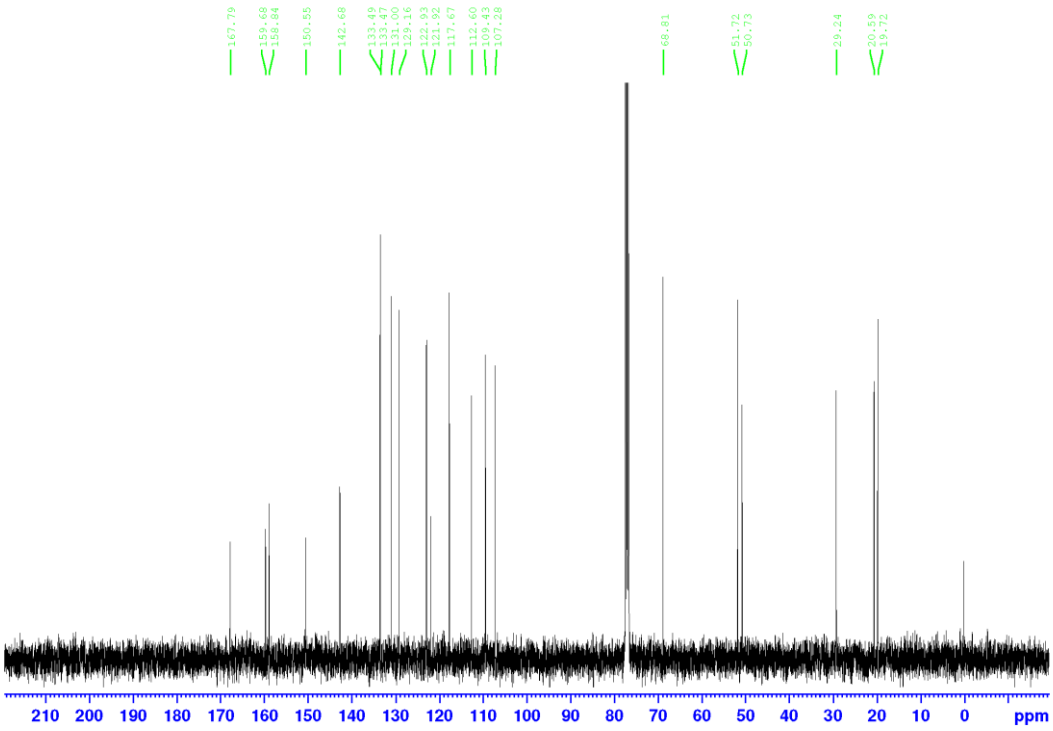

Figure S21. ^{13}C NMR spectrum of **8b**.

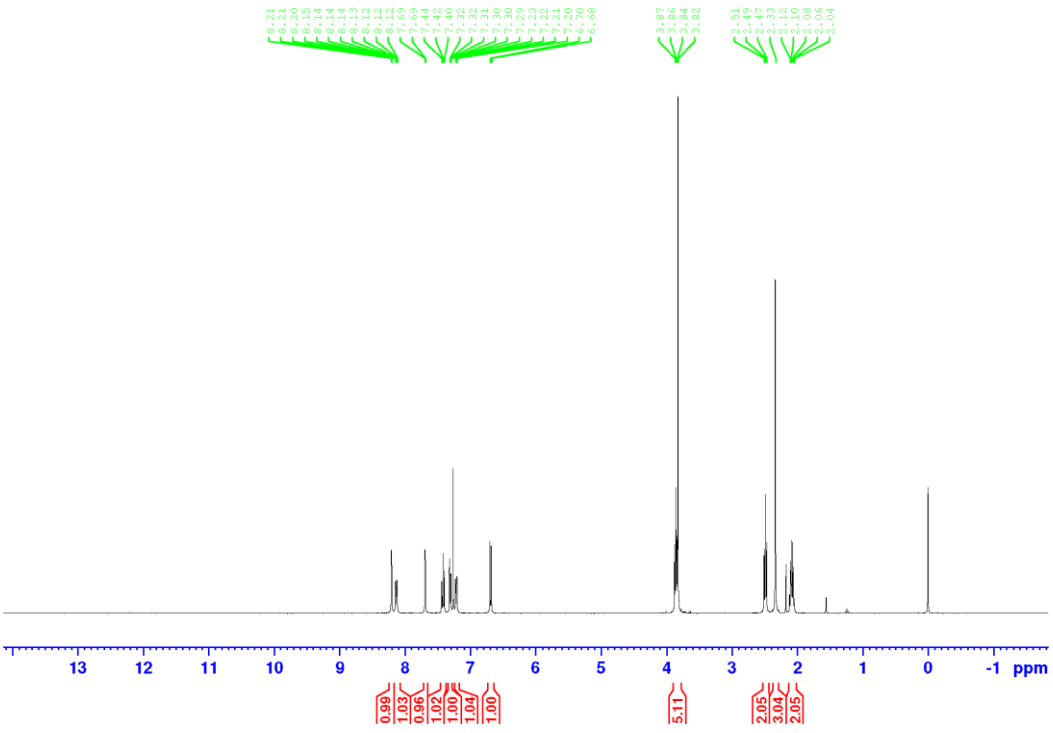

Figure S22. ^{1}H NMR spectrum of **8d**.

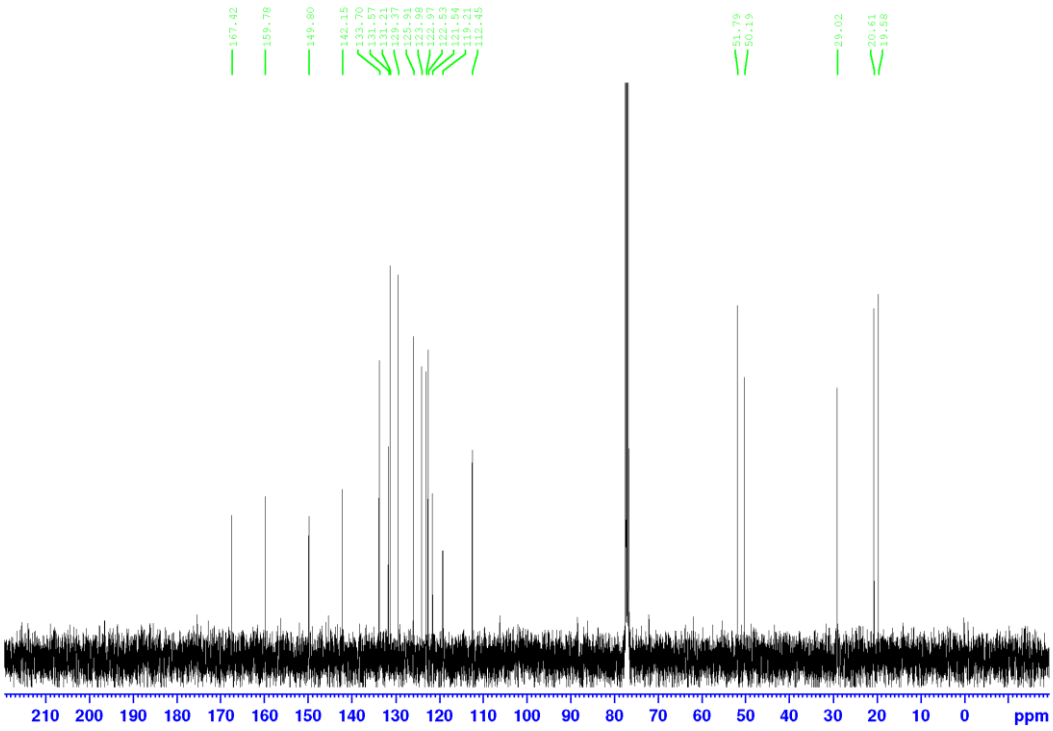

Figure S23. ^{13}C NMR spectrum of **8d**.

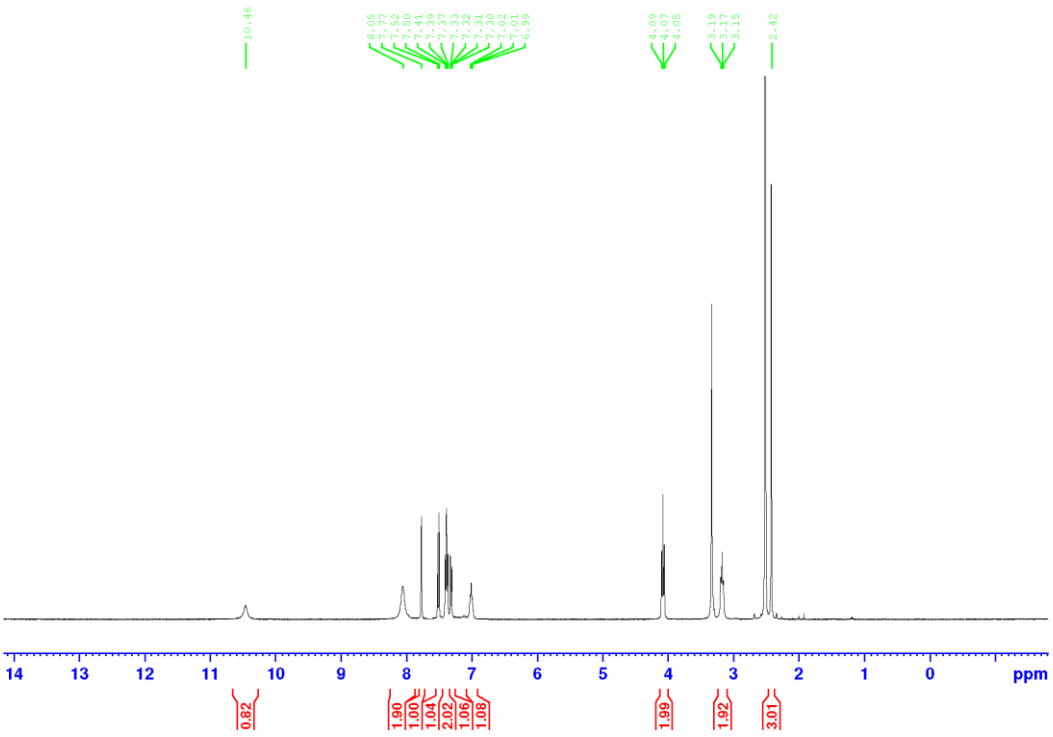

Figure S24. ^{1}H NMR spectrum of **9a**.

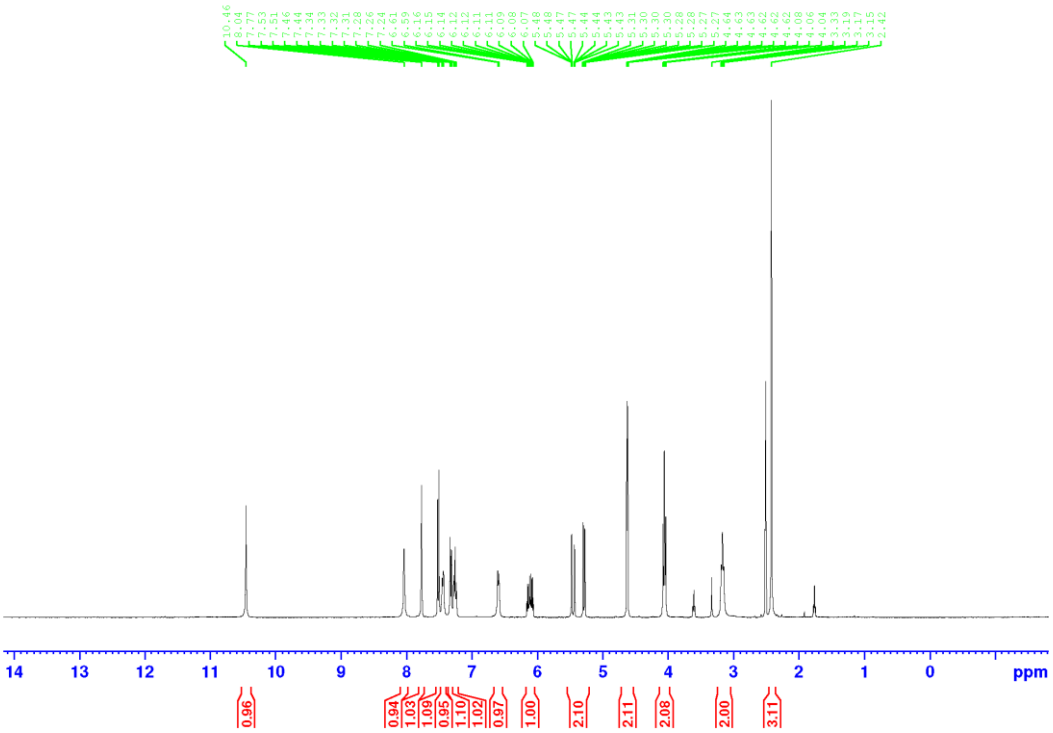

Figure S25. ^{1}H NMR spectrum of **9b**.

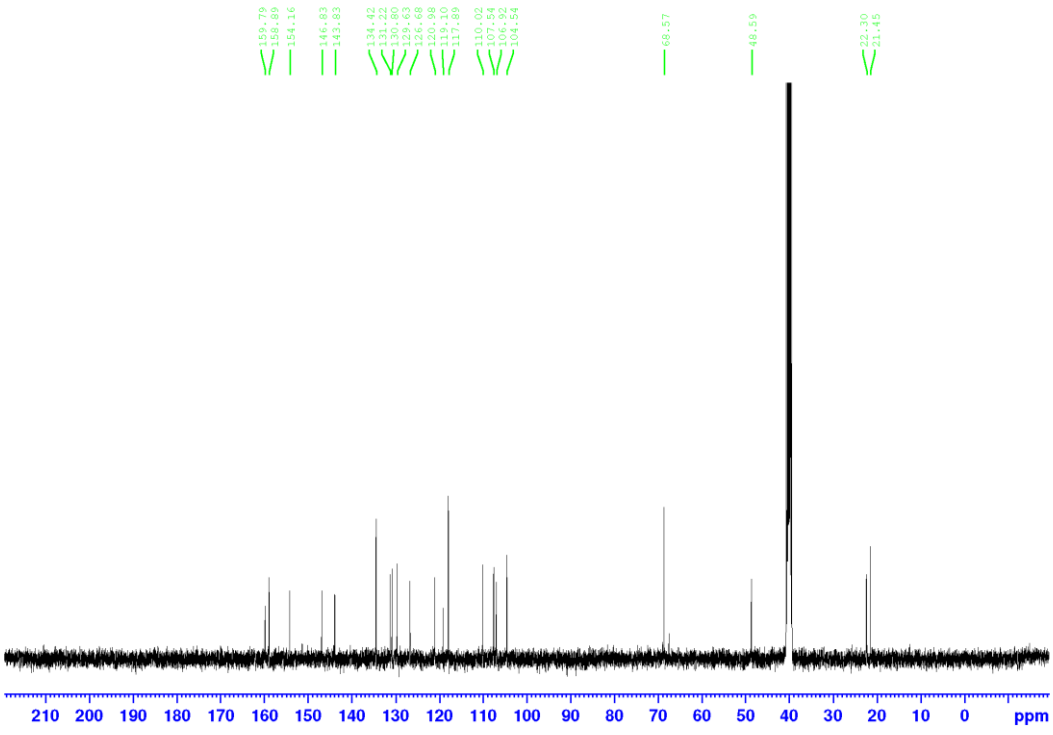

Figure S26. ^{13}C NMR spectrum of **9b**.

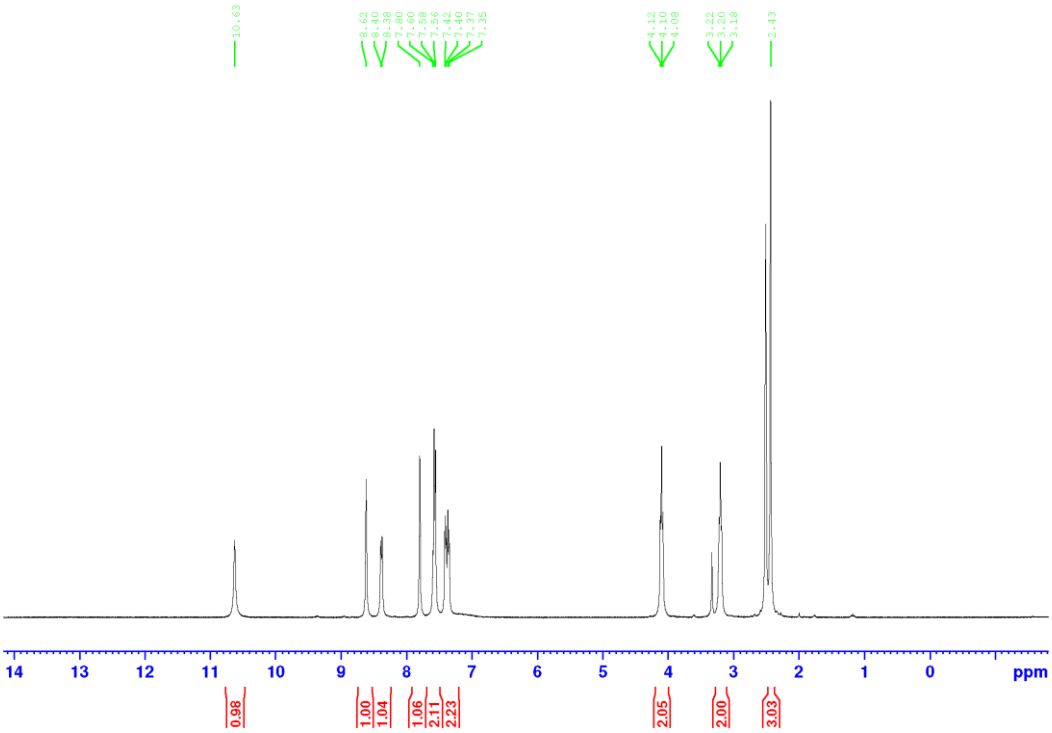

Figure S27. ^{1}H NMR spectrum of **9d**.

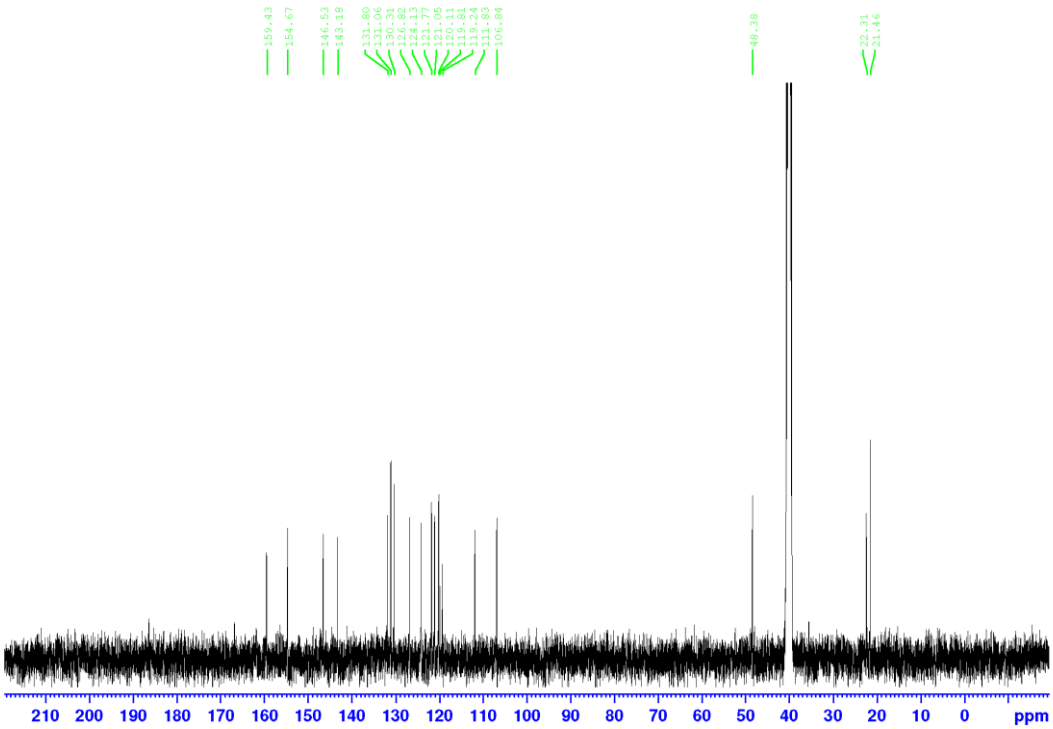

Figure S28. ^{13}C NMR spectrum of **9d**.

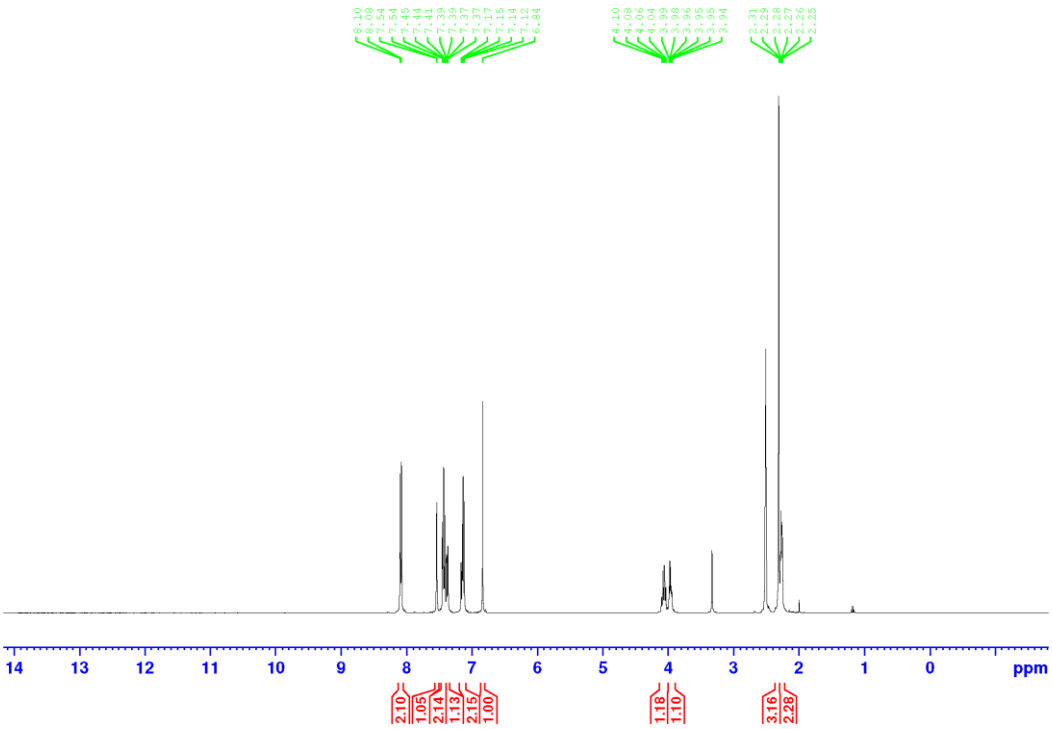

Figure S29. ^{1}H NMR spectrum of (*S*)-**1**.

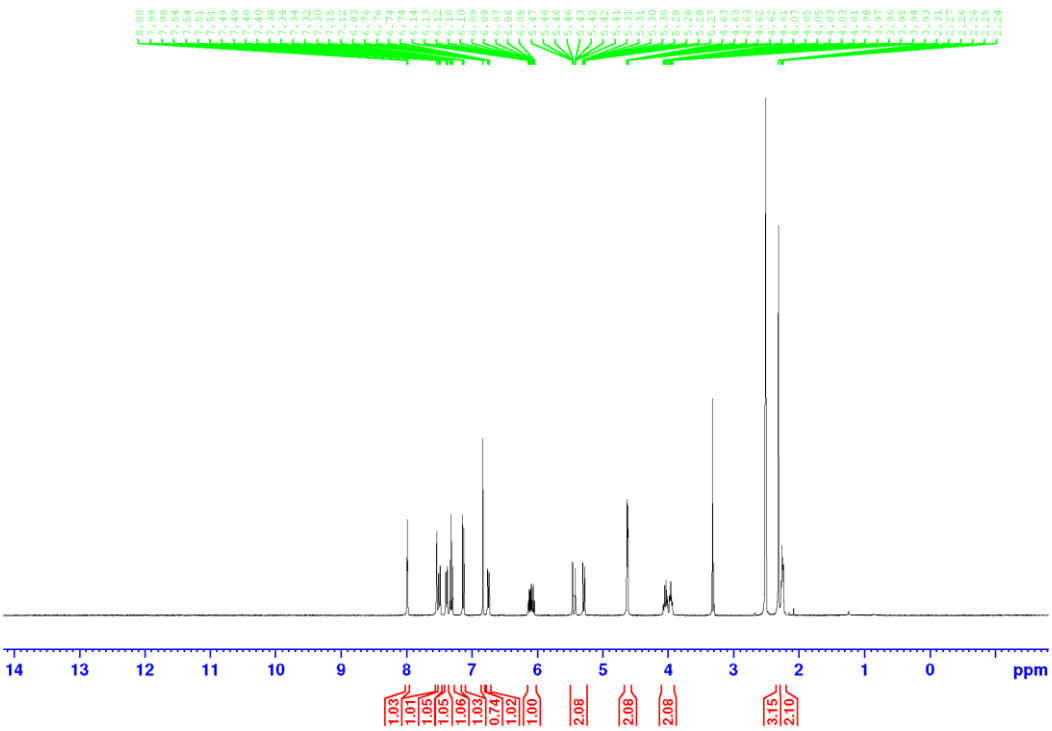

Figure S30. ^{1}H NMR spectrum of (*S*)-**11**.

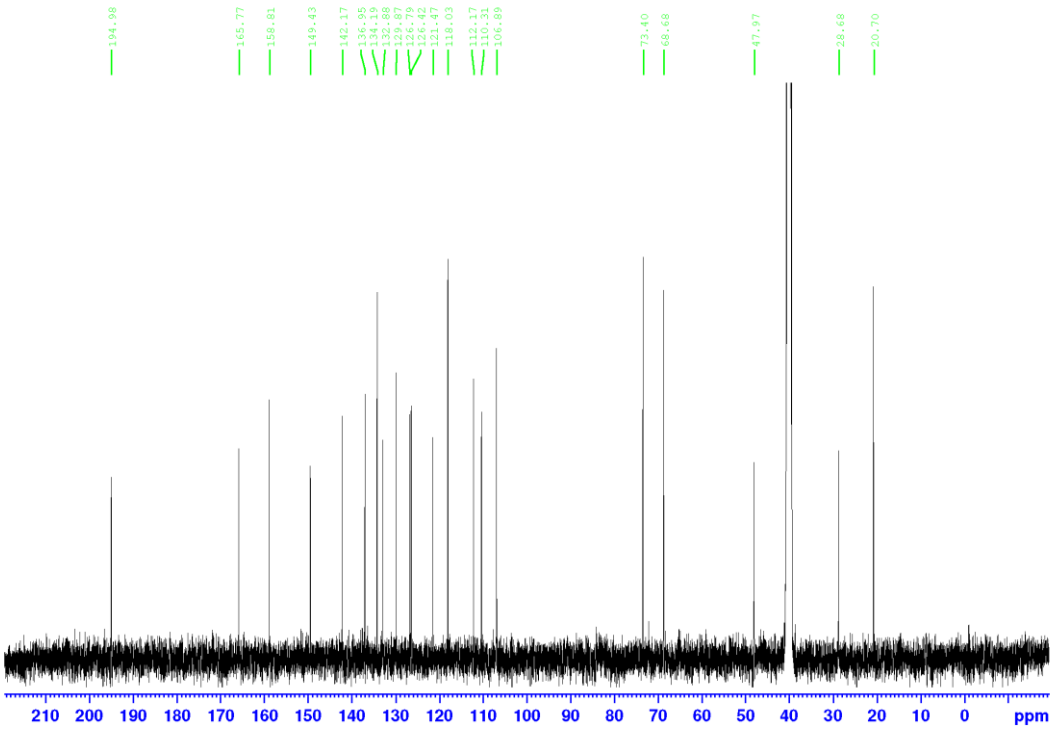

Figure S31. ^{13}C NMR spectrum of (*S*)-**11**.

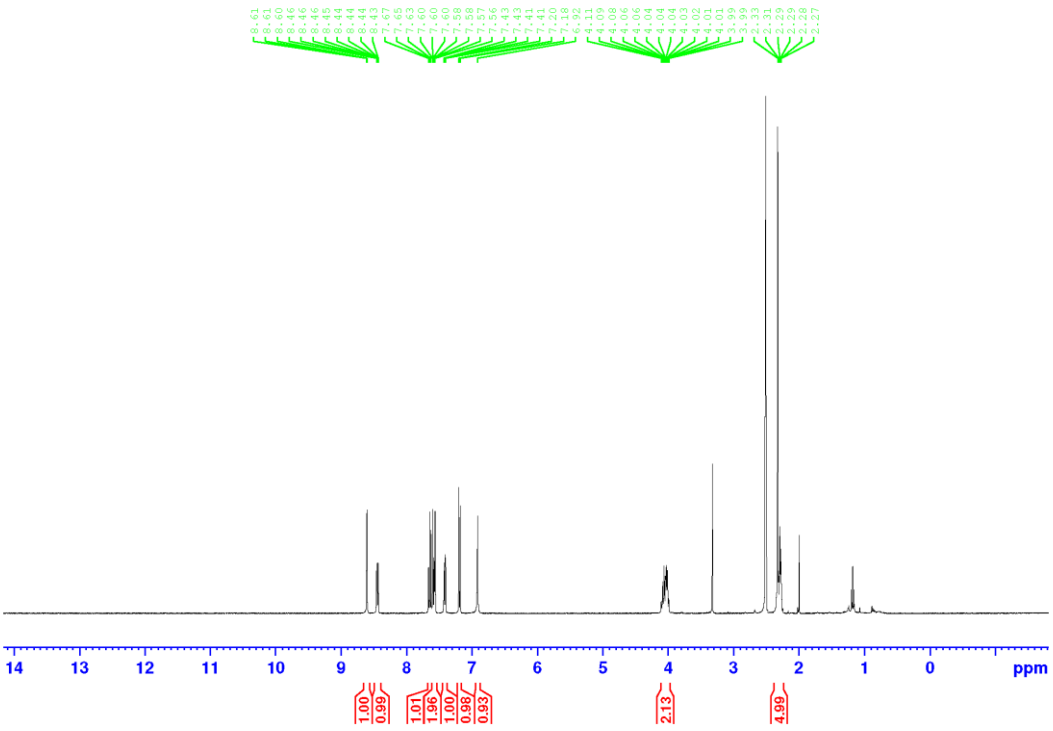

Figure S32. ^{1}H NMR spectrum of (*S*)-**13**.

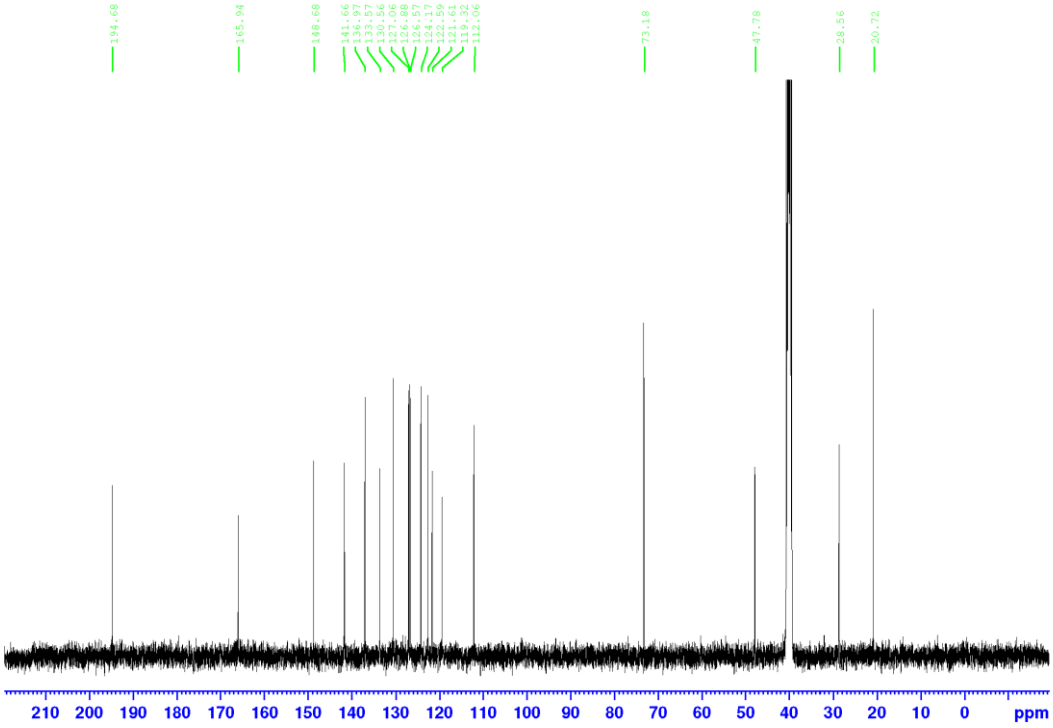

Figure S33. ^{13}C NMR spectrum of (*S*)-**13**.

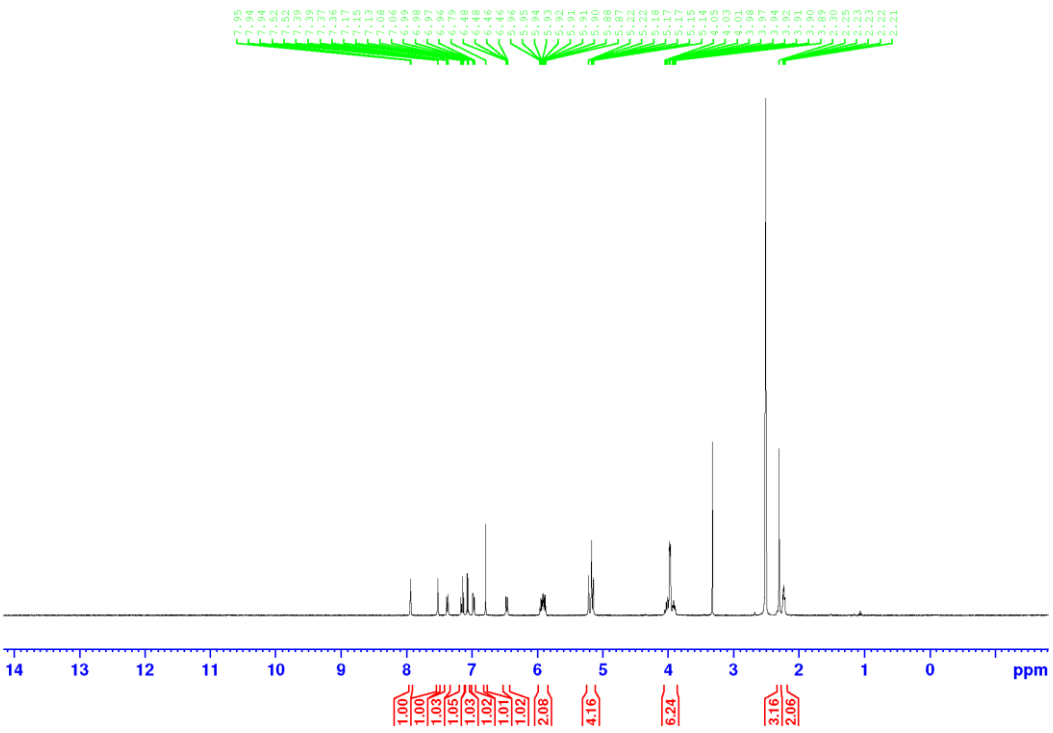

Figure S34. ^{1}H NMR spectrum of (*S*)-**12**.

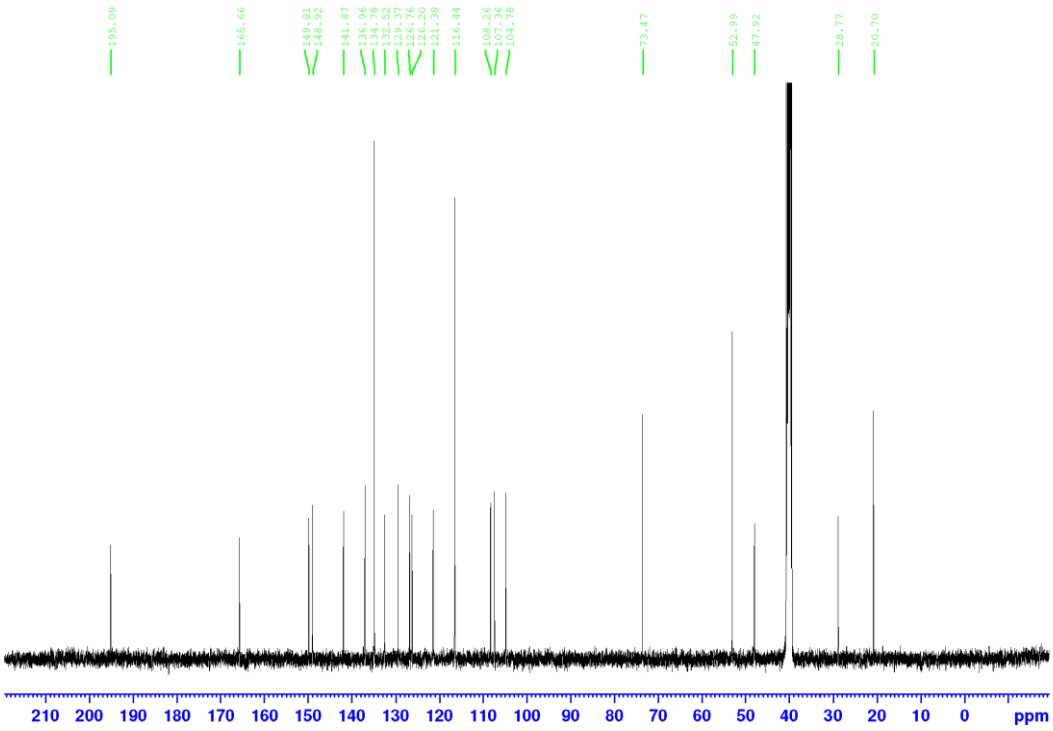

Figure S35. ^{13}C NMR spectrum of (*S*)-**12**.

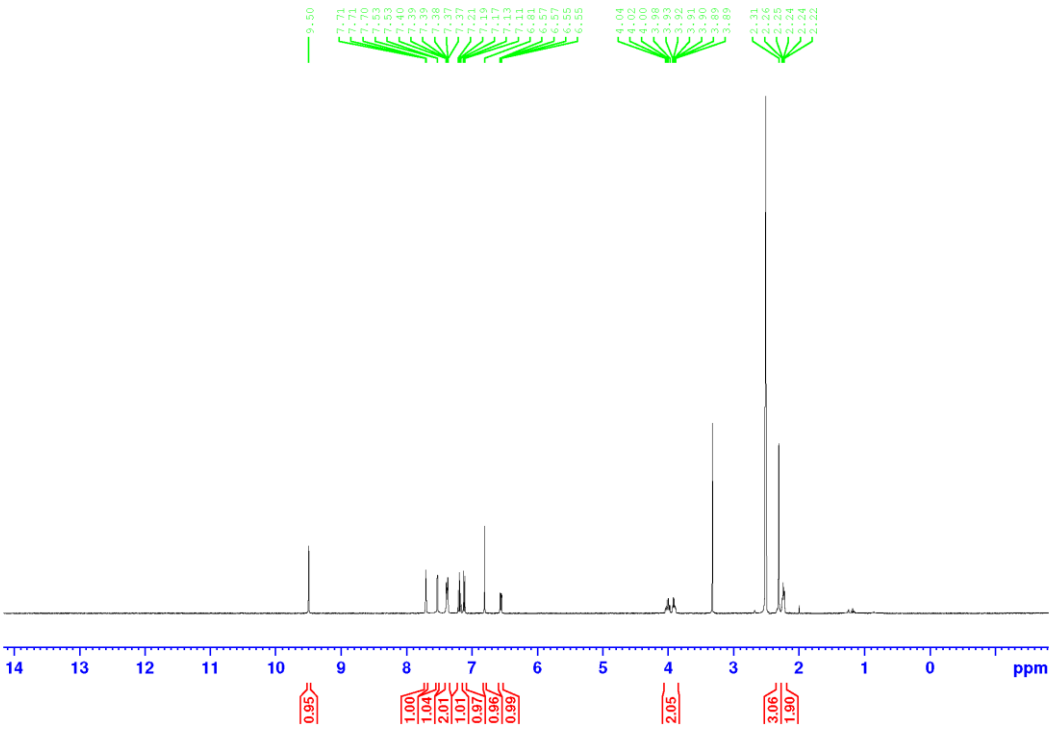

Figure S36. ^{1}H NMR spectrum of (*S*)-**2**.

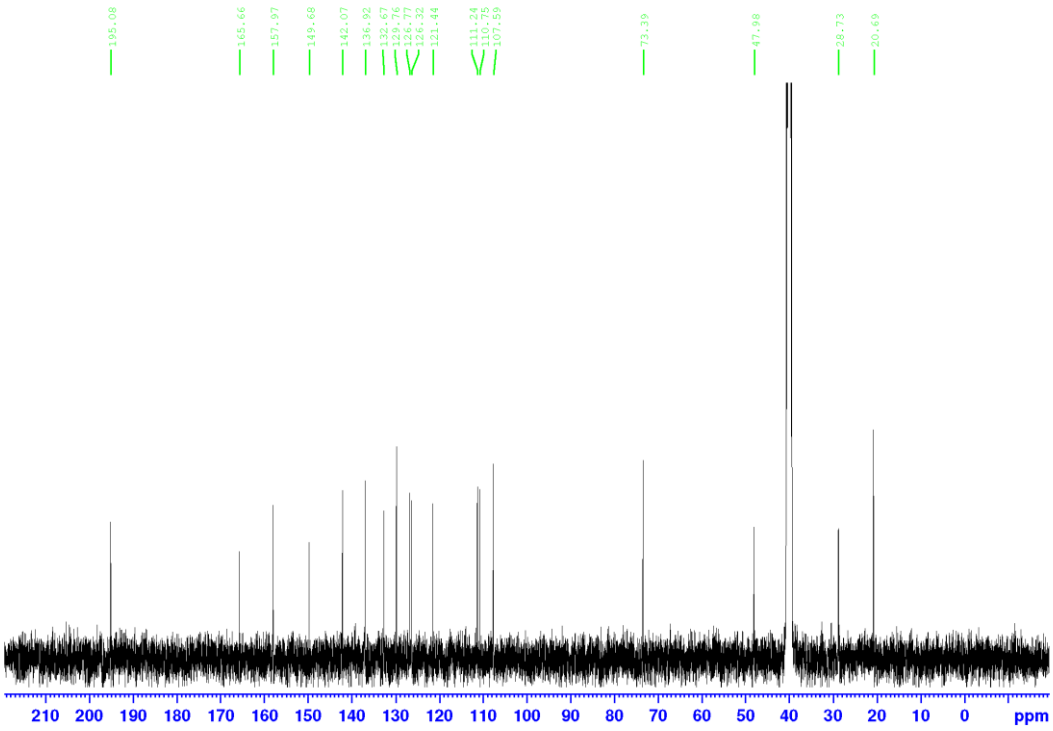

Figure S37. ^{13}C NMR spectrum of (*S*)-**2**.

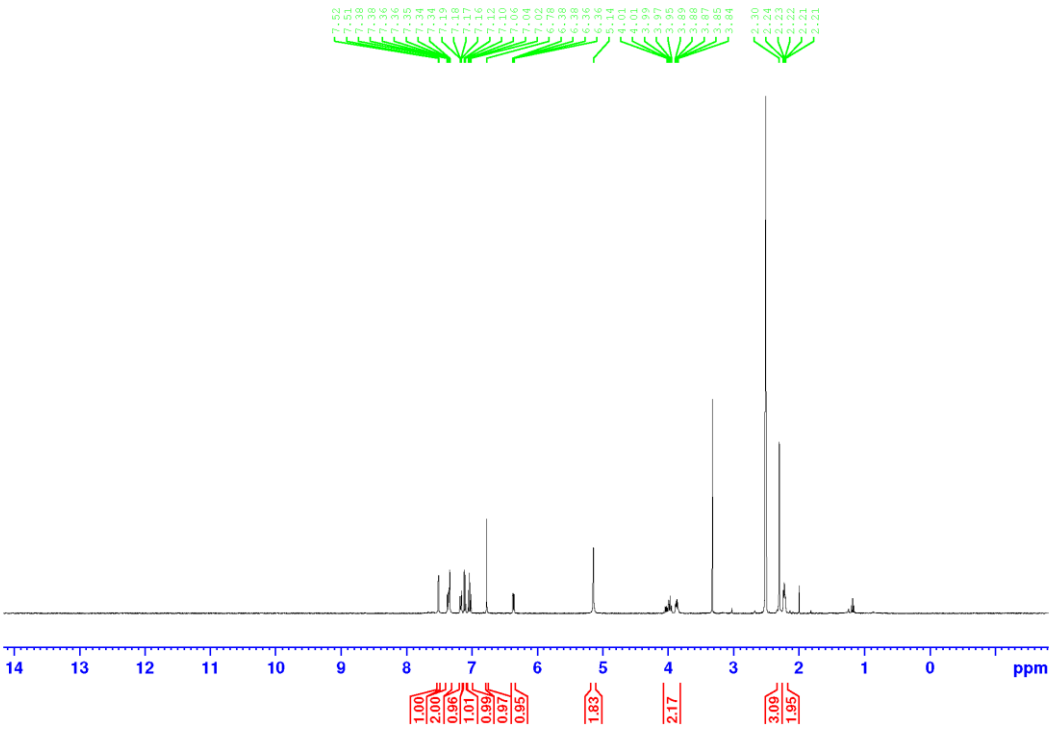

Figure S38. ^{1}H NMR spectrum of (*S*)-**3**.

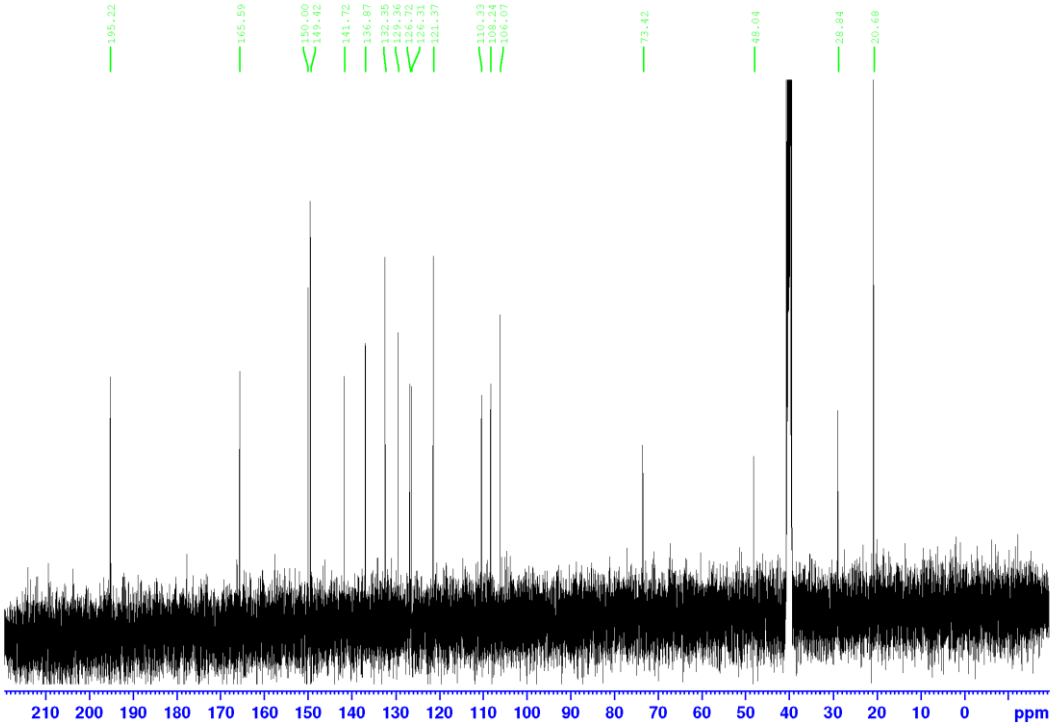

Figure S39. ^{13}C NMR spectrum of (*S*)-**3**.

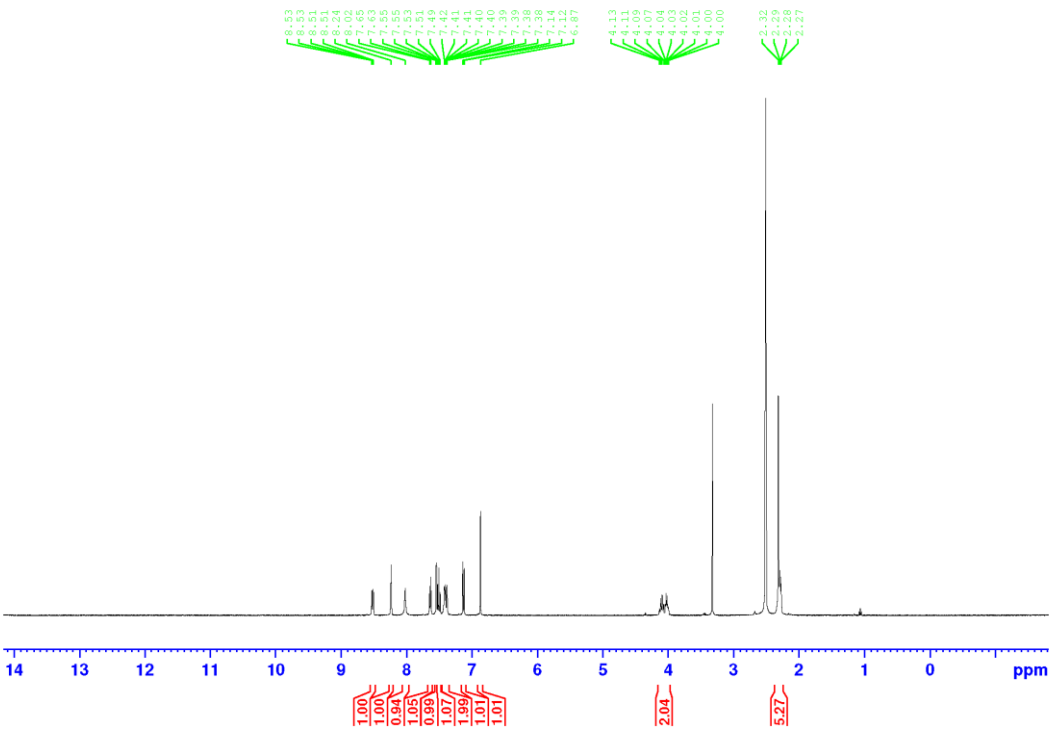

Figure S40. ^{1}H NMR spectrum of (*S*)-**16**.

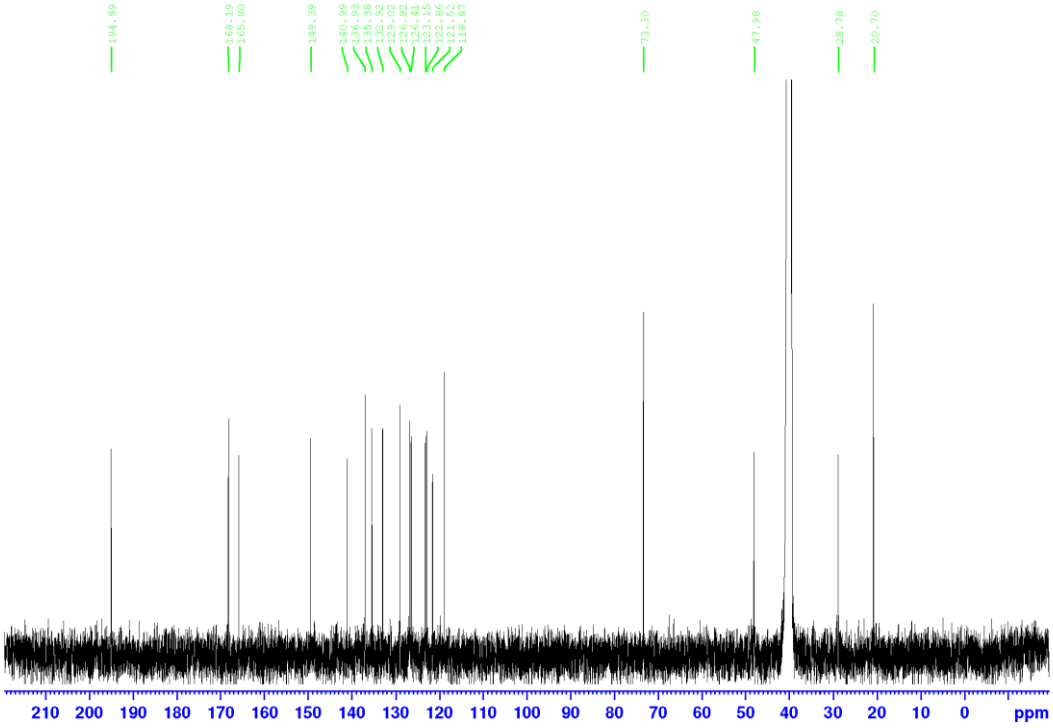

Figure S41. ^{13}C NMR spectrum of (*S*)-**16**.

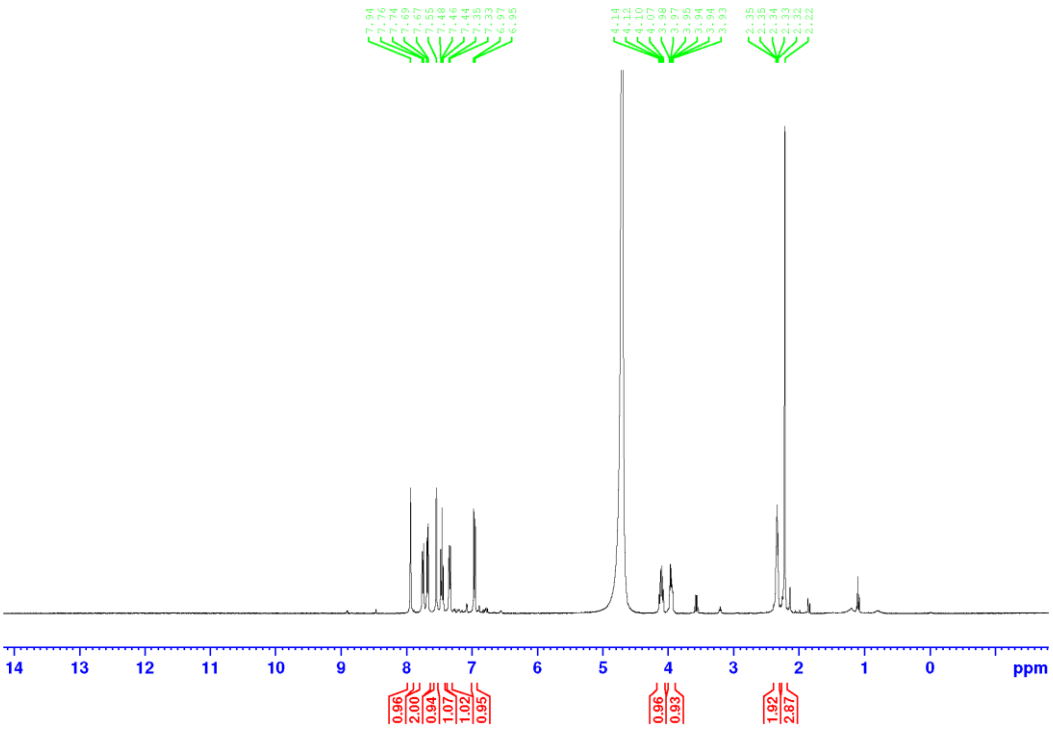

Figure S42. ^{1}H NMR spectrum of (*S*)-**17**.

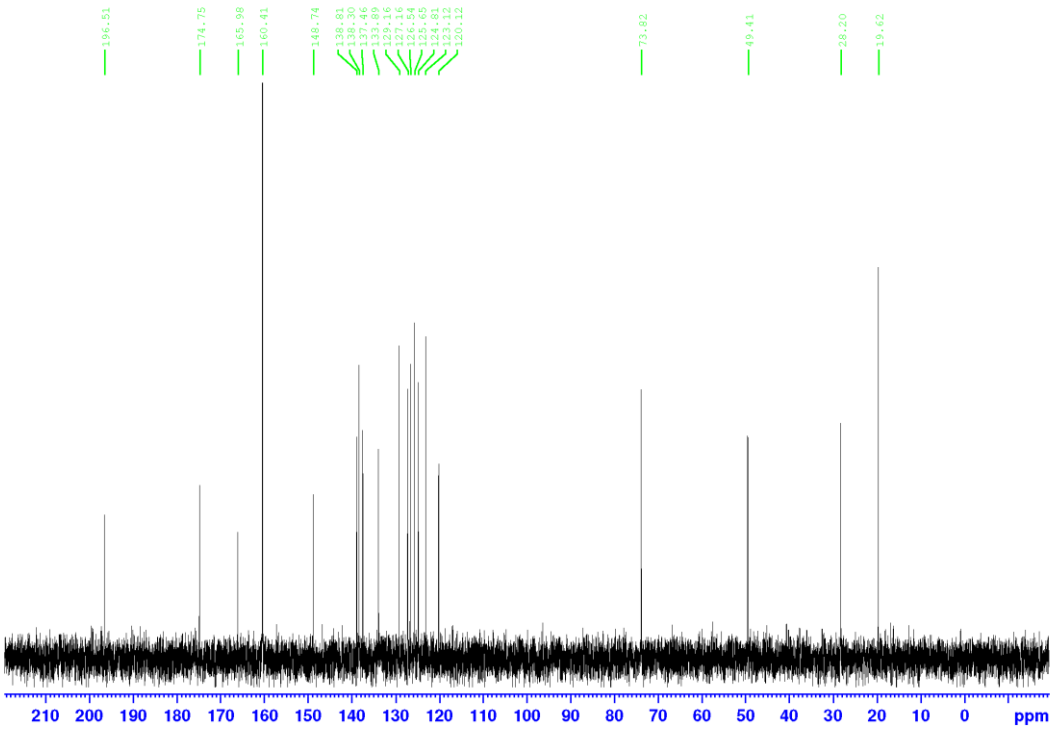

Figure S43. ^{13}C NMR spectrum of (*S*)-**17**.

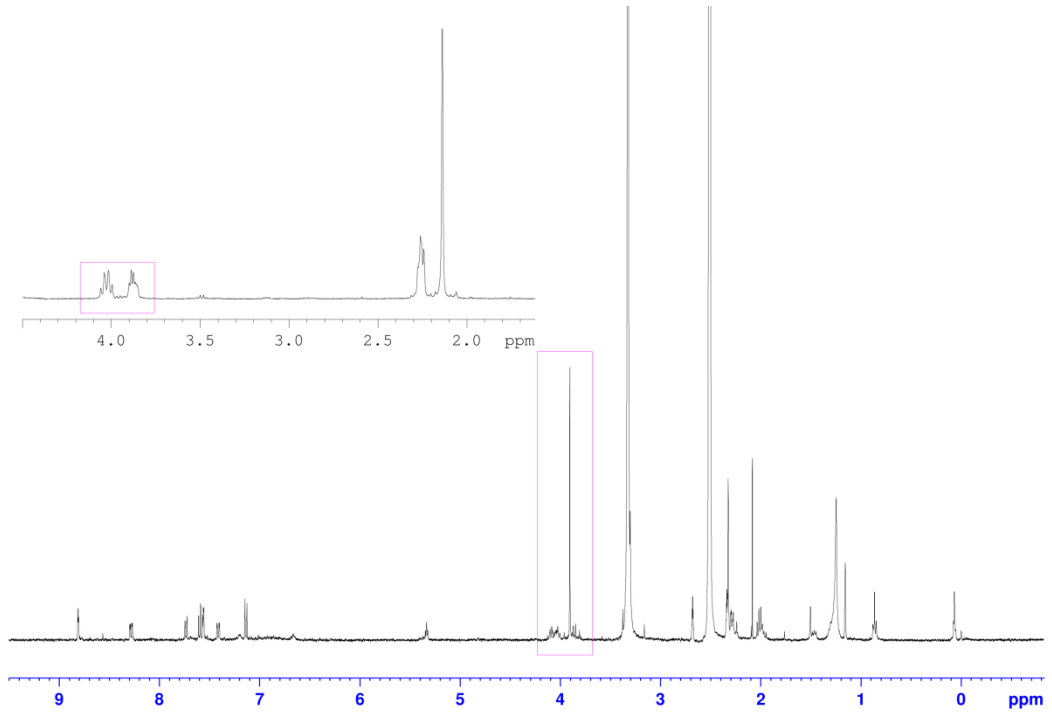

Figure S44. Proof of formation of corresponding methyl ester of (*S*)-**17** *via* ^{1}H NMR (overlay of (*S*)-**17**).

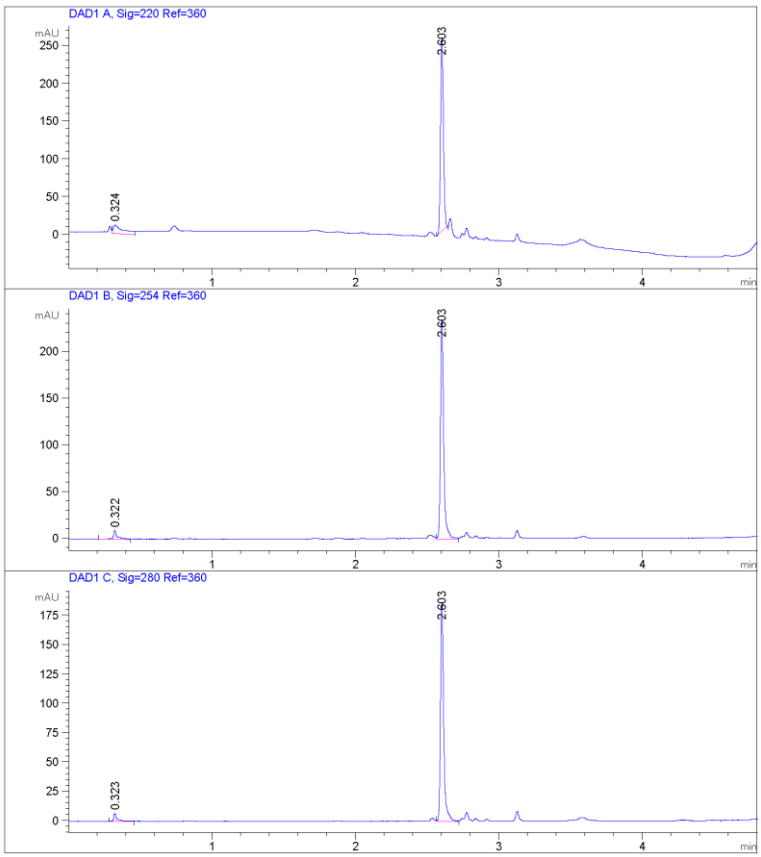

Figure S45. Proof of formation of corresponding methyl ester of (*S*)-**17** *via* LC.

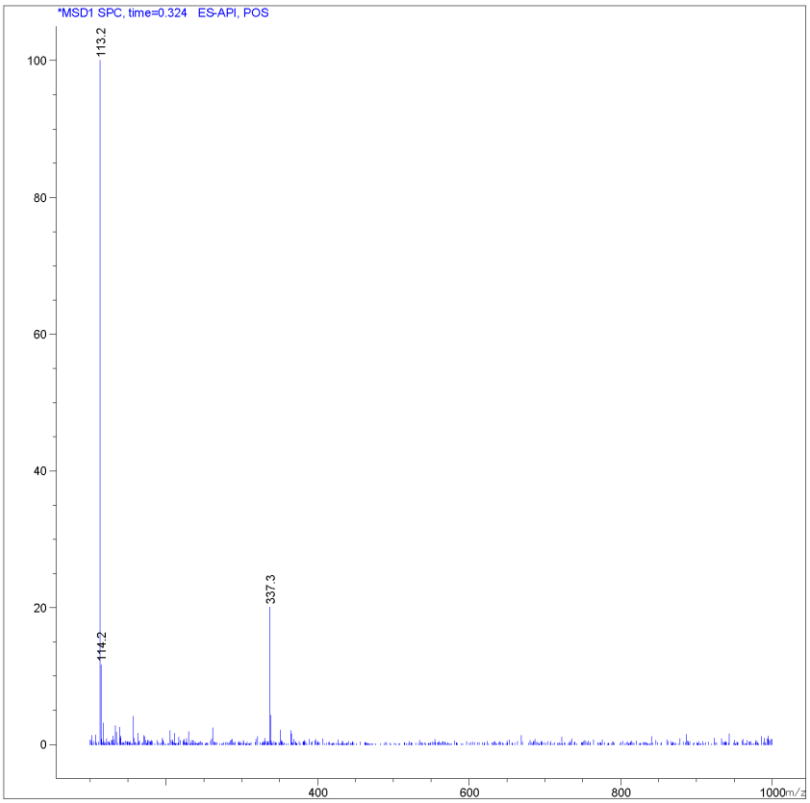

Figure S46. Proof of formation of corresponding methyl ester of (*S*)-**17** *via* MS (MS-spectrum of compound with t_R = 0.324 min in Figure S45).

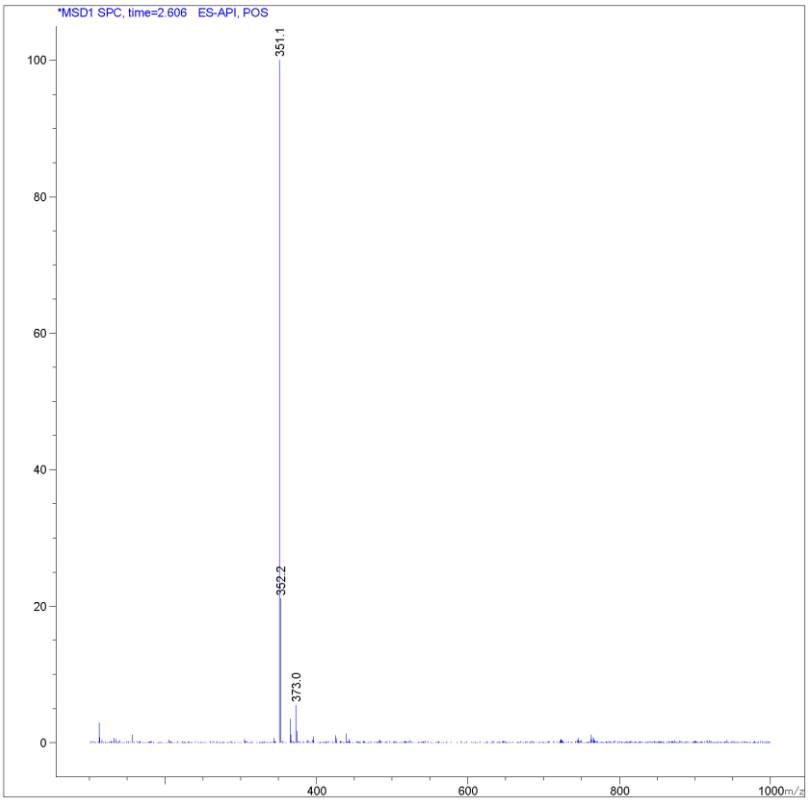

Figure S47. Proof of formation of corresponding methyl ester of (*S*)-**17** *via* MS (MS-spectrum of compound with t_R = 2.606 min in Figure S45).

4. Chiral HPLC chromatograms

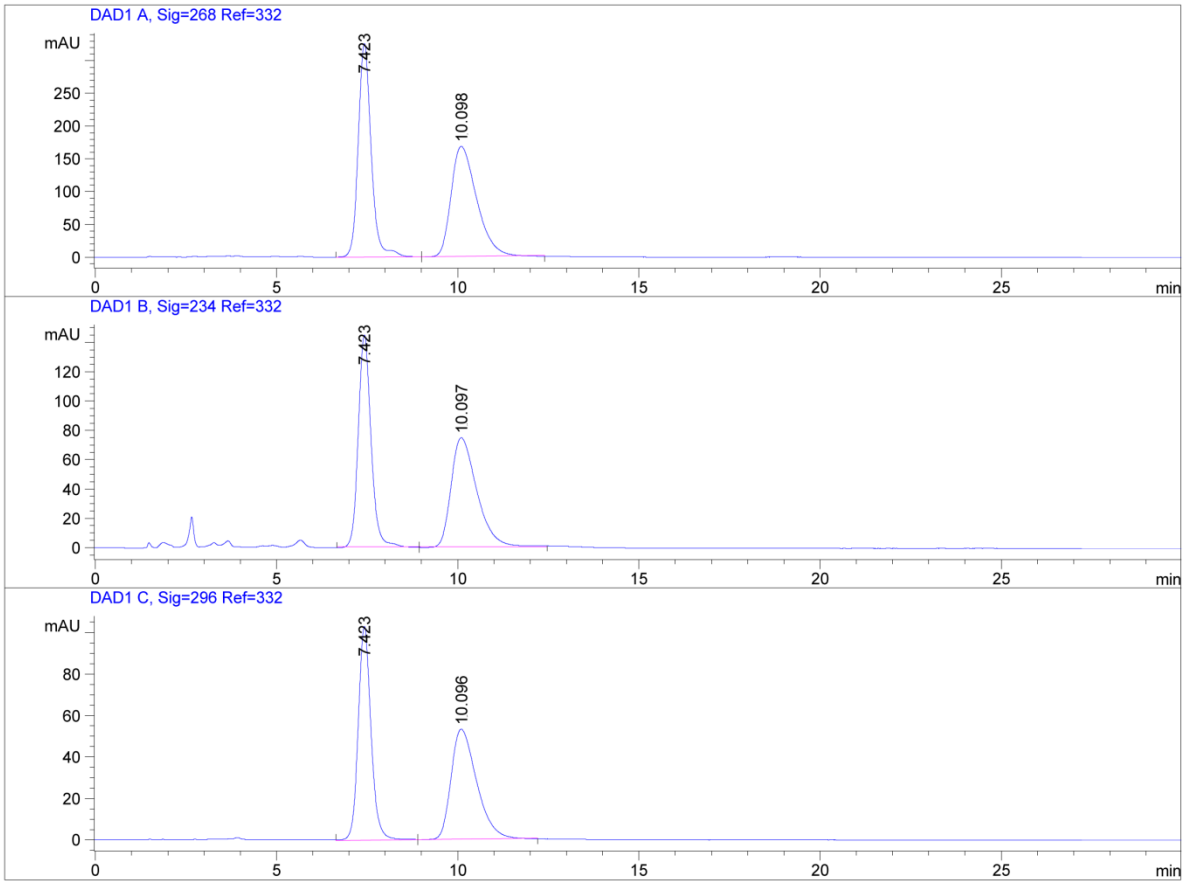

Figure S48. Chiral HPLC chromatogram of (*S*)-**1** spiked with (*R*)-**1**.

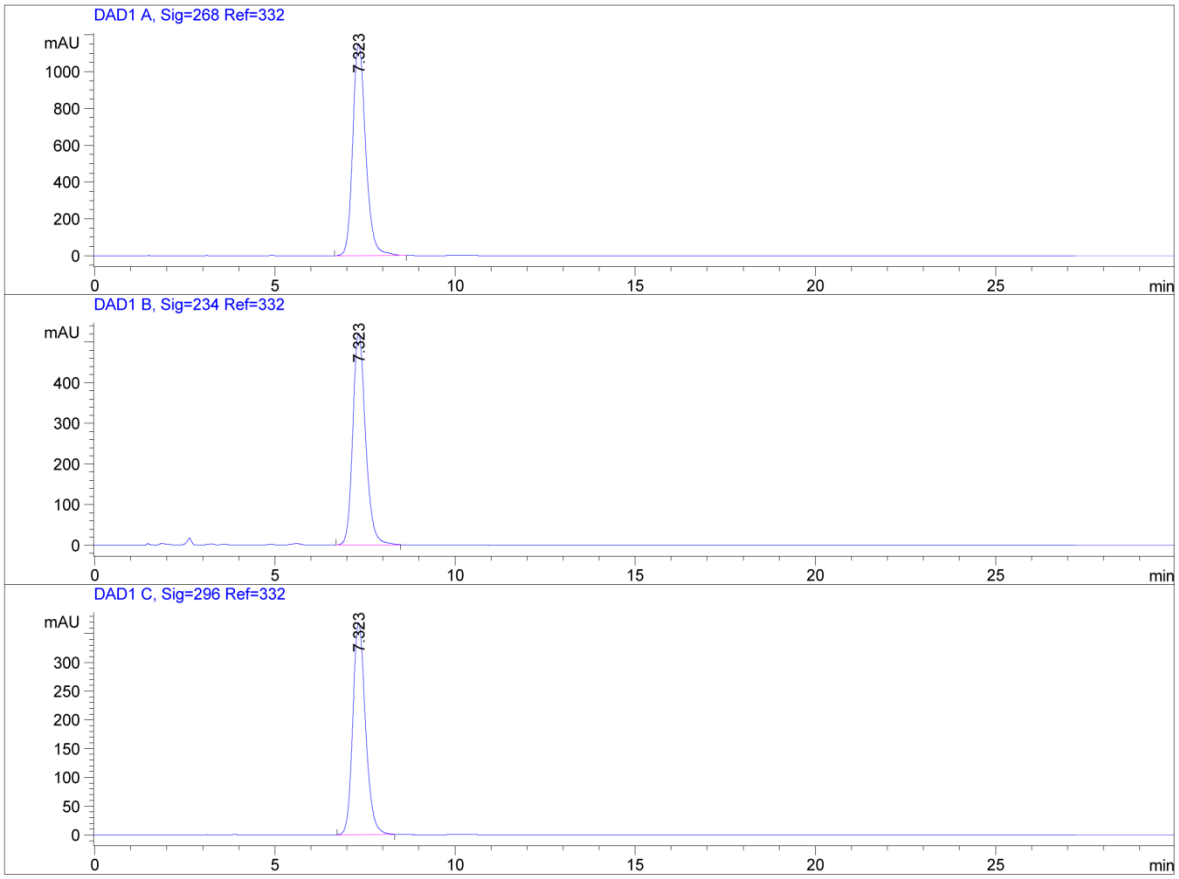


```
=====================================================================
                      Area Percent Report
=====================================================================

Signal 1: DAD1 A, Sig=268 Ref=332

Peak RetTime Type  Width     Area      Height     Area
  #   [min]        [min]   [mAU*s]     [mAU]       %
----|-------|----|-------|----------|----------|--------|
   1   7.323 BB    0.3873 2.87565e4  1151.78931 100.0000

Totals :                  2.87565e4  1151.78931


Signal 2: DAD1 B, Sig=234 Ref=332

Peak RetTime Type  Width     Area      Height     Area
  #   [min]        [min]   [mAU*s]     [mAU]       %
----|-------|----|-------|----------|----------|--------|
   1   7.323 BB    0.3836 1.28542e4   521.51294 100.0000

Totals :                  1.28542e4   521.51294


Signal 3: DAD1 C, Sig=296 Ref=332

Peak RetTime Type  Width     Area      Height     Area
  #   [min]        [min]   [mAU*s]     [mAU]       %
----|-------|----|-------|----------|----------|--------|
   1   7.323 BB    0.3825 9053.86914  368.64407 100.0000

Totals :                  9053.86914  368.64407

=====================================================================
                      *** End of Report ***
```

Figure S49. Chiral HPLC chromatogram of (*S*)-**1**.

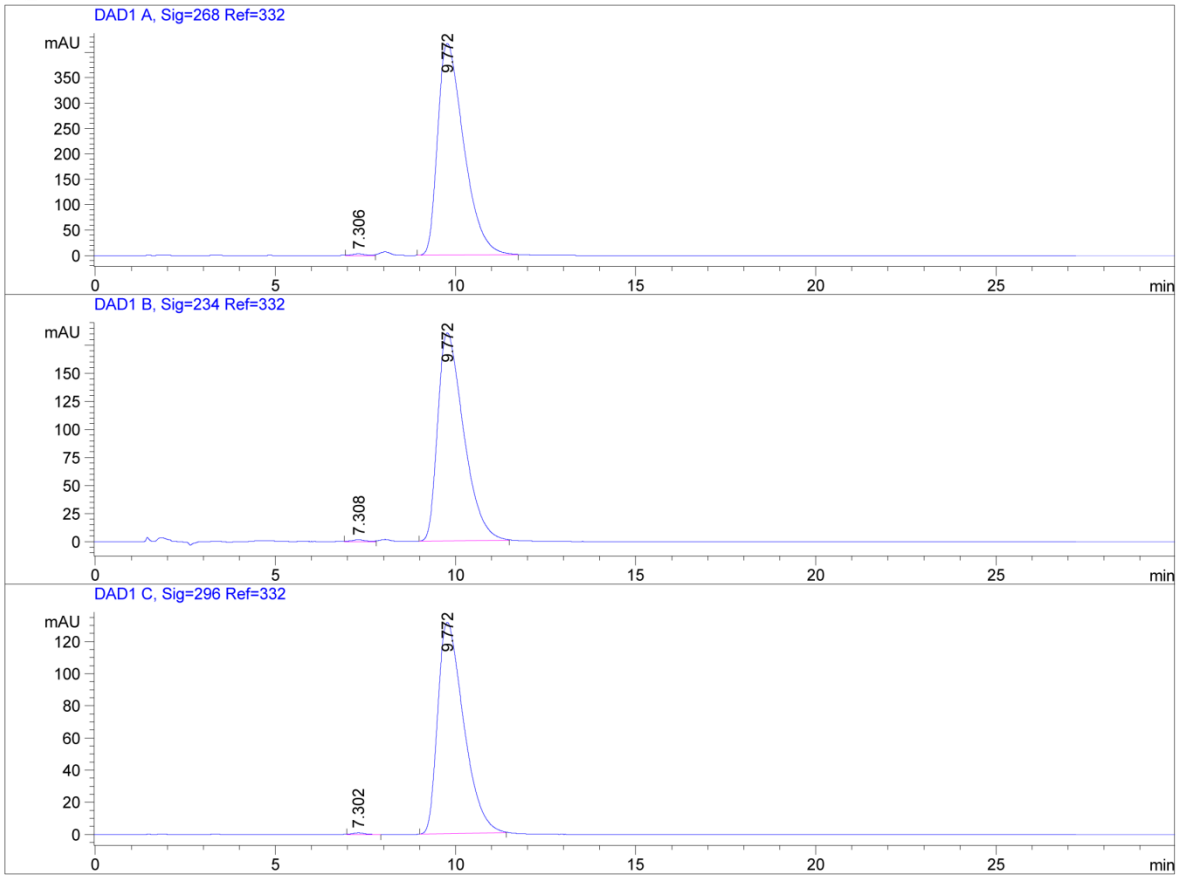


```
=====================================================================
                        Area Percent Report
=====================================================================

Signal 1: DAD1 A, Sig=268 Ref=332

Peak RetTime Type  Width     Area      Height     Area
  #   [min]        [min]   [mAU*s]     [mAU]       %
----|-------|----|-------|----------|----------|--------|
   1   7.306 MM    0.4439   90.45800    3.39619   0.4286
   2   9.772 BB    0.7747 2.10152e4   416.46057  99.5714

Totals :                  2.11057e4   419.85677


Signal 2: DAD1 B, Sig=234 Ref=332

Peak RetTime Type  Width     Area      Height     Area
  #   [min]        [min]   [mAU*s]     [mAU]       %
----|-------|----|-------|----------|----------|--------|
   1   7.308 MM    0.4416   41.44268    1.56393   0.4441
   2   9.772 BB    0.7687 9289.46973  185.36247  99.5559

Totals :                  9330.91241  186.92641


Signal 3: DAD1 C, Sig=296 Ref=332

Peak RetTime Type  Width     Area      Height     Area
  #   [min]        [min]   [mAU*s]     [mAU]       %
----|-------|----|-------|----------|----------|--------|
   1   7.302 MM    0.3934   24.31529    1.03012   0.3682
   2   9.772 BB    0.7720 6578.78711  131.42290  99.6318

Totals :                  6603.10240  132.45302

=====================================================================
                        *** End of Report ***
```

Figure S50. Chiral HPLC chromatogram of (*R*)-**1**.

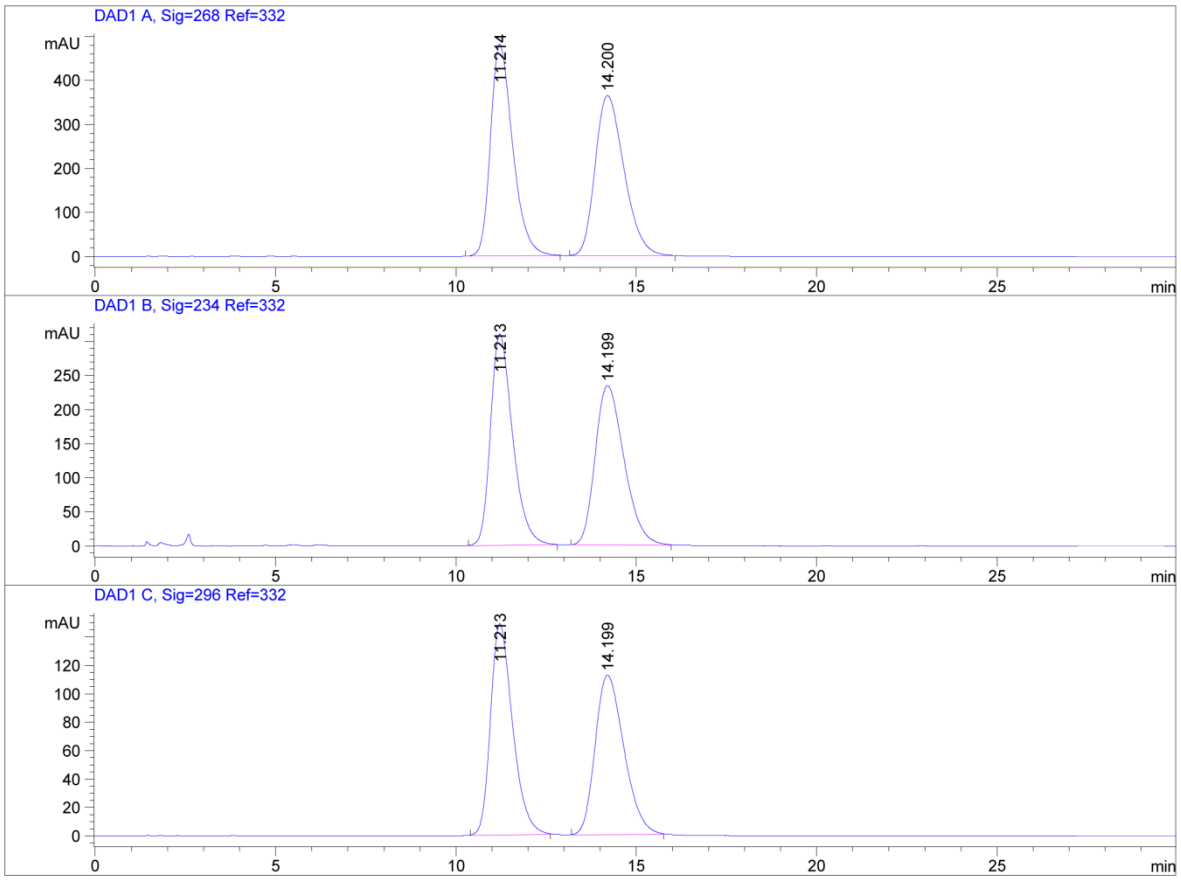

Figure S51. Chiral HPLC chromatogram of (*S*)-**11** spiked with (*R*)-**11**.

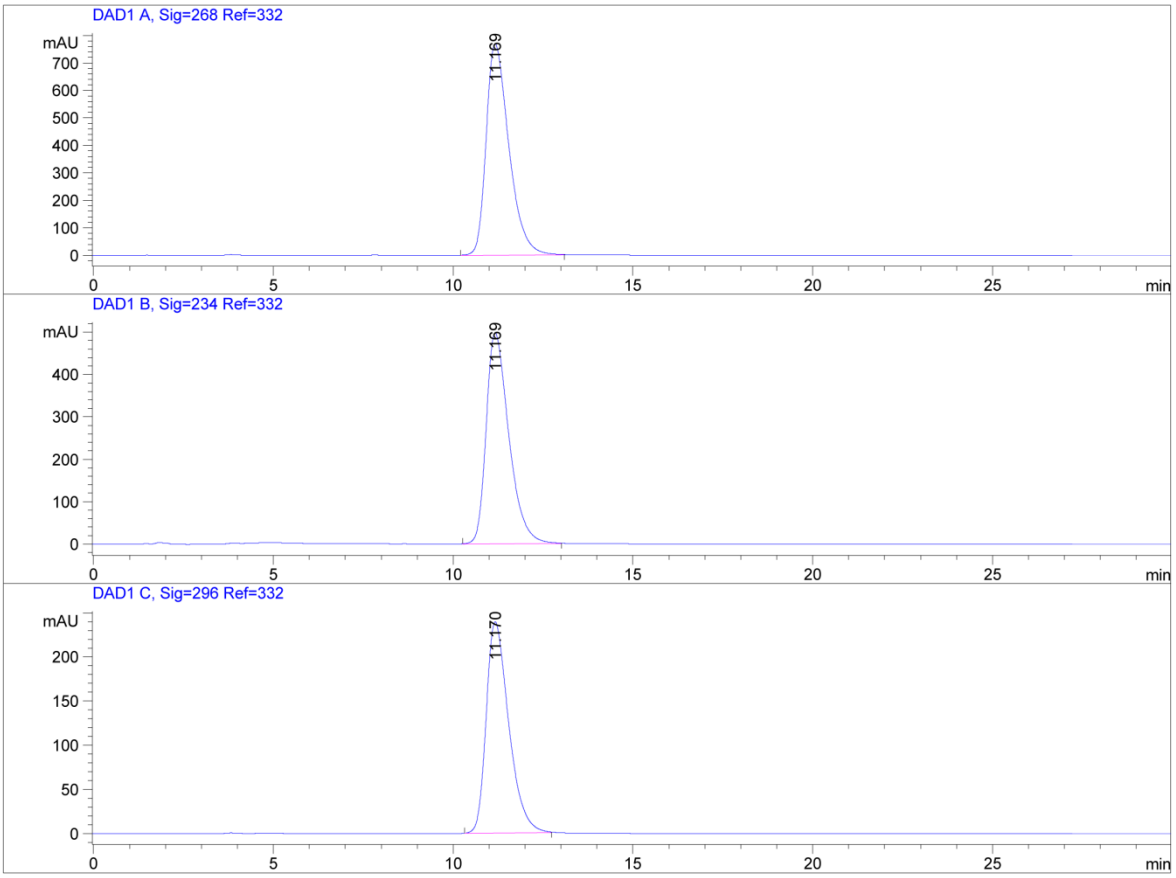


```
=====================================================================
                    Area Percent Report
=====================================================================

Signal 1: DAD1 A, Sig=268Ref=332

Peak RetTime Type  Width     Area      Height     Area
  #   [min]        [min]   [mAU*s]     [mAU]       %
----|-------|----|-------|----------|----------|--------|
   1  11.169 BB    0.6729 3.38424e4   769.84790 100.0000

Totals :                  3.38424e4   769.84790


Signal 2: DAD1 B, Sig=234 Ref=332

Peak RetTime Type  Width     Area      Height     Area
  #   [min]        [min]   [mAU*s]     [mAU]       %
----|-------|----|-------|----------|----------|--------|
   1  11.169 BB    0.6684 2.18080e4   498.43903 100.0000

Totals :                  2.18080e4   498.43903


Signal 3: DAD1 C, Sig=296 Ref=332

Peak RetTime Type  Width     Area      Height     Area
  #   [min]        [min]   [mAU*s]     [mAU]       %
----|-------|----|-------|----------|----------|--------|
   1  11.170 BB    0.6643 1.04204e4   239.15958 100.0000

Totals :                  1.04204e4   239.15958


=====================================================================
                    *** End of Report ***
```

Figure S52. Chiral HPLC chromatogram of (*S*)-**11**.

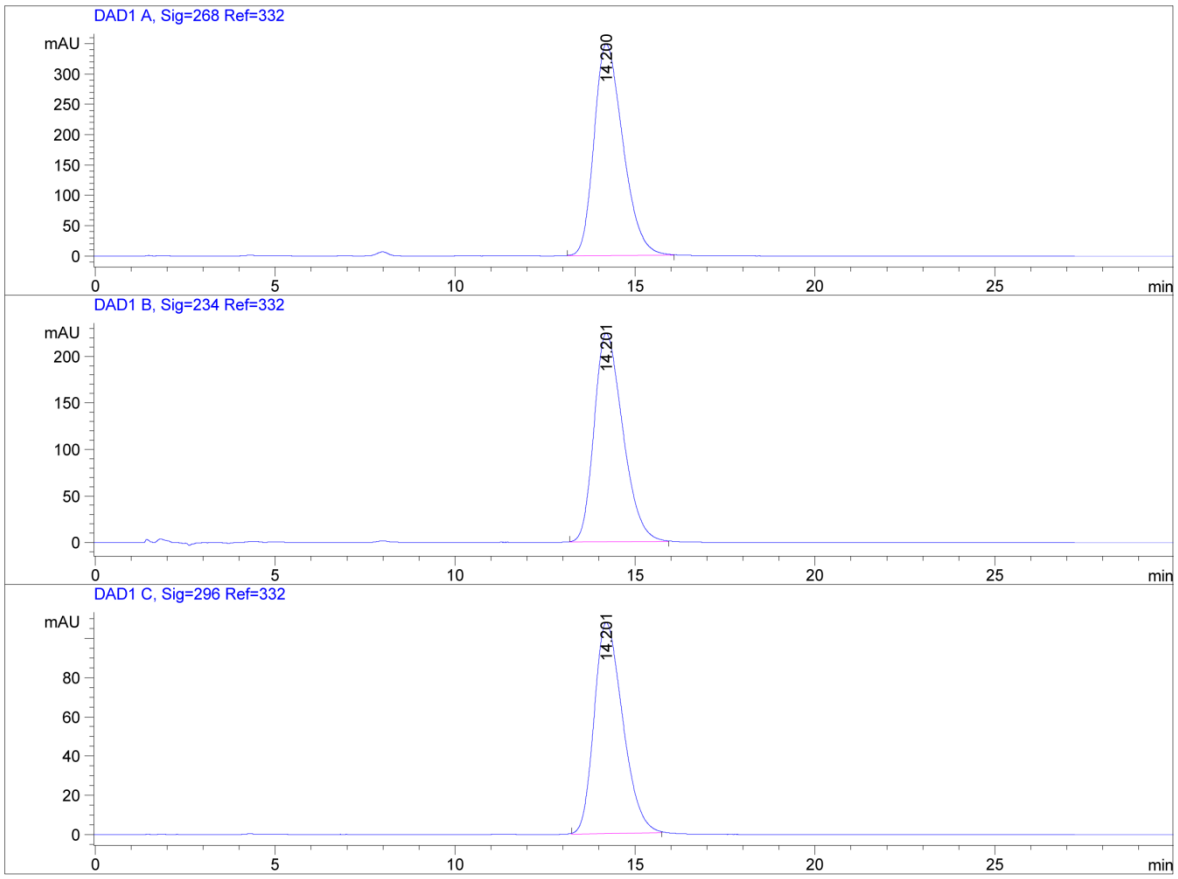


```
=====================================================================
                    Area Percent Report
=====================================================================

Signal 1: DAD1 A, Sig=268 Ref=332

Peak RetTime Type  Width     Area      Height     Area
  #   [min]        [min]   [mAU*s]     [mAU]       %
----|-------|----|-------|----------|----------|--------|
   1  14.200 BB    0.8613 1.93767e4   348.15967 100.0000

Totals :                  1.93767e4   348.15967


Signal 2: DAD1 B, Sig=234 Ref=332

Peak RetTime Type  Width     Area      Height     Area
  #   [min]        [min]   [mAU*s]     [mAU]       %
----|-------|----|-------|----------|----------|--------|
   1  14.201 BB    0.8504 1.24005e4   223.81982 100.0000

Totals :                  1.24005e4   223.81982


Signal 3: DAD1 C, Sig=296 Ref=332

Peak RetTime Type  Width     Area      Height     Area
  #   [min]        [min]   [mAU*s]     [mAU]       %
----|-------|----|-------|----------|----------|--------|
   1  14.201 BB    0.8413 5921.57861  107.39657 100.0000

Totals :                  5921.57861  107.39657

=====================================================================
                    *** End of Report ***
```

Figure S53. Chiral HPLC chromatogram of (*R*)-**11**.

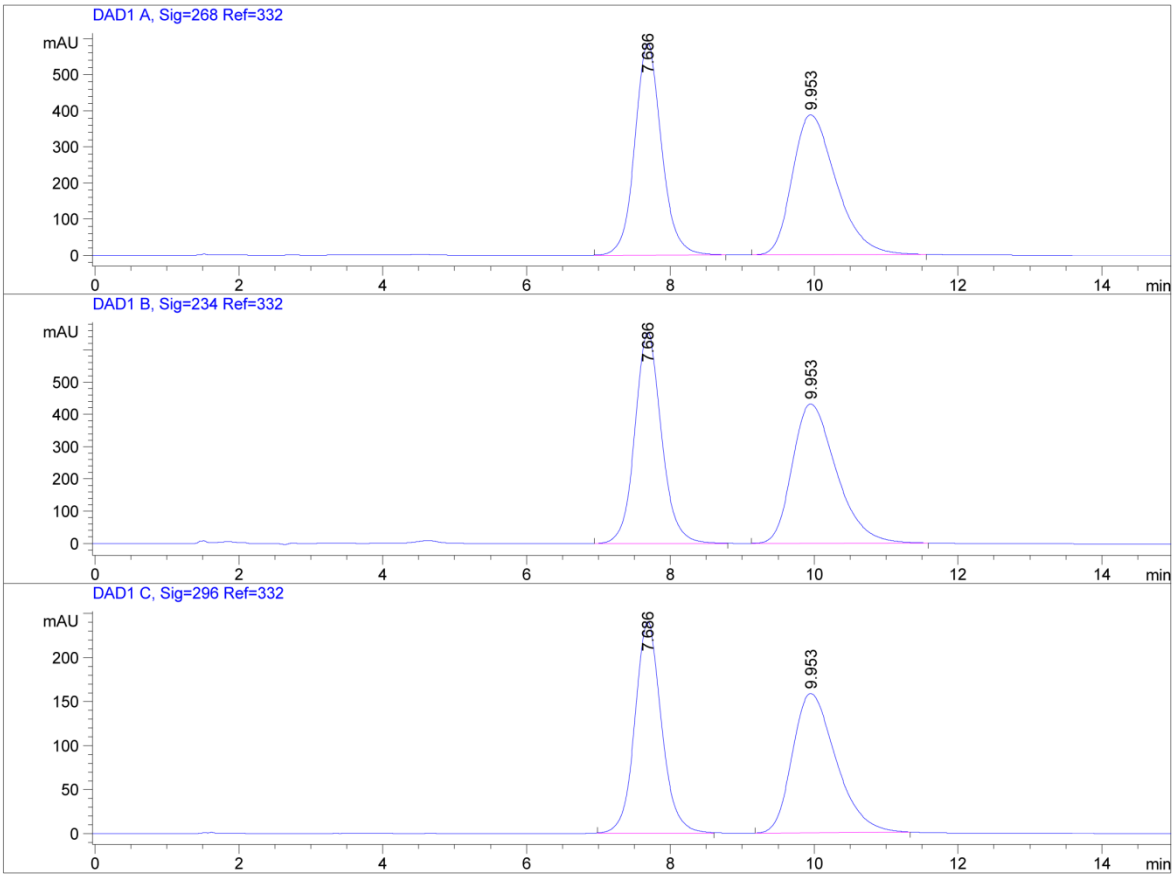

Figure S54. Chiral HPLC chromatogram of (*S*)-**13** spiked with (*R*)-**13**.

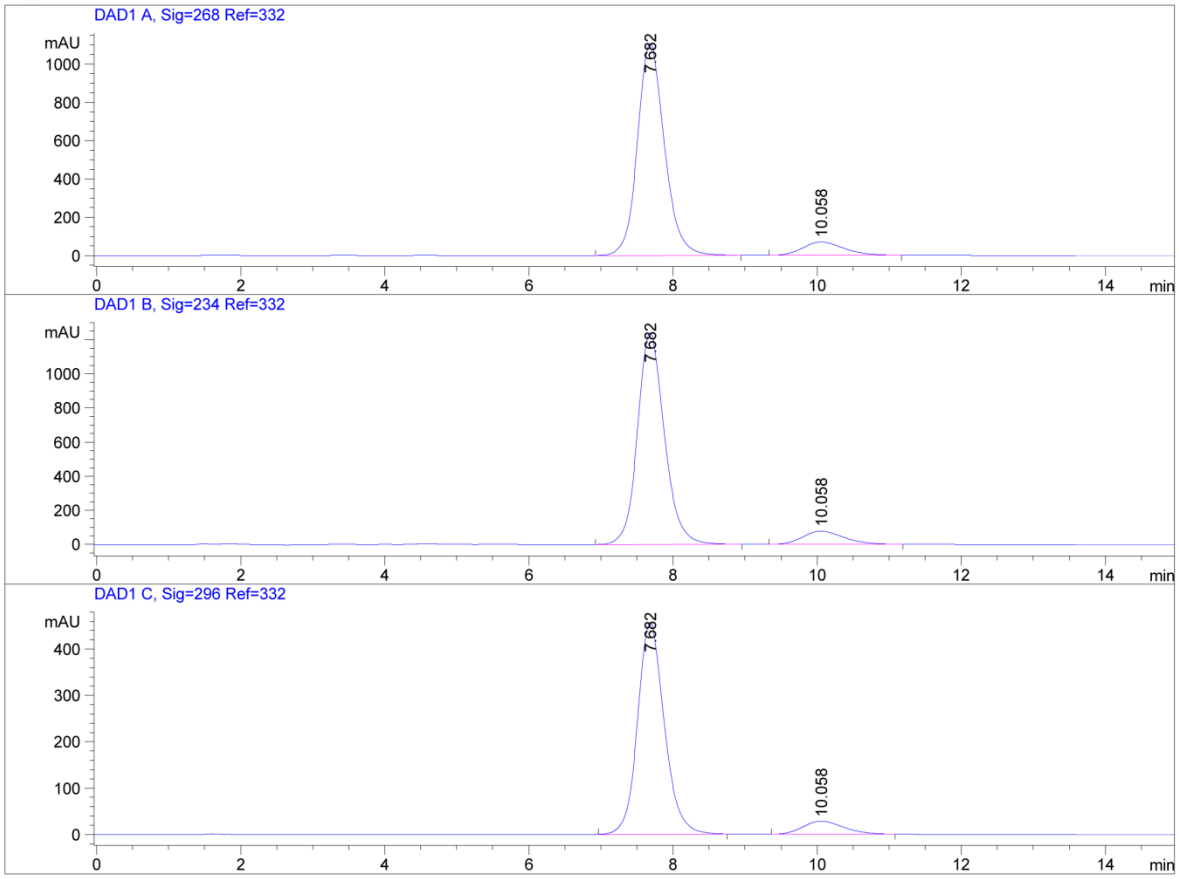


```
================================================================================
                              Area Percent Report
================================================================================

Signal 1: DAD1 A, Sig=268 Ref=332

Peak RetTime Type  Width     Area      Height     Area
  #   [min]        [min]   [mAU*s]     [mAU]       %
----|-------|----|-------|----------|----------|--------|
   1   7.682 BB    0.3997 2.88199e4  1107.00513  91.2478
   2  10.058 BB    0.6109 2764.30127   69.66653   8.7522

Totals :                  3.15842e4  1176.67166


Signal 2: DAD1 B, Sig=234 Ref=332

Peak RetTime Type  Width     Area      Height     Area
  #   [min]        [min]   [mAU*s]     [mAU]       %
----|-------|----|-------|----------|----------|--------|
   1   7.682 BB    0.3990 3.21849e4  1239.12463  91.2803
   2  10.058 BB    0.6093 3074.50684   77.41396   8.7197

Totals :                  3.52594e4  1316.53860


Signal 3: DAD1 C, Sig=296 Ref=332

Peak RetTime Type  Width     Area      Height     Area
  #   [min]        [min]   [mAU*s]     [mAU]       %
----|-------|----|-------|----------|----------|--------|
   1   7.682 BB    0.3976 1.18118e4   456.91171  91.3423
   2  10.058 BB    0.6065 1119.56445   28.36450   8.6577

Totals :                  1.29314e4   485.27621

================================================================================
                            *** End of Report ***
```

Figure S55. Chiral HPLC chromatogram of (*S*)-**13**.

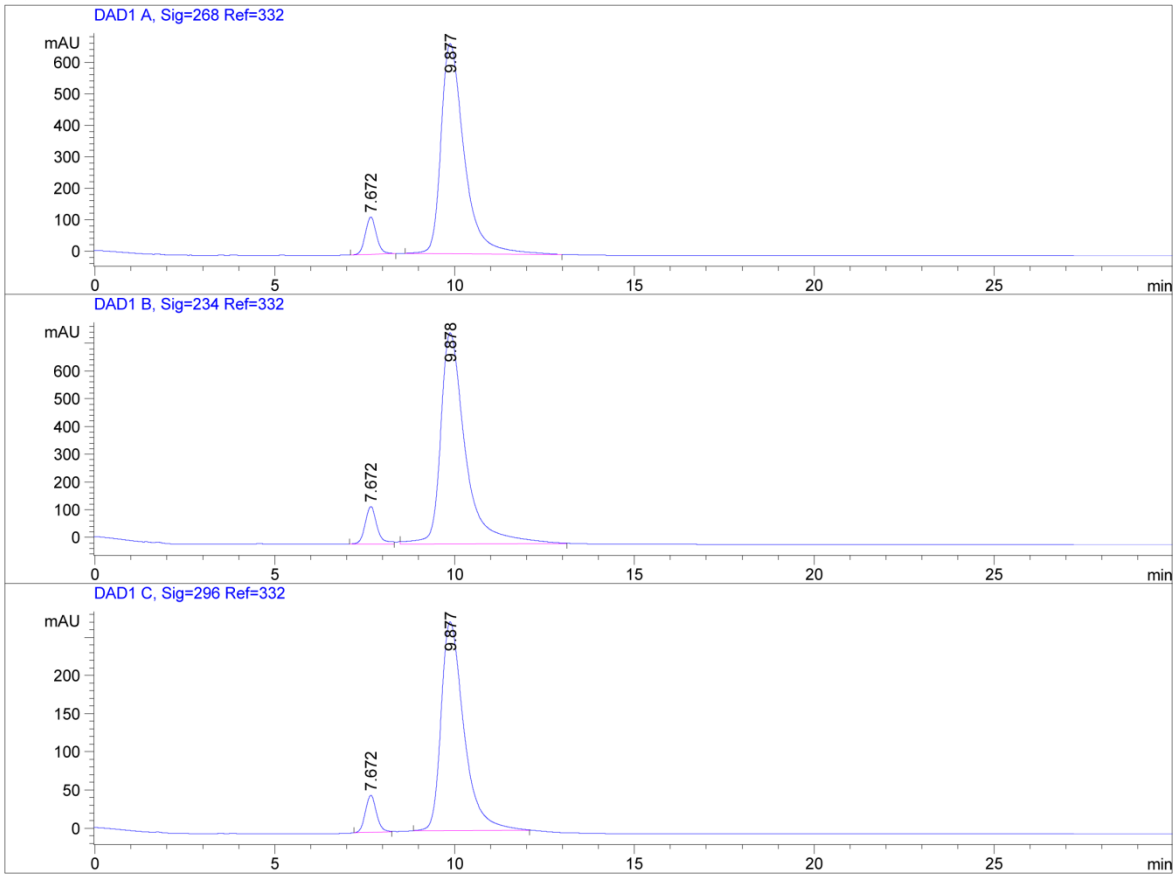


```
=====================================================================
                        Area Percent Report
=====================================================================

Signal 1: DAD1 A, Sig=268 Ref=332

Peak RetTime Type  Width     Area      Height     Area
  #   [min]        [min]   [mAU*s]     [mAU]       %
----|-------|----|-------|----------|----------|--------|
   1   7.672 BB    0.3327 2570.77197  118.67730   7.8563
   2   9.877 BB    0.6827 3.01517e4   667.91925  92.1437

Totals :                  3.27224e4   786.59655


Signal 2: DAD1 B, Sig=234 Ref=332

Peak RetTime Type  Width     Area      Height     Area
  #   [min]        [min]   [mAU*s]     [mAU]       %
----|-------|----|-------|----------|----------|--------|
   1   7.672 BB    0.3476 3097.24463  135.04044   7.8597
   2   9.878 BB    0.7090 3.63092e4   760.50641  92.1403

Totals :                  3.94064e4   895.54684


Signal 3: DAD1 C, Sig=296 Ref=332

Peak RetTime Type  Width     Area      Height     Area
  #   [min]        [min]   [mAU*s]     [mAU]       %
----|-------|----|-------|----------|----------|--------|
   1   7.672 BB    0.3323 1040.56470   48.50504   7.8915
   2   9.877 BB    0.6694 1.21454e4   273.87204  92.1085

Totals :                  1.31859e4   322.37708

=====================================================================
                        *** End of Report ***
```

Figure S56. Chiral HPLC chromatogram of (*R*)-**13**.

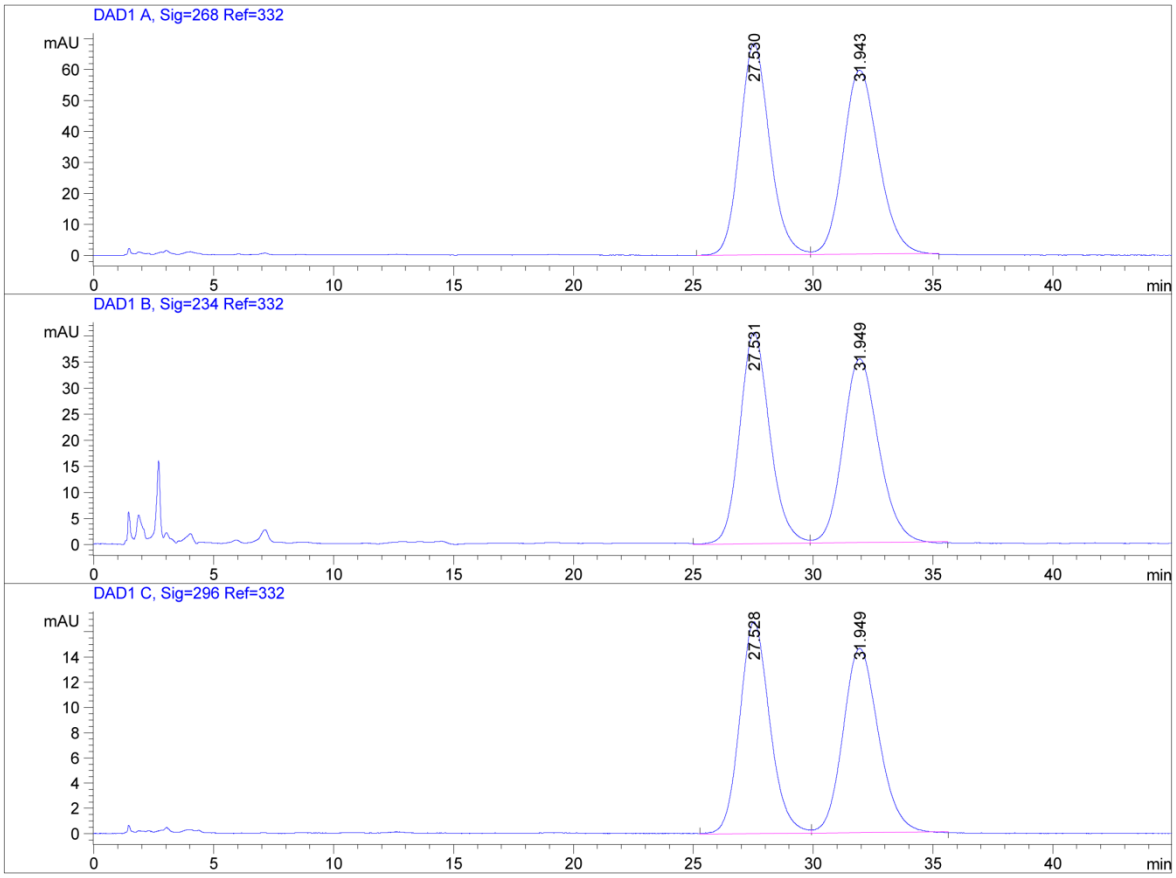

Figure S57. Chiral HPLC chromatogram of (*S*)-**12** spiked with (*R*)-**12**.

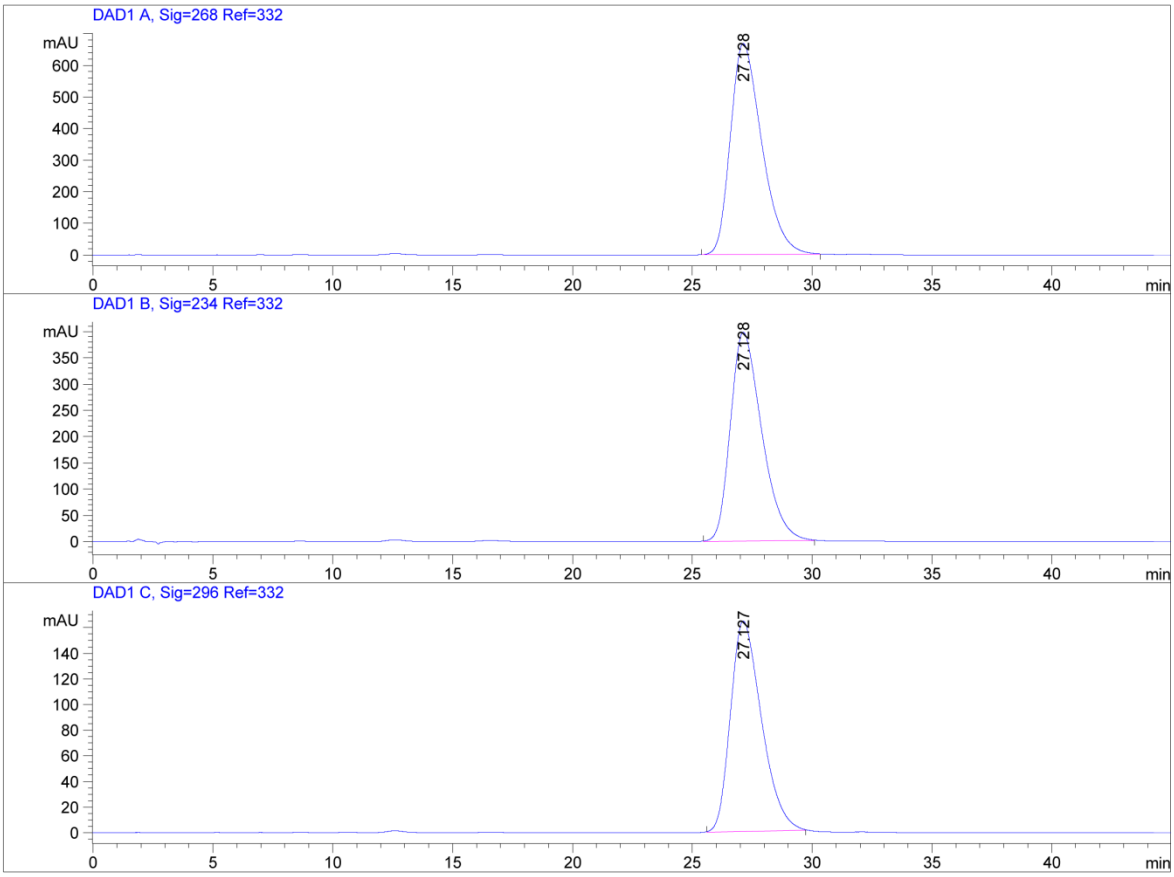


```
=====================================================================
                        Area Percent Report
=====================================================================
Signal 1: DAD1 A, Sig=268 Ref=332

Peak RetTime Type  Width     Area      Height     Area
  #   [min]        [min]   [mAU*s]     [mAU]       %
----|-------|----|-------|----------|----------|--------|
   1  27.128 BB    1.3829 6.08378e4   667.77954 100.0000

Totals :                  6.08378e4   667.77954


Signal 2: DAD1 B, Sig=234 Ref=332

Peak RetTime Type  Width     Area      Height     Area
  #   [min]        [min]   [mAU*s]     [mAU]       %
----|-------|----|-------|----------|----------|--------|
   1  27.128 BB    1.3808 3.59935e4   397.36972 100.0000

Totals :                  3.59935e4   397.36972


Signal 3: DAD1 C, Sig=296 Ref=332

Peak RetTime Type  Width     Area      Height     Area
  #   [min]        [min]   [mAU*s]     [mAU]       %
----|-------|----|-------|----------|----------|--------|
   1  27.127 BB    1.3393 1.47638e4   164.14957 100.0000

Totals :                  1.47638e4   164.14957

=====================================================================
                        *** End of Report ***
```

Figure S58. Chiral HPLC chromatogram of (*S*)-**12**.

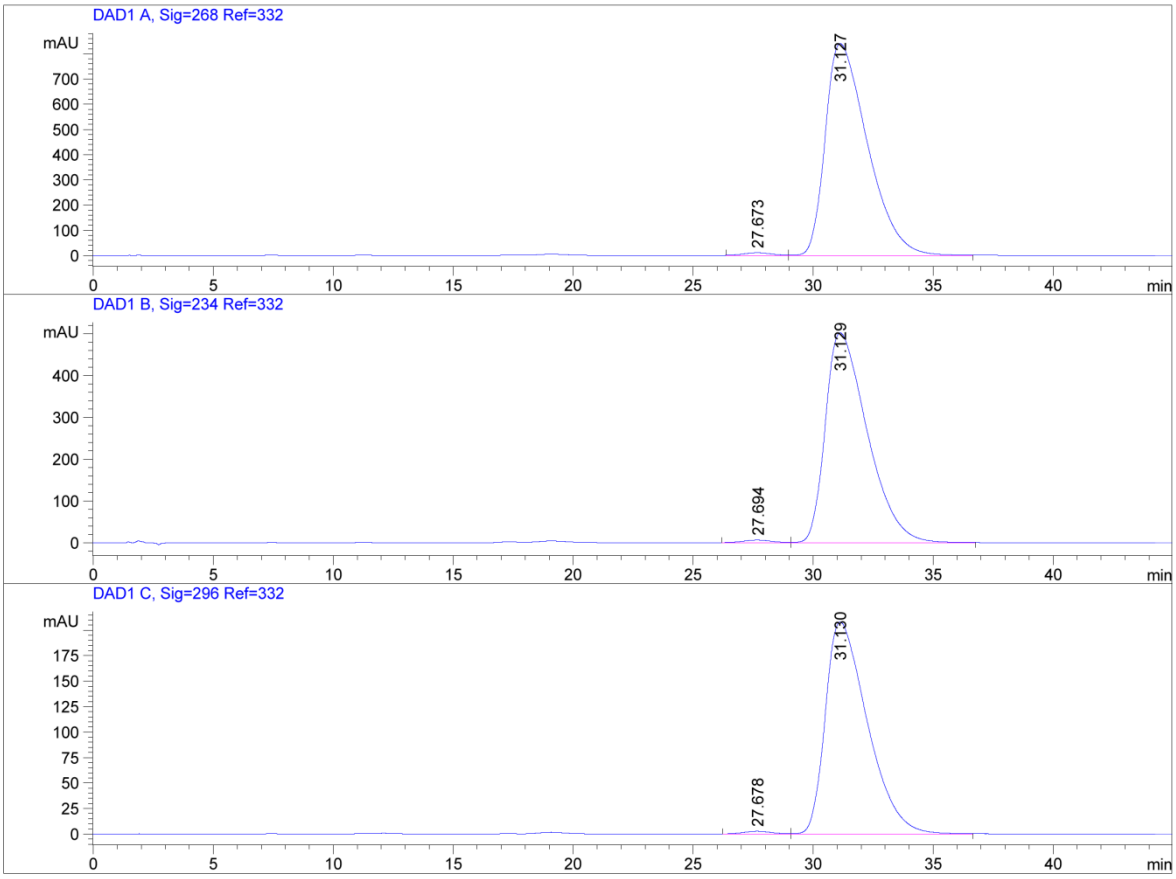


```
=====================================================================
                        Area Percent Report
=====================================================================
Signal 1: DAD1 A, Sig=268 Ref=332

Peak RetTime Type  Width     Area      Height     Area
  #   [min]        [min]   [mAU*s]     [mAU]       %
----|-------|----|-------|----------|----------|--------|
   1  27.673 MF    1.3623  871.79840   10.66553   0.8416
   2  31.127 FM    2.0364 1.02721e5   840.72552  99.1584

Totals :                  1.03593e5   851.39105


Signal 2: DAD1 B, Sig=234 Ref=332

Peak RetTime Type  Width     Area      Height     Area
  #   [min]        [min]   [mAU*s]     [mAU]       %
----|-------|----|-------|----------|----------|--------|
   1  27.694 MF    1.4911  607.42621    6.78967   0.9820
   2  31.129 FM    2.0307 6.12460e4   502.67957  99.0180

Totals :                  6.18535e4   509.46924


Signal 3: DAD1 C, Sig=296 Ref=332

Peak RetTime Type  Width     Area      Height     Area
  #   [min]        [min]   [mAU*s]     [mAU]       %
----|-------|----|-------|----------|----------|--------|
   1  27.678 MF    1.3385  206.94585    2.57690   0.8111
   2  31.130 FM    2.0282 2.53068e4   207.96075  99.1889

Totals :                  2.55137e4   210.53765

=====================================================================
                        *** End of Report ***
```

Figure S59. Chiral HPLC chromatogram of (*R*)-**12**.

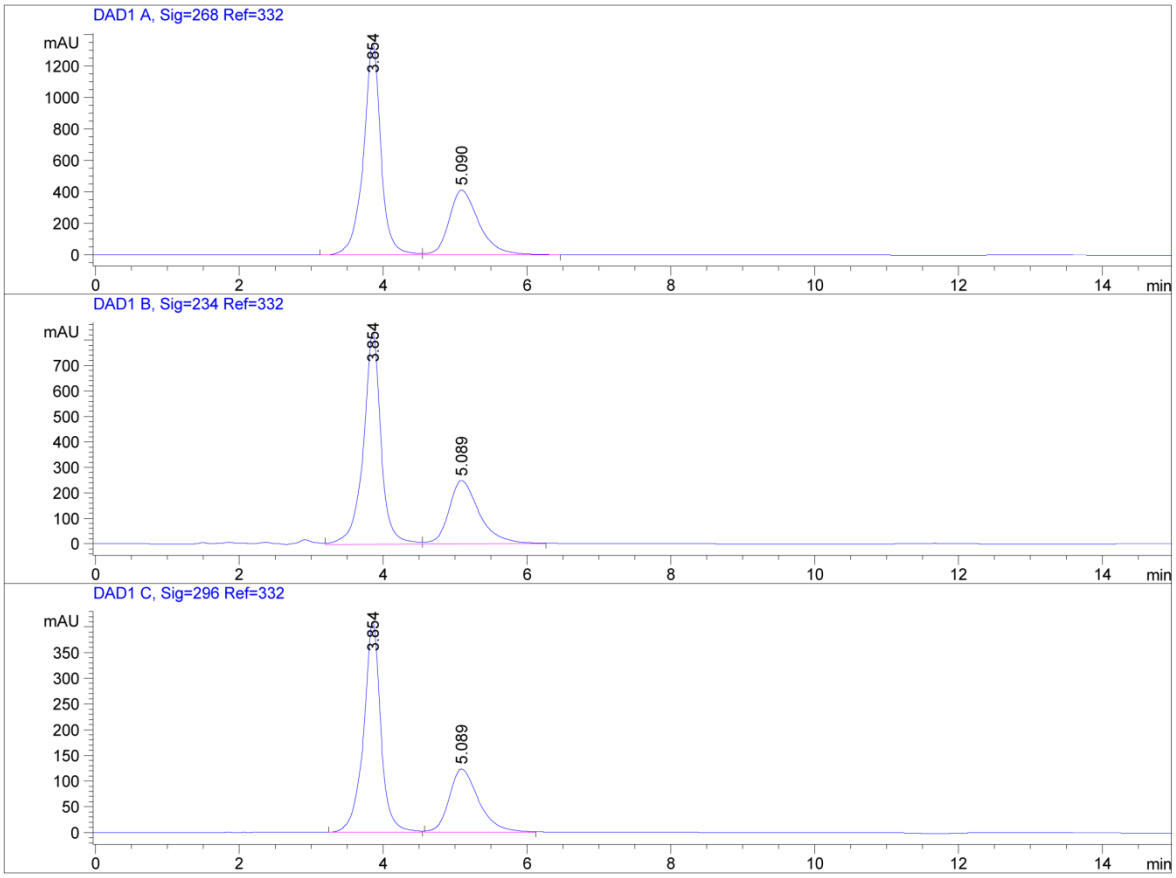

Figure S60. Chiral HPLC chromatogram of (*S*)-**2** spiked with (*R*)-**2**.

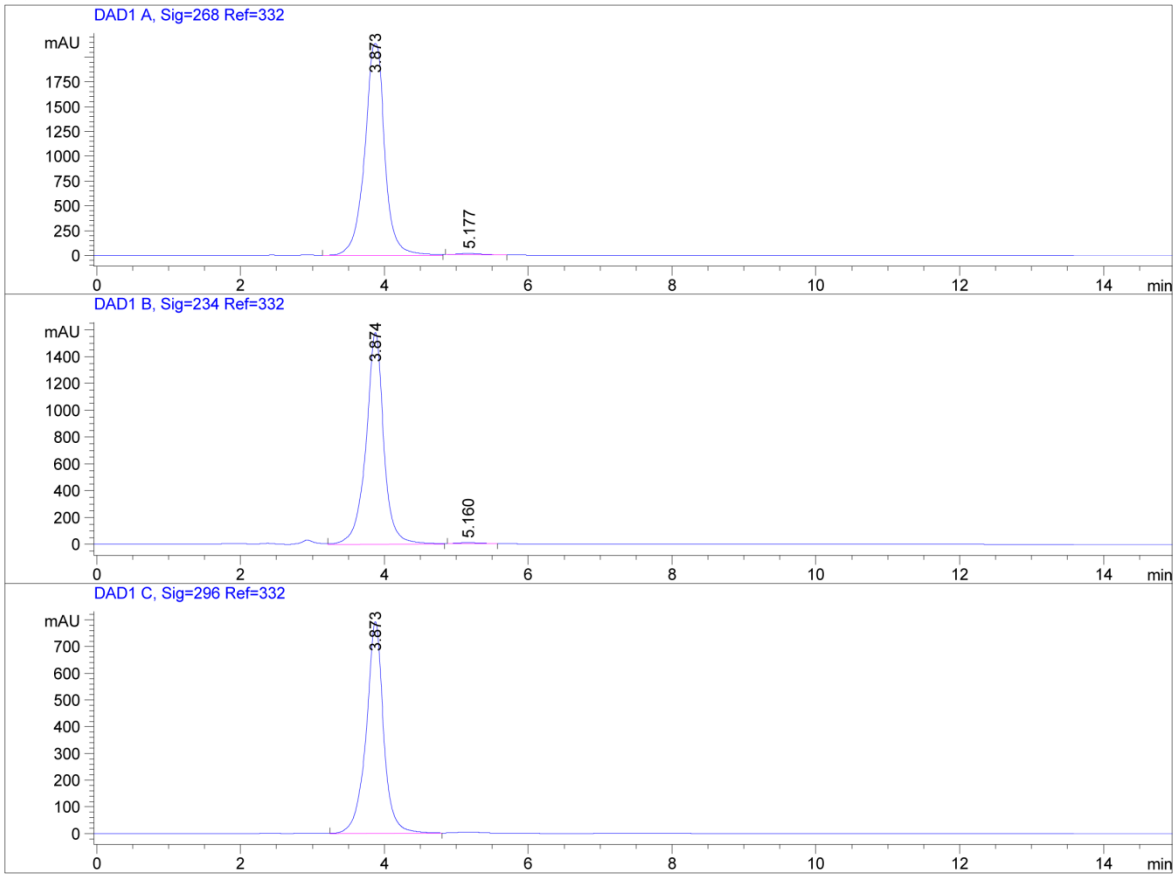


```
=====================================================================
                        Area Percent Report
=====================================================================
Signal 1: DAD1 A, Sig=268 Ref=332

Peak RetTime Type  Width     Area      Height     Area
  #   [min]        [min]   [mAU*s]     [mAU]       %
----|-------|----|-------|----------|----------|--------|
   1   3.873 VV    0.2874 4.12882e4  2136.97314  99.5102
   2   5.177 MM    0.3361  203.22523   10.07786   0.4898

Totals :                   4.14914e4  2147.05101


Signal 2: DAD1 B, Sig=234 Ref=332

Peak RetTime Type  Width     Area      Height     Area
  #   [min]        [min]   [mAU*s]     [mAU]       %
----|-------|----|-------|----------|----------|--------|
   1   3.874 VB    0.2519 2.73658e4  1581.08496  99.3489
   2   5.160 MM    0.4011  179.34746    7.45250   0.6511

Totals :                   2.75451e4  1588.53747


Signal 3: DAD1 C, Sig=296 Ref=332

Peak RetTime Type  Width     Area      Height     Area
  #   [min]        [min]   [mAU*s]     [mAU]       %
----|-------|----|-------|----------|----------|--------|
   1   3.873 BB    0.2471 1.33921e4   792.67151 100.0000

Totals :                   1.33921e4   792.67151

=====================================================================
                        *** End of Report ***
```

Figure S61. Chiral HPLC chromatogram of (*S*)-**2**.

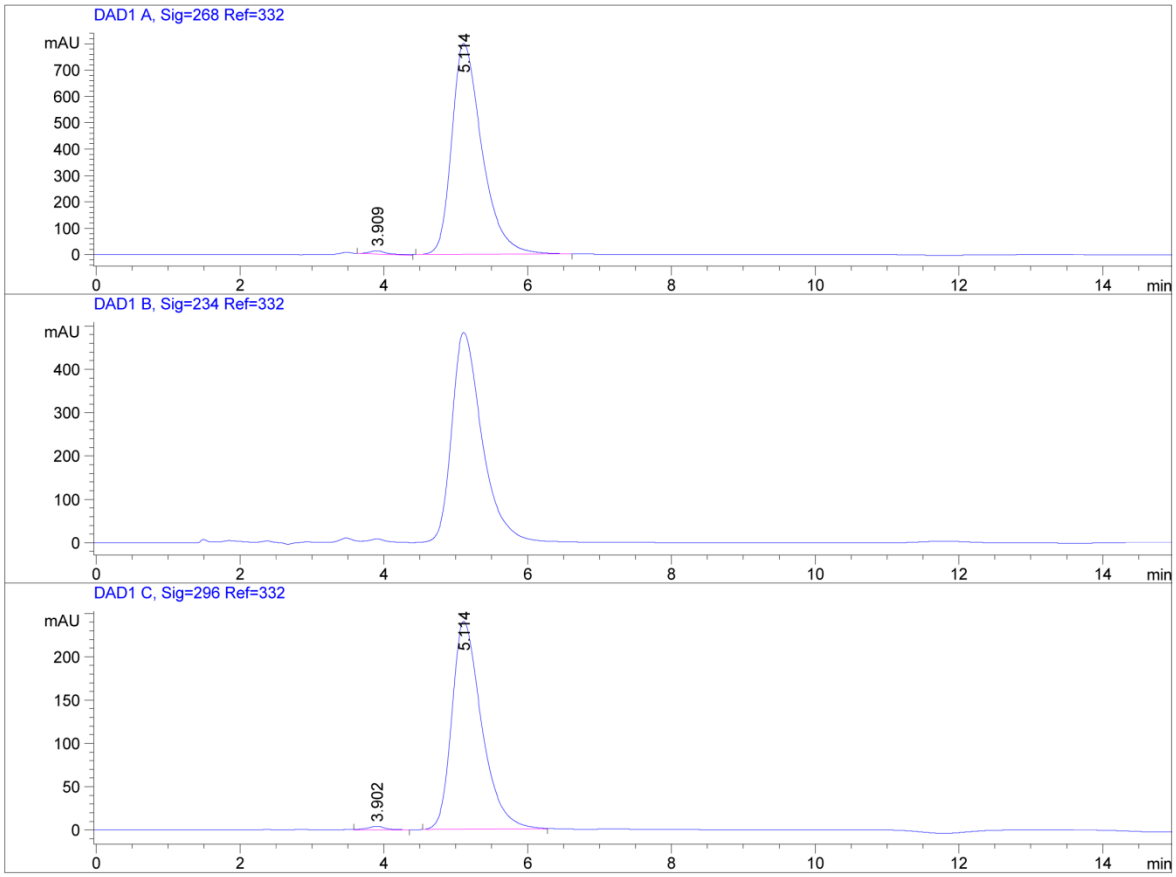


```
=====================================================================
                        Area Percent Report
=====================================================================
Signal 1: DAD1 A, Sig=268 Ref=332

Peak RetTime Type  Width     Area      Height     Area
  #   [min]        [min]   [mAU*s]     [mAU]       %
----|-------|----|-------|----------|----------|--------|
   1   3.909 MM    0.2895  223.11160   12.84487   0.9448
   2   5.114 BB    0.4409 2.33913e4   800.55347  99.0552

Totals :                  2.36144e4   813.39834


Signal 2: DAD1 B, Sig=234 Ref=332

Signal 3: DAD1 C, Sig=296 Ref=332

Peak RetTime Type  Width     Area      Height     Area
  #   [min]        [min]   [mAU*s]     [mAU]       %
----|-------|----|-------|----------|----------|--------|
   1   3.902 MM    0.2626   62.92564    3.99308   0.9004
   2   5.114 BB    0.4367 6925.93701  239.98106  99.0996

Totals :                  6988.86266  243.97414

=====================================================================
                        *** End of Report ***
```

Figure S62. Chiral HPLC chromatogram of (*R*)-**2**.

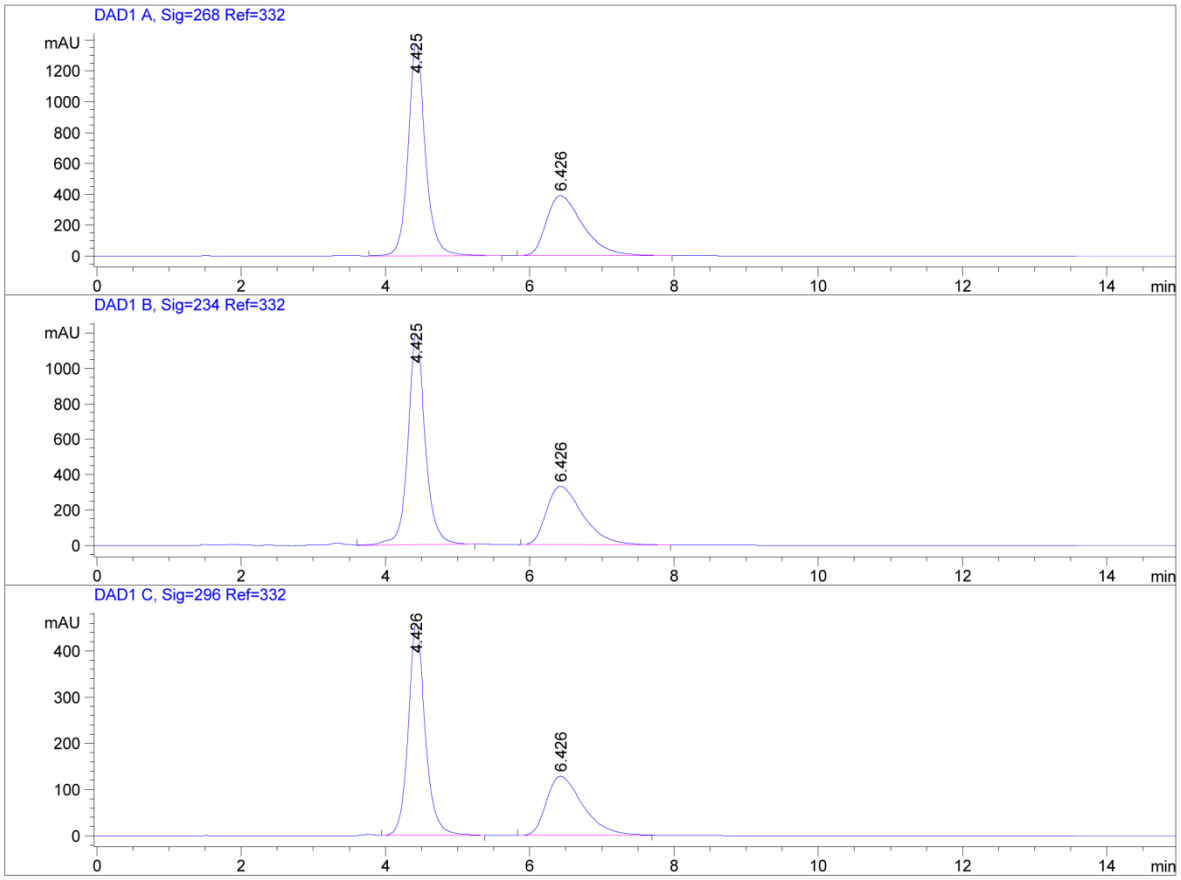

Figure S63. Chiral HPLC chromatogram of (*S*)-**3** spiked with (*R*)-**3**.

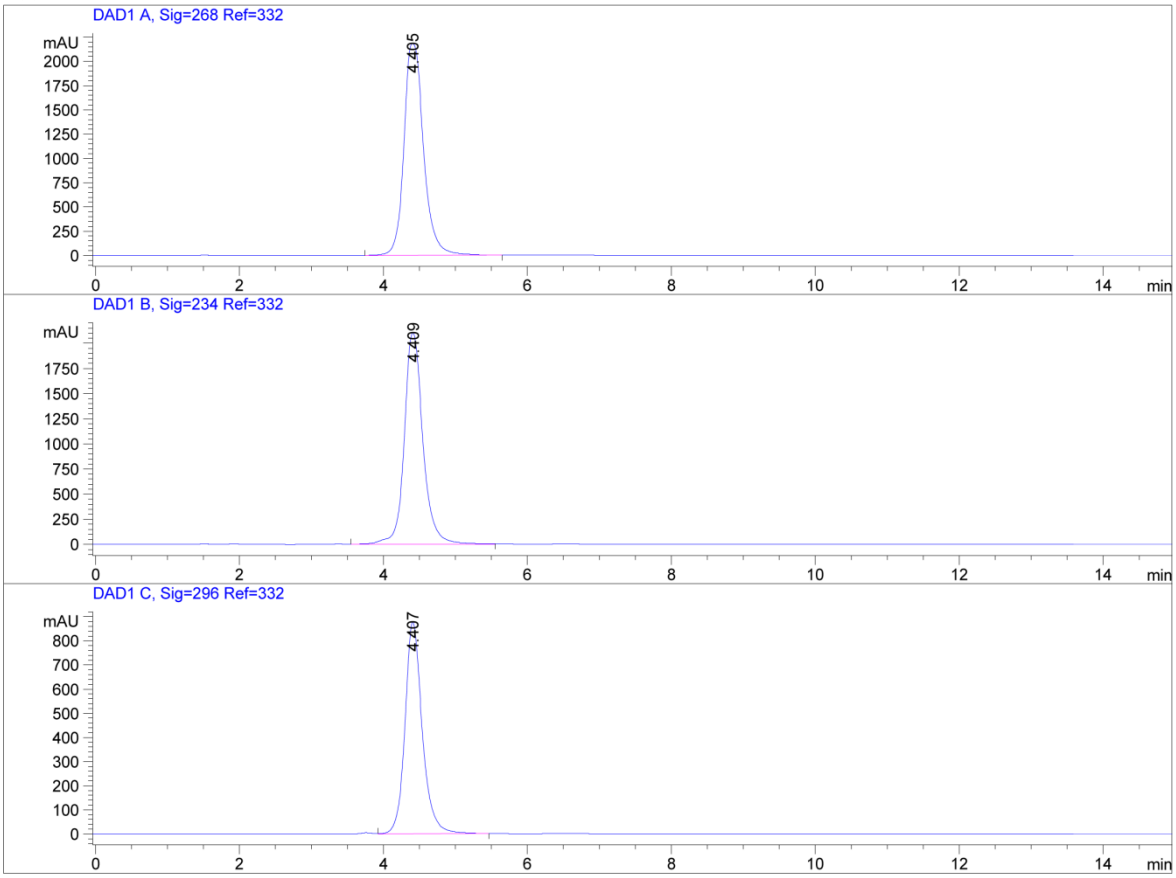


```
=====================================================================
                        Area Percent Report
=====================================================================
Signal 1: DAD1 A, Sig=268 Ref=332

Peak RetTime Type  Width     Area      Height     Area
  #   [min]        [min]   [mAU*s]     [mAU]       %
----|-------|----|-------|----------|----------|--------|
   1   4.405 BB    0.2861 4.11661e4  2181.87695 100.0000

Totals :                  4.11661e4  2181.87695


Signal 2: DAD1 B, Sig=234 Ref=332

Peak RetTime Type  Width     Area      Height     Area
  #   [min]        [min]   [mAU*s]     [mAU]       %
----|-------|----|-------|----------|----------|--------|
   1   4.409 VB    0.2707 3.80011e4  2104.52466 100.0000

Totals :                  3.80011e4  2104.52466


Signal 3: DAD1 C, Sig=296 Ref=332

Peak RetTime Type  Width     Area      Height     Area
  #   [min]        [min]   [mAU*s]     [mAU]       %
----|-------|----|-------|----------|----------|--------|
   1   4.407 VB    0.2481 1.46083e4   877.95654 100.0000

Totals :                  1.46083e4   877.95654

=====================================================================
                        *** End of Report ***
```

Figure S64. Chiral HPLC chromatogram of (*S*)-**3**.

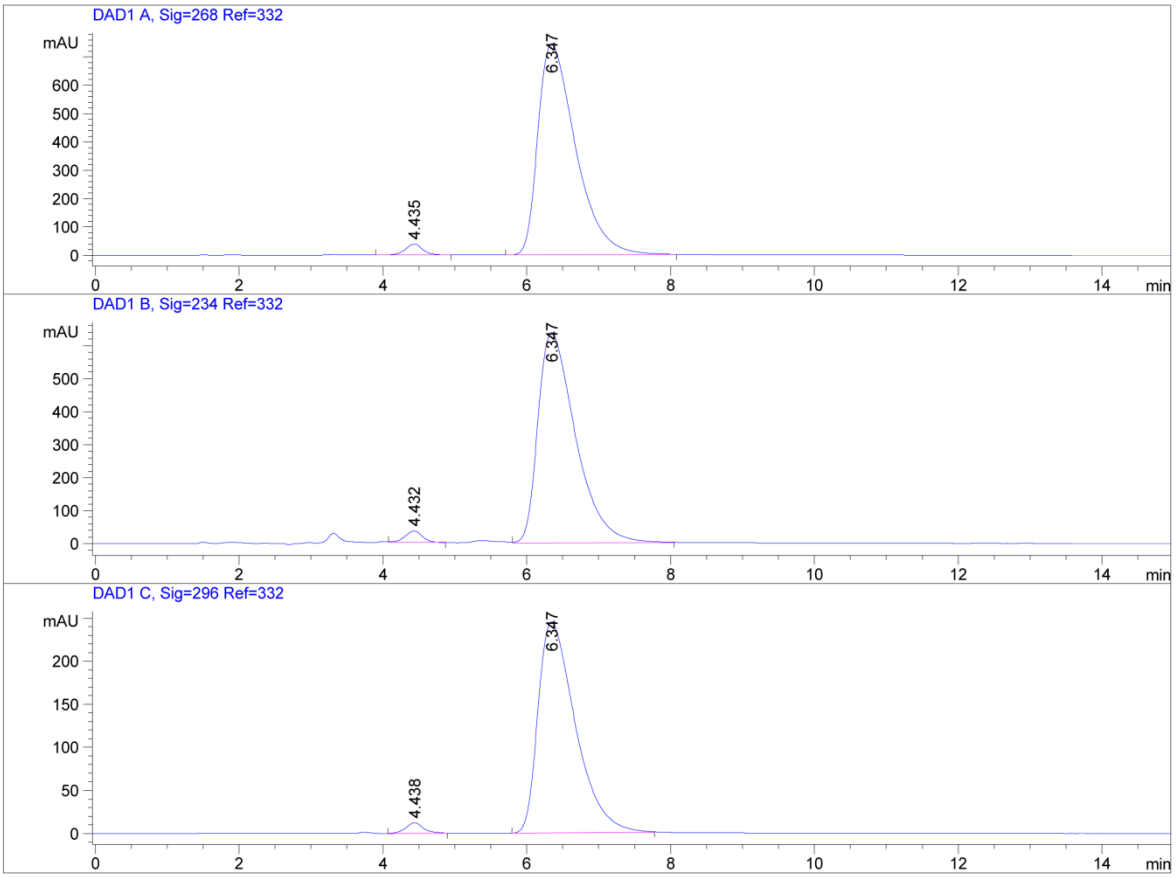


```
=====================================================================
                        Area Percent Report
=====================================================================
Signal 1: DAD1 A, Sig=268 Ref=332

Peak RetTime Type  Width     Area      Height     Area
  #   [min]        [min]   [mAU*s]     [mAU]       %
----|-------|----|-------|----------|----------|--------|
   1   4.435 BB    0.2544  664.35297   39.07228   2.3951
   2   6.347 VB    0.5575 2.70738e4   745.89117  97.6049

Totals :                  2.77381e4   784.96345


Signal 2: DAD1 B, Sig=234 Ref=332

Peak RetTime Type  Width     Area      Height     Area
  #   [min]        [min]   [mAU*s]     [mAU]       %
----|-------|----|-------|----------|----------|--------|
   1   4.432 MM    0.2649  533.29248   33.55628   2.2503
   2   6.347 VB    0.5576 2.31657e4   638.06116  97.7497

Totals :                  2.36990e4   671.61744


Signal 3: DAD1 C, Sig=296 Ref=332

Peak RetTime Type  Width     Area      Height     Area
  #   [min]        [min]   [mAU*s]     [mAU]       %
----|-------|----|-------|----------|----------|--------|
   1   4.438 BB    0.2553  215.70221   12.49881   2.3778
   2   6.347 BB    0.5509 8855.63086  245.45146  97.6222

Totals :                  9071.33307  257.95027

=====================================================================
                        *** End of Report ***
```

Figure S65. Chiral HPLC chromatogram of (*R*)-**3**.

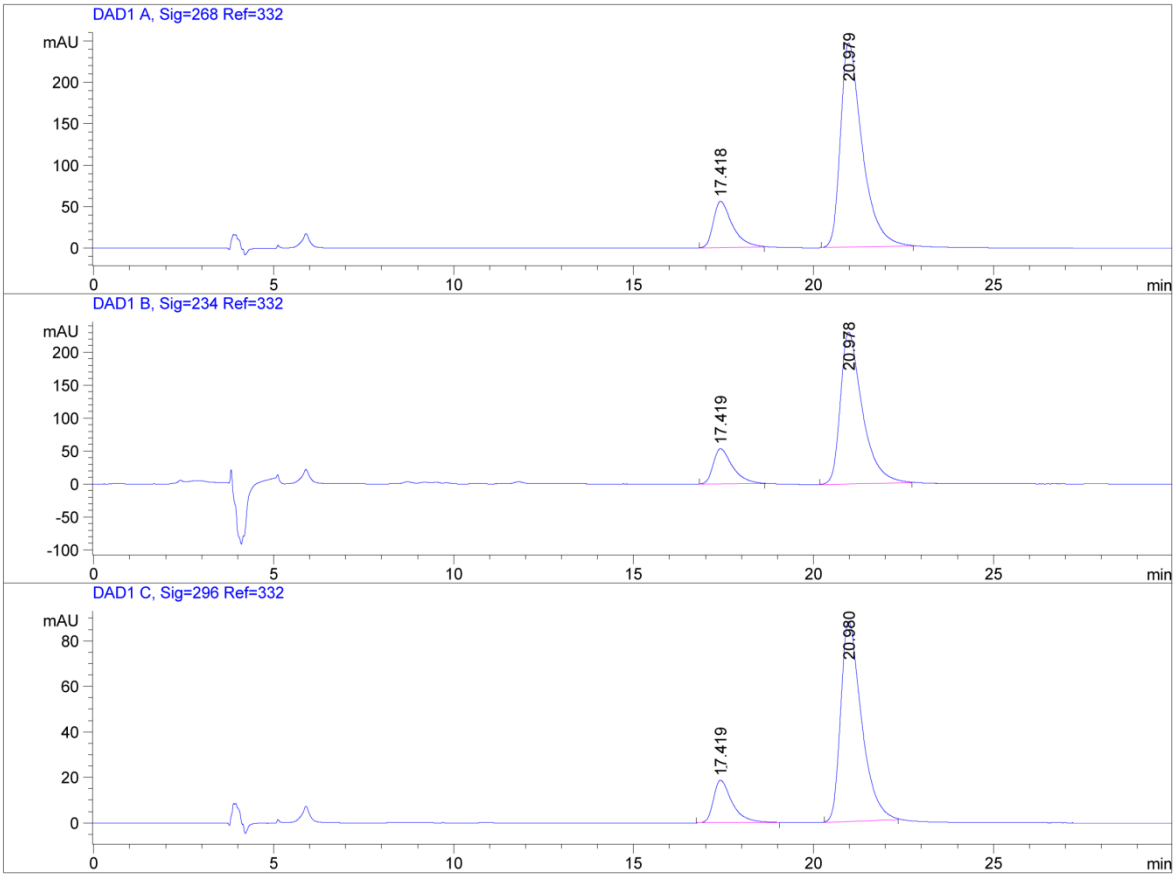

Figure S66. Chiral HPLC chromatogram of (*S*)-**16** spiked with (*R*)-**16**.

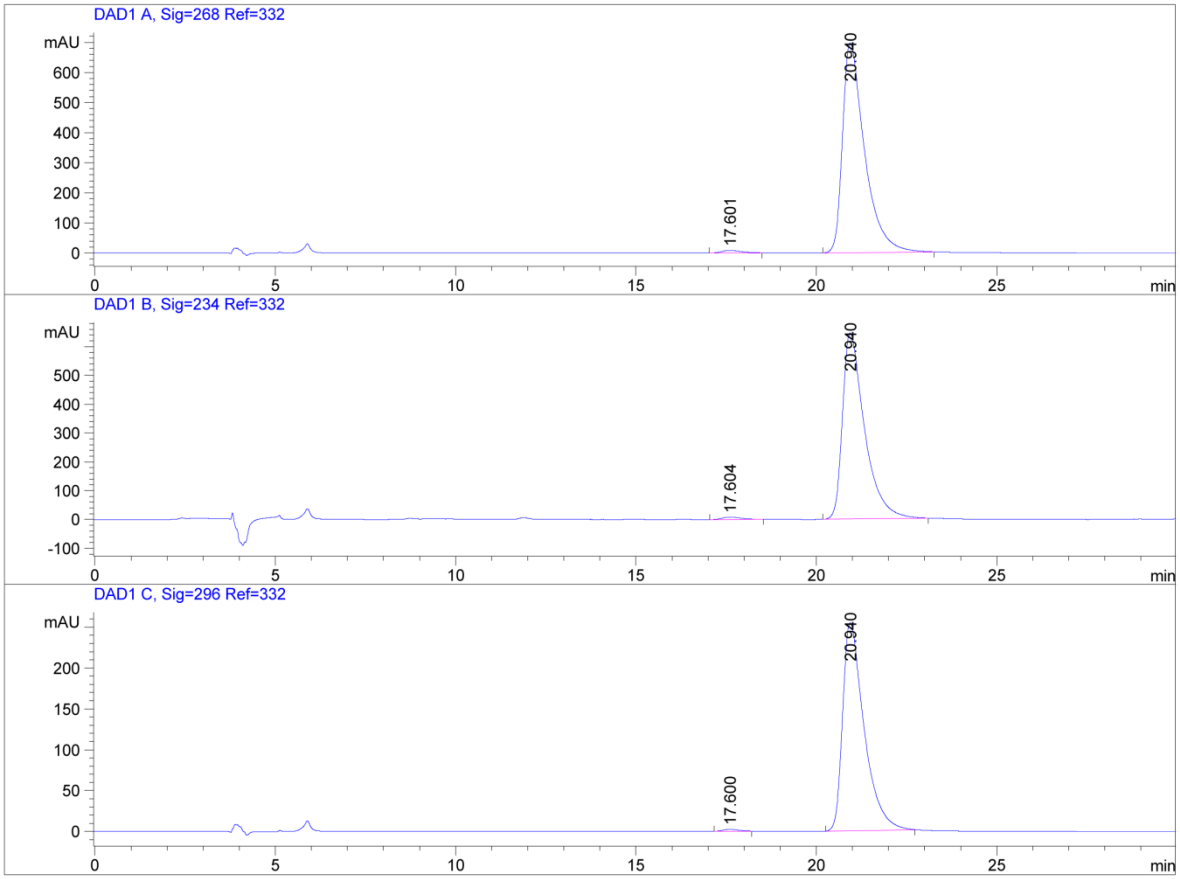


```
=====================================================================
                        Area Percent Report
=====================================================================

Signal 1: DAD1 A, Sig=268 Ref=332

Peak RetTime Type  Width     Area      Height     Area
  #   [min]        [min]   [mAU*s]     [mAU]       %
----|-------|----|-------|----------|----------|--------|
   1  17.601 BB    0.5252  317.24835    8.70569   1.0604
   2  20.940 BB    0.6337 2.95999e4   696.71820  98.9396

Totals :                  2.99171e4   705.42389


Signal 2: DAD1 B, Sig=234 Ref=332

Peak RetTime Type  Width     Area      Height     Area
  #   [min]        [min]   [mAU*s]     [mAU]       %
----|-------|----|-------|----------|----------|--------|
   1  17.604 BB    0.4516  307.24445    8.42317   1.1065
   2  20.940 BB    0.6315 2.74591e4   646.46808  98.8935

Totals :                  2.77663e4   654.89125


Signal 3: DAD1 C, Sig=296 Ref=332

Peak RetTime Type  Width     Area      Height     Area
  #   [min]        [min]   [mAU*s]     [mAU]       %
----|-------|----|-------|----------|----------|--------|
   1  17.600 BB    0.4188   74.67025    2.33699   0.7036
   2  20.940 BB    0.6148 1.05373e4   254.60912  99.2964

Totals :                  1.06119e4   256.94611

=====================================================================
                        *** End of Report ***
```

Figure S67. Chiral HPLC chromatogram of (*S*)-**16**.

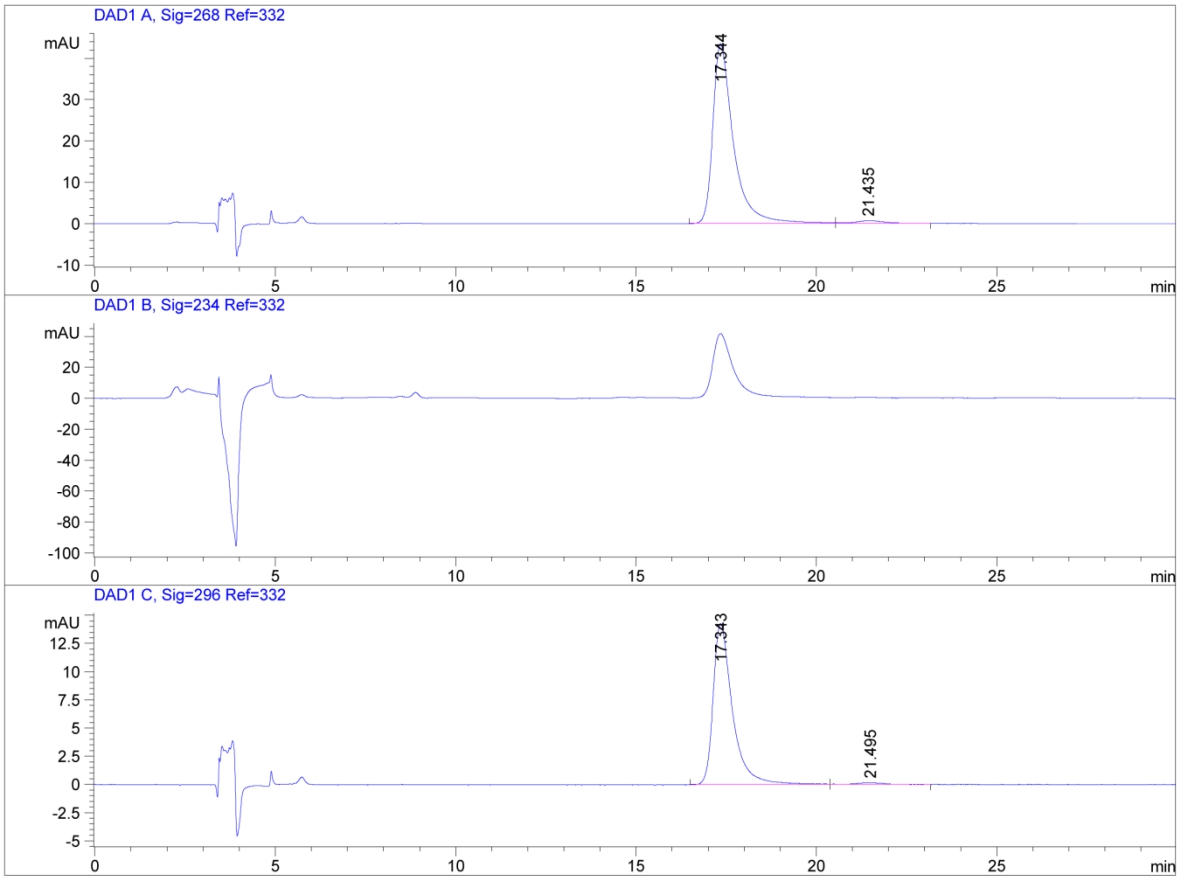


```
=====================================================================
                      Area Percent Report
=====================================================================
Signal 1: DAD1 A, Sig=268 Ref=332

Peak RetTime Type  Width     Area      Height     Area
  #   [min]        [min]   [mAU*s]     [mAU]       %
----|-------|----|-------|----------|----------|--------|
   1  17.344 MF    0.6593 1716.79102   43.40181  98.1276
   2  21.435 FM    0.8589   32.75820 6.35648e-1   1.8724

Totals :                  1749.54921   44.03746


Signal 2: DAD1 B, Sig=234 Ref=332

Signal 3: DAD1 C, Sig=296 Ref=332

Peak RetTime Type  Width     Area      Height     Area
  #   [min]        [min]   [mAU*s]     [mAU]       %
----|-------|----|-------|----------|----------|--------|
   1  17.343 MF    0.6173  527.94348   14.25369  98.7468
   2  21.495 FM    0.7191    6.70038 1.55299e-1   1.2532

Totals :                   534.64386   14.40899

=====================================================================
                      *** End of Report ***
```

Figure S68. Chiral HPLC chromatogram of (*R*)-**16**.

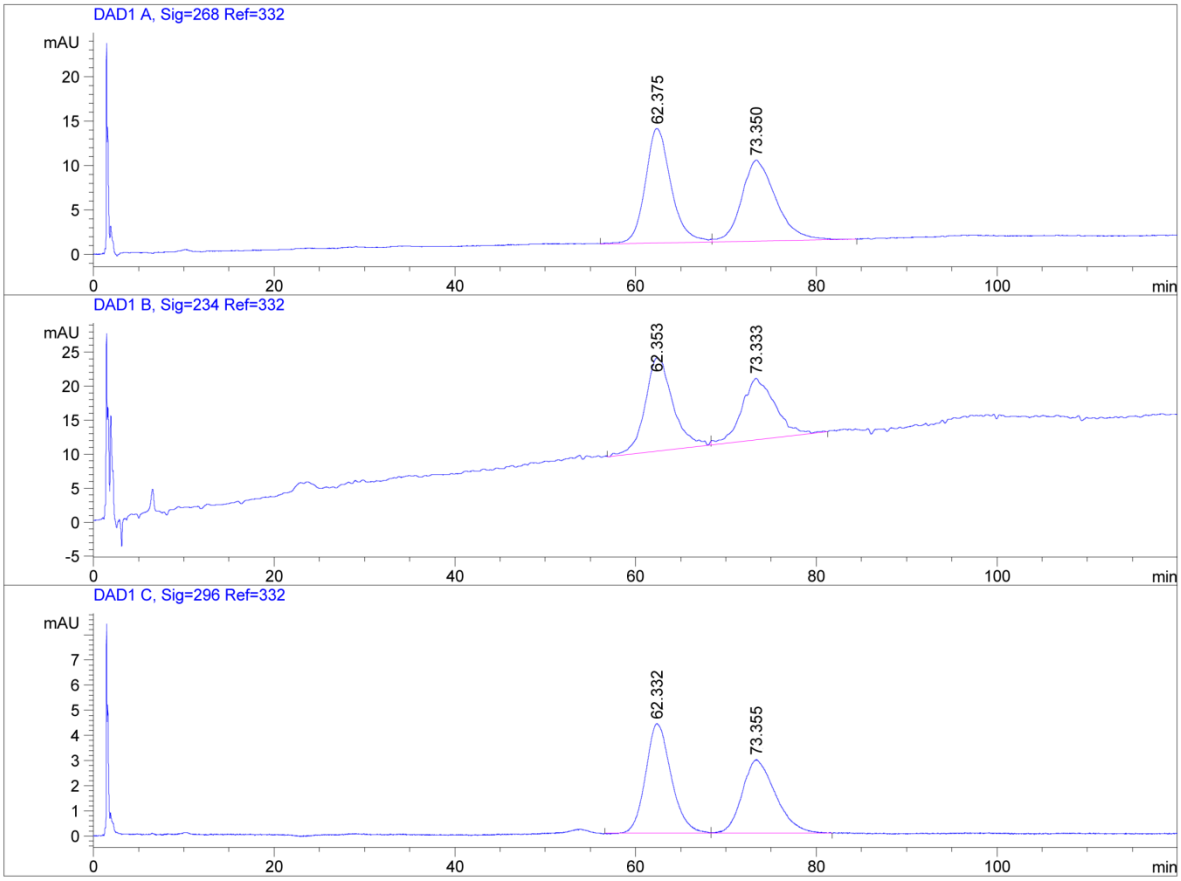

Figure S69. Chiral HPLC chromatogram of corresponding methyl ester of (*S*)-**17** spiked with corresponding methyl ester of (*R*)-**17**.

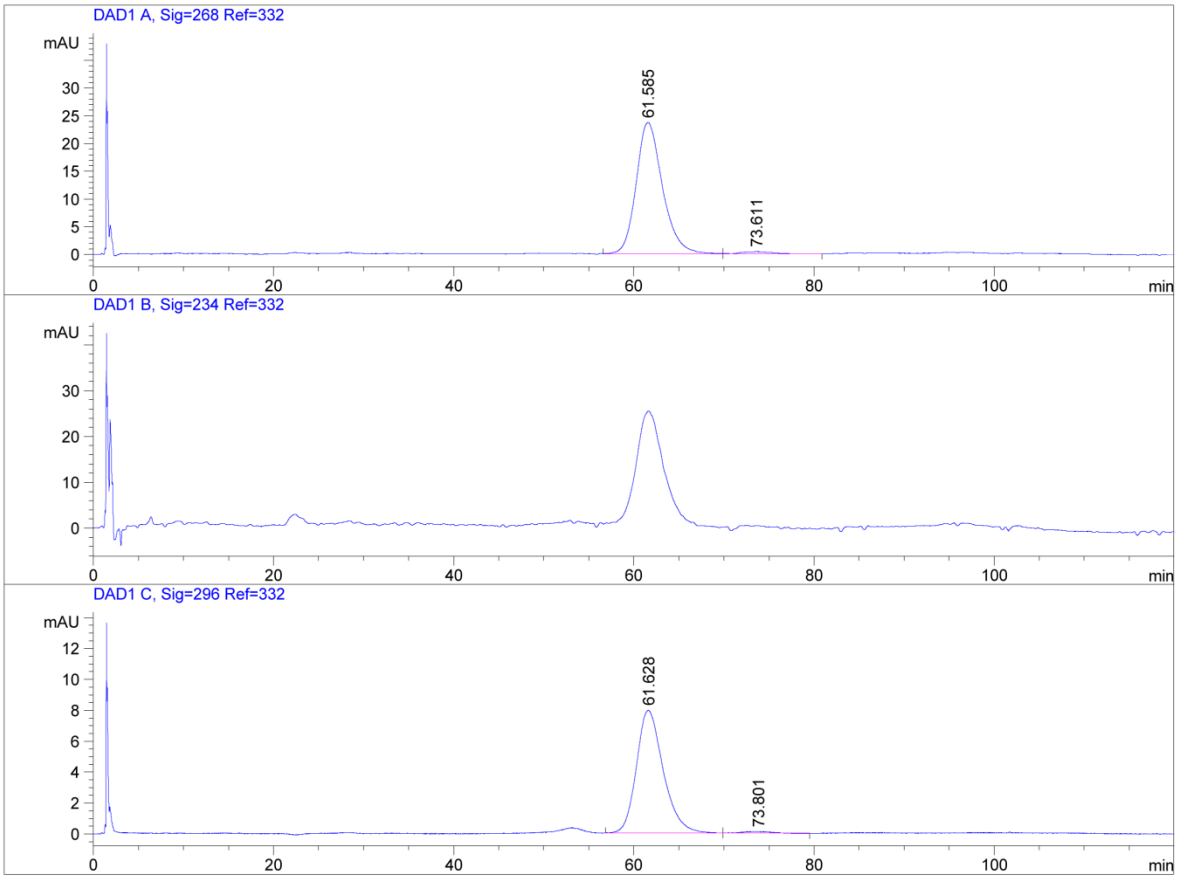


```
=====================================================================
                      Area Percent Report
=====================================================================
Signal 1: DAD1 A, Sig=268 Ref=332

Peak RetTime Type  Width     Area      Height     Area
  #   [min]        [min]   [mAU*s]     [mAU]       %
----|-------|----|-------|----------|----------|--------|
   1  61.585 MF    3.3990 4836.27002   23.71438  97.9039
   2  73.611 FM    3.9964  103.54269 4.31814e-1   2.0961

Totals :                  4939.81271   24.14620


Signal 2: DAD1 B, Sig=234 Ref=332

Signal 3: DAD1 C, Sig=296 Ref=332

Peak RetTime Type  Width     Area      Height     Area
  #   [min]        [min]   [mAU*s]     [mAU]       %
----|-------|----|-------|----------|----------|--------|
   1  61.628 MF    3.4460 1646.15820    7.96159  98.7528
   2  73.801 FM    3.0216   20.79068 1.14679e-1   1.2472

Totals :                  1666.94889    8.07627

=====================================================================
                      *** End of Report ***
```

Figure S70. Chiral HPLC chromatogram of corresponding methyl ester of (*S*)-**17**.

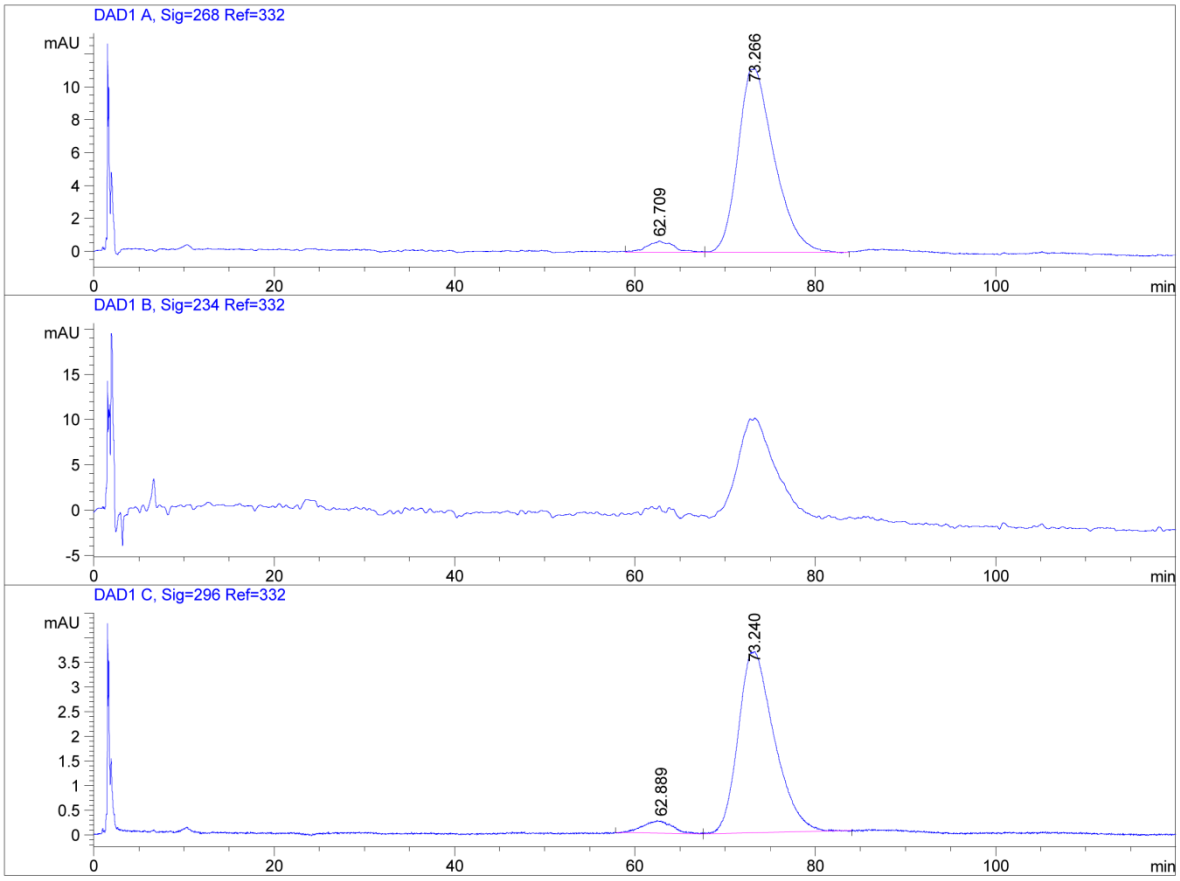


```
=====================================================================
                      Area Percent Report
=====================================================================
Signal 1: DAD1 A, Sig=268 Ref=332

Peak RetTime Type  Width     Area      Height     Area
  #   [min]        [min]   [mAU*s]     [mAU]       %
----|-------|----|-------|----------|----------|--------|
   1  62.709 MF    3.3176  134.67136 6.76541e-1   4.1551
   2  73.266 FM    4.6232 3106.40894   11.19864  95.8449

Totals :                  3241.08029   11.87518


Signal 2: DAD1 B, Sig=234 Ref=332

Signal 3: DAD1 C, Sig=296 Ref=332

Peak RetTime Type  Width     Area      Height     Area
  #   [min]        [min]   [mAU*s]     [mAU]       %
----|-------|----|-------|----------|----------|--------|
   1  62.889 MM    3.6880   55.83808 2.52340e-1   5.1917
   2  73.240 MM    4.6262 1019.69373    3.67362  94.8083

Totals :                  1075.53181    3.92596

=====================================================================
                      *** End of Report ***
```

Figure S71. Chiral HPLC chromatogram of corresponding methyl ester of (*R*)-**17**.

5. Actin-activated ATPase assay

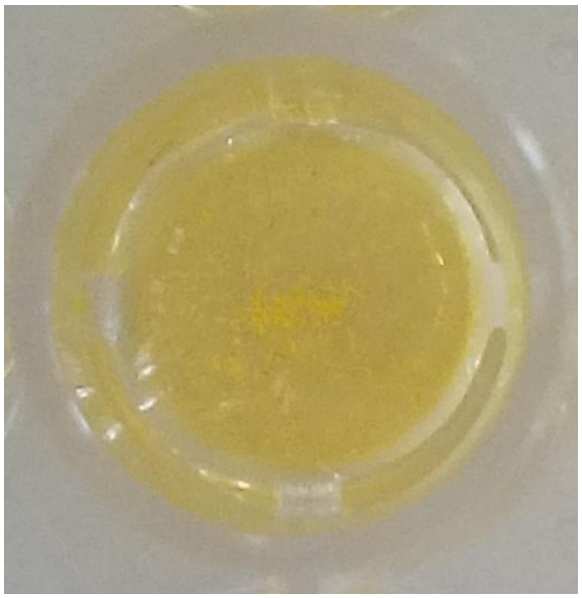

Figure S72. Observed (*S*)-**13** precipitation in assay buffer when applied at concentrations higher than 40 μM.

6. Microscopic imaging of fluorescence

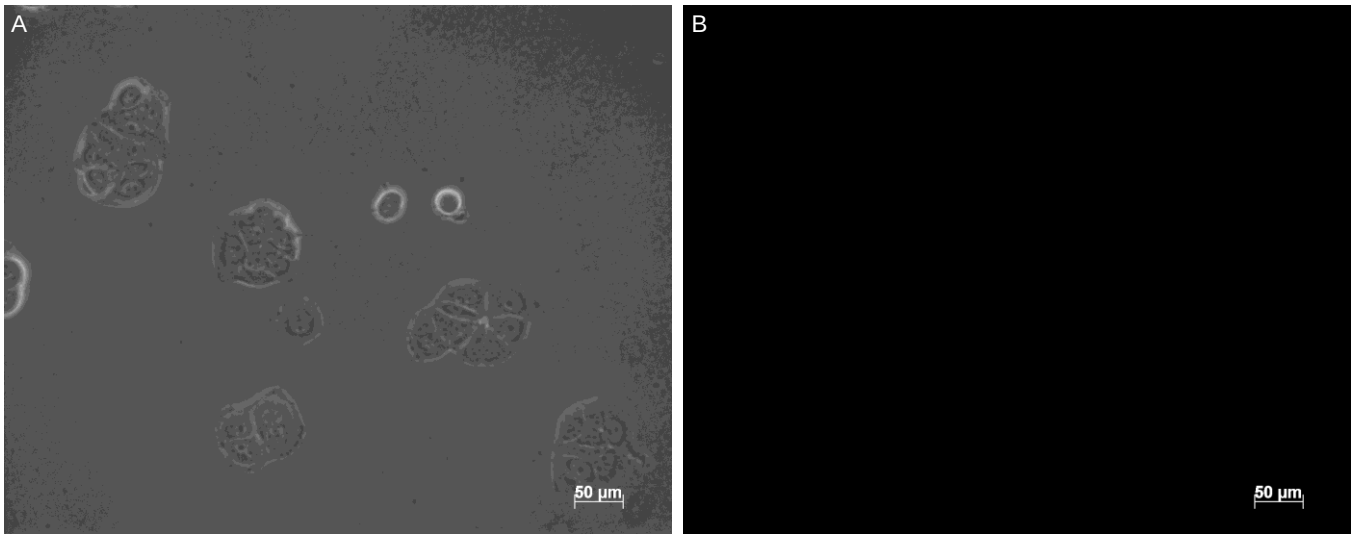

Figure S73. Fluorescence imaging of GFP-negative MCF-7/6 breast carcinoma cells treated with 0.1% DMSO as a solvent control. (A) Brightfield image. (B) Fluorescence image (488 nm excitation).

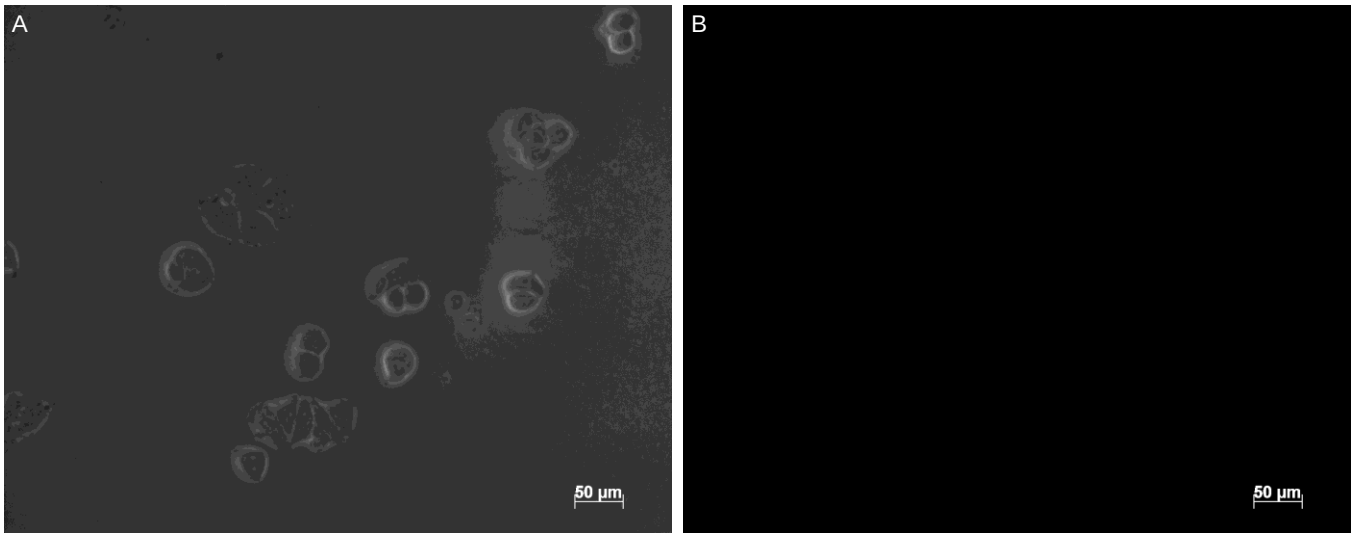

Figure S74. Fluorescence imaging of GFP-negative MCF-7/6 breast carcinoma cells treated with 5 µM of (*S*)-3'-aminoblebbistatin (*S*)-**3**. (A) Brightfield image. (B) Fluorescence image (488 nm excitation).

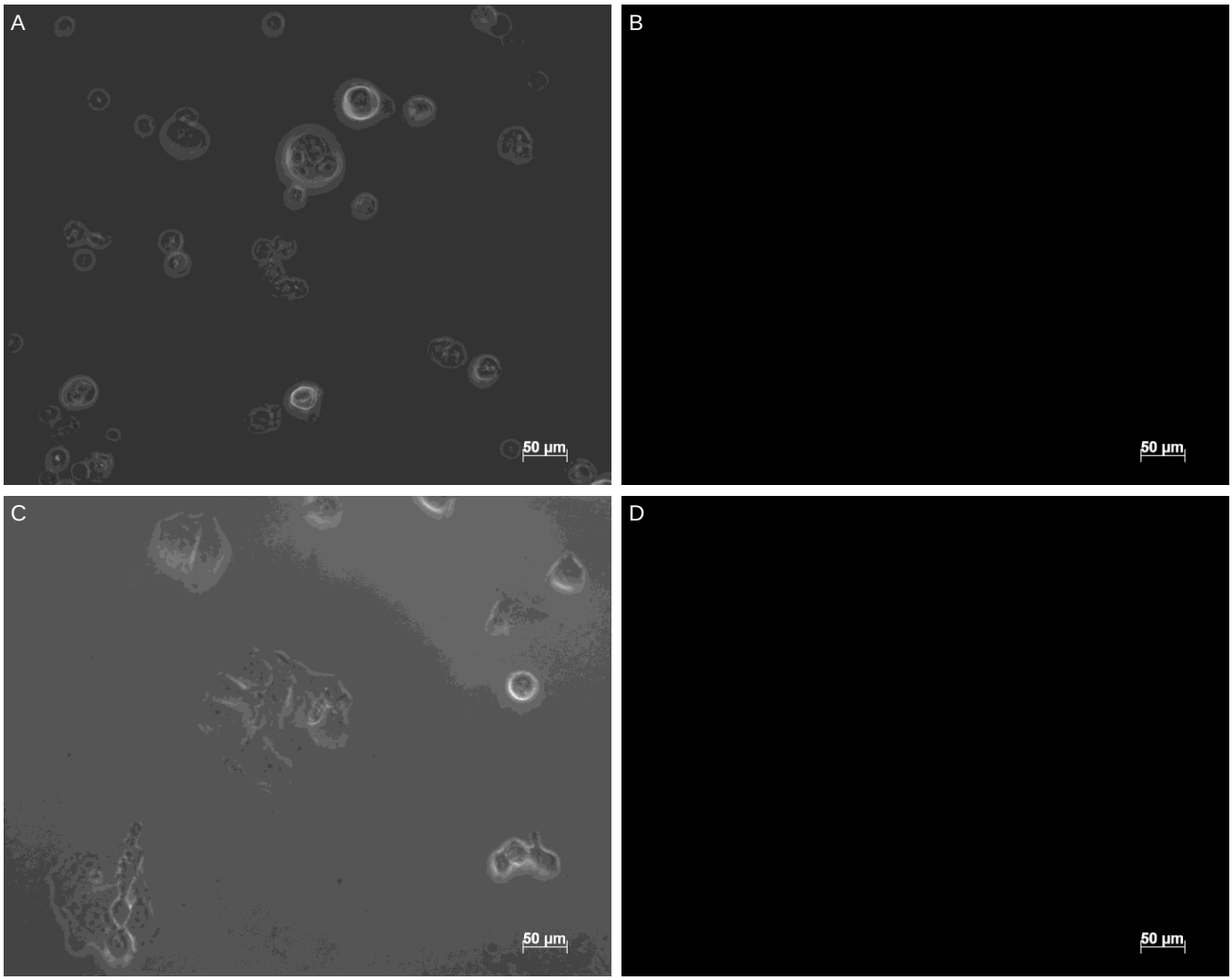

Figure S75. Fluorescence imaging of GFP-negative MCF-7/6 human breast carcinoma cells treated with (*S*)-3'-hydroxyblebbistatin (*S*)-**2**. (A) Brightfield image and (B) fluorescence image (488 nm excitation) of treatment with 5 µM of (*S*)-3'-hydroxyblebbistatin (*S*)-**2**. (C) Brightfield image and (D) fluorescence image (488 nm excitation) of treatment with 50 µM of (*S*)-3'-hydroxyblebbistatin (*S*)-**2**.

7. References

1. D. H. Brown Ripin and M. Vetelino, *Synlett*, 2003, **15**, 2353-2353.

2. S. Buchan and H. McCombie, *J. Chem. Soc.*, 1932, 2857-2860.

3. A. Dahlen, A. Petersson and G. Hilmersson, *Org. Biomol. Chem.*, 2003, **1**, 2423-2426.

4. S. Vandekerckhove, S. Van Herreweghe, J. Willems, B. Danneels, T. Desmet, C. de Kock, P. J. Smith, K. Chibale and M. D'Hooghe, *Eur. J. Med. Chem.*, 2015, **92**, 91-102.

5. D. L. Reger, T. C. Grattan, K. J. Brown, C. A. Little, J. J. S. Lamba, A. L. Rheingold and R. D. Sommer, *J. Organomet. Chem.*, 2000, **607**, 120-128.

6. S. Trofimenko, *J. Am. Chem. Soc.*, 1970, **92**, 5118-5126.

7. S. Juliá, J. M. del Mazo, L. Avila and J. Elguero, *Org. Prep. Proc. Int.*, 1984, **16**, 299-307.

8. E. Haldón, E. Álvarez, M. C. Nicasio and P. J. Pérez, *Inorg. Chem.*, 2012, **51**, 8298-8306.

9. P. Lipp and F. Caspers, *Ber. Dtsch. Chem. Ges. B: Abhandlungen*, 1925, **58B**, 1011-1014.

10. H.-J. Cristau, P. P. Cellier, J.-F. Spindler and M. Taillefer, *Chem. Eur. J.*, 2004, **10**, 5607-5622.

11. J. Ackermann, K. Bleicher, S. Ceccarelli Grenz, O. Chomienne, P. Mattei, T. Schulz-Gasch. WO 2007/063012 A1, 2007.

12. C. P. A. T. Lawson, A. M. Z. Slawin and N. J. Westwood, *Chem. Commun.*, 2011, **47**, 1057-1059.

13. I. Niculescu-Duvaz, M. Ionescu, A. Cambanis, M. Vitan and V. Feyns, *J. Med. Chem.*, 1968, **11**, 500-503.

14. E. Schuler, N. Juanico, J. Teixido, E. L. Michelotti and J. I. Borrell, *Heterocycles*, 2006, **67**, 161-173.

15. C. Lucas-Lopez, S. Patterson, T. Blum, A. F. Straight, J. Toth, A. M. Z. Slawin, T. J. Mitchison, J. R. Sellers and N. J. Westwood, *Eur. J. Org. Chem.*, 2005, 1736-1740.

16. Center For Disease Control and Prevention. Diazomethane. http://www.cdc.gov/niosh/ipcsneng/neng1256.html, (accessed February 2016).

17. International Programme on Chemical Safety. Diazomethane. http://www.inchem.org/documents/icsc/icsc/eics1256.htm, (accessed February 2016).

18. Rigaku Oxford Diffraction (2015). *CrysAlis PRO*. Rigaku Oxford Diffraction, Yarnton, England.

19. O. V. Dolomanov, L. J. Bourhis, R. J. Gildea, J. A. K. Howard and H. Puschmann, *J. Appl. Cryst.*, 2009, **42**, 339-341.

20. G. M. Sheldrick, *Acta Crystallogr.*, 2008, **A64**, 112-122.